Identification of novel prognostic targets in coronary artery disease and related complications using bioinformatics and next generation sequencing data analysis

Basavaraj Vastrad[1], Chanabasayya Vastrad*[2]

1. Department of Pharmaceutical Chemistry, K.L.E. College of Pharmacy, Gadag, Karnataka 582101, India.

2. Biostatistics and Bioinformatics, Chanabasava Nilaya, Bharthinagar, Dharwad 580001, Karnataka, India.

* Chanabasayya Vastrad

channu.vastrad@gmail.com

Ph: +919480073398

Chanabasava Nilaya, Bharthinagar,

Dharwad 580001 , Karanataka, India

Abstract

Coronary artery disease (CAD) is the most common cardiovascular disorder and the leading cause of heart-related deaths in world. Increasing molecular targets have been discovered for CAD and CAD - related complications prognosis and therapy. However, there is still an urgent need to identify novel biomarkers. Therefore, we evaluated biomarkers that might help the diagnosis and treatment of CAD and CAD - related complications. We searched next generation sequencing (NGS) dataset (GSE202625) and identified differentially expressed genes (DEGs) by comparing CAD and normal control samples using DESeq2. Gene ontology (GO) and pathway enrichment analyses of the DEGs were performed using the g:Profiler online database. The protein-protein interaction (PPI) network was plotted with IMEx interactome and visualized using Cytoscape. Module analysis of the PPI network was done using PEWCC1. MiRNA - hub gene regulatory network and TF - hub gene regulatory network analysis was performed to identify the hub genes, miRNAs and TFs. Receiver operating characteristic (ROC) curve analysis was used to predict the diagnostic effectiveness of the hub genes. A total of 118 DEGs (479 up regulated genes and 479 down regulated genes) were detected. The GO enrichment analysis indicated that the DEGs most significantly enriched in cellular response to stimulus and biosynthetic process. The REACTOME pathway enrichment analysis revealed that the DEGs were most significantly enriched in immune system and eukaryotic translation elongation. PPI network, modules, miRNA - hub gene regulatory network and TF - hub gene regulatory network analysis demonstrated that EGR1, SIRT1, STAT1, LRRK2, HIF1A, CSNK2B, RPS3, RPS2, RPS4X and HDAC11 were the hub genes. On the whole, the findings of this study enhance our understanding of the potential molecular mechanisms of CAD and CAD-related complications, and provide potential targets for further research.

Keywords: Coronary artery disease; Bioinformatics analysis; Differentially expressed genes; Biomarkers; Protein-protein network analysis

Introduction

Coronary artery disease (CAD) refers to the complete obstruction of blood flow through the coronary arteries occurs resulting in insufficient oxygen and nutrient delivery to the heart muscles, potentially causing the death of the heart muscle cells and subsequent dysfunction of a portion of the heart muscle itself [1]. CAD and CAD-related complications have become key causes of mortality and morbidity through the world [2]. Incidence of CAD accounts for 8.14 million deaths (16.8%) globally [3]. Myocardial infarction [4], atherosclerosis [5], arrhythmias [6], heart failure [7], atrial fibrillation [8] and dilated cardiomyopathy [9] are associated with CAD. Insulin resistance [10], type 1 and type 2 diabetes mellitus [11-12], non-alcoholic fatty liver disease [13], hypertension [14], obesity [15] and hypercholesterolemia [16] are thought to be the contributing complications to CAD. However, the molecular mechanism underlying many CAD cases remains unclear, resulting in a lack of effective treatment [17]. The higher pervasiveness and finite treatments of CAD lead to considerable public health and economic hardship [18]. Therefore, it is necessary to improve our understanding of CAD molecular pathogenesis and to advance better screening methods for CAD.

In recent years, scholars worldwide have made remarkable achievements in biomarkers and aberrant molecular signaling pathways are involved in the CAD. Data identified several signaling pathways include NF-κB signaling pathway [19], RhoA/ROCK-1 signaling pathway [20], Wnt signaling pathway [21], TLR4 signaling pathway [22] and transforming growth factor β signaling pathway [23], and genes include SCARB1 [24], TP53 [25], RRM1, RRM2 and ERCC2 [26], IL17RA [27] and COX2 [28] that were significantly associated with CAD. In particular, the novel molecular characteristics can be tested in initial risk assessment, the recognition of better specific biomarkers, and the advancement of clinic treatment and survival.

The fast development of next generation sequencing (NGS) technology and bioinformatics analysis based on high-throughput data provide new tactics to identify differentially expressed genes (DEGs) and discover therapeutic targets for the initiation and evolution of CAD and CAD-related complications [29]. However, the differentially expressed genes (DEGs) identified with NGS data large samples and unknown confounding factors. To identify new important DEGs

that remained representative and accurate, we used integrated bioinformatics methods genes obtained from NGS data.

In the current investigation, we downloaded NGS dataset, namely, GSE202625 [30] from the NCBI Gene Expression Omnibus (GEO) database (https://www.ncbi.nlm.nih.gov/geo/) [31], including NGS data. We identified DEGs using the DESeq2 package in R bioconductor. The Gene ontology (GO) and pathway enrichment analyses were performed via g:Profiler. Subsequently, we integrated the DEG protein-protein interaction (PPI) network with module screening to identify hub genes in CAD. Subsequently we constructed miRNA-hub gene regulatory network and TF-hub gene regulatory network to identify hub genes, miRNA and TFs. Finally, we validated the hub genes by receiver operating characteristic (ROC) curve analysis. Identifying key genes and their enriched functions and signaling pathways might help provide a convenient and effective approach for clinical prevention, treatment and management of CAD and CAD-related complications.

Materials and Methods

Next generation sequencing data source

NGS dataset was downloaded from the GEO database. GSE202625 [30] dataset includes 76 CAD samples and 62 normal control samples. The GSE202625 dataset based on GPL23934 Ion Torrent S5 (Homo sapiens).

Identification of DEGs

DESeq2 [32] an R package from Bioconductor was used to identify DEGs between samples from patients with CAD and normal controls. We defined DEGs as a fold change (FC) > 0.333 for up regulated genes and fold change (FC) < -0.2803 for down regulated genes. The Benjamini and Hochberg (BH) method was accomplished to adjust P value to cut down the false positive error [33]. A P value < 0.05 was considered statistically significant. ggplot2 and gplot packages of R software was applied to generate volcano plot and heatmap.

GO and pathway enrichment analyses of DEGs

GO enrichment analysis (GO, http://www.geneontology.org) [34] which means gene ontology analysis now is prevalently used to define genes and it is an actual useful method for our daily extensive scale of functional enrichment study. GO enrichment analysis can be classified into three different gene functions includes biological process (BP), molecular function (MF), and cellular component (CC). REACTOME (https://reactome.org/) [35] pathway database keeps a lot of data about biological pathways, diseases, and chemical substances. In our study, we used the database for g:Profiler (http://biit.cs.ut.ee/gprofiler/) [36] to analyze DEG enrichment of BP, CC, and MF and the REACTOME pathways. $P < 0.05$ was considered statistically significant.

Construction of the PPI network and module analysis

In order to find the hub genes in CAD, we integrated the cross correlation of DEGs through the IMEx interactome (https://www.imexconsortium.org/) [37] database. Later, with the help of the Cytoscape (http://www.cytoscape.org/) [38] software, a PPI network of DEGs was constructed, which was helpful for systematic study on the molecular mechanisms of diseases and therapeutic targets. Finally, for the sake of screening out the hub genes from the PPI network according to the degree [39] , betweenness [40], stress [41] and closeness [42] values in the Cytoscape plugin Network Analyzer. The PEWCC1 [43] of Cytoscape was carried out to module analyze and visualize the result of PPI network.

Construction of the miRNA-hub gene regulatory network

miRNAs can play a role in maintaining physiological stability by regulating the expression of hub genes. We used miRNet database (https://www.mirnet.ca/) [44] to find miRNAs regulating hub genes, taking the intersection of the results of this database. In addition, we visualized miRNA-hub gene regulatory network with Cytoscape software [38].

Construction of the TF-hub gene regulatory network

TFs can play a role in maintaining physiological stability by regulating the expression of hub genes. We used NetworkAnalyst database (https://www.networkanalyst.ca/) [45] database to find TFs regulating hub genes,

taking the intersection of the results of this database. In addition, we visualized TF-hub gene regulatory network with Cytoscape software [38].

Receiver operating characteristic curve (ROC) analysis

ROC analysis was performed to predict the diagnostic effectiveness of biomarkers for CAD by pROC package in R software [46]. The area under the ROC curve (AUC) value was utilized to determine the diagnostic effectiveness in discriminating CAD from normal control samples in the GSE64566 dataset.

Results

Identification of DEGs

Comparing the genes of CAD samples with normal control samples in GSE202625, we found 958 DEGs, including 479 up regulated and 479 down regulated genes (Table 1). The volcano plot of the distribution of DEGs in GSE202625 is shown in Fig. 1. Hierarchical clustering analysis revealed a clear distinction of DEGs between patients with CAD and normal controls (Fig. 2).

GO and pathway enrichment analyses of DEGs

GO and REACTOME enrichment analysis of DEGs between CAD and normal controls groups were performed (Table 2 and Table 3). In GO BP analysis, up regulated genes were primarily rich in cellular response to stimulus and biological regulation, while down regulated genes were primarily rich in biosynthetic process and organonitrogen compound metabolic process. In GO CC analysis, up regulated genes were mainly rich in endomembrane system and intracellular anatomical structure, while down regulated genes were primarily rich in intracellular organelle lumen and cytoplasm. In GO MF analysis, up regulated genes were mainly rich in ion binding and enzyme binding, while down regulated genes were mainly rich in structural molecule activity and nucleic acid binding. In REACTOME pathway enrichment analysis, up regulated genes were rich in immune system and cytokine signaling in immune system, while down regulated genes were rich in eukaryotic translation elongation and disease.

Construction of the PPI network and module analysis

The PPI network of the DEGs was constructed using IMEx interactome . In the PPI network, there were 4863 nodes and 13037 interactions (Fig 3). The hub nodes were EGR1, SIRT1, STAT1, LRRK2, HIF1A, CSNK2B, RPS3, RPS2, RPS4X and HDAC11 (Table 4). The PEWCC1 plug-in was used to screen functional modules of the PPI network, which show a sub-network of highly interconnected proteins. The module 1 contained 26 nodes and 78 interactions (Fig. 4A). Module 1 was linked with immune system, cytokine signaling in immune system, cellular response to stimulus, biological regulation, intracellular anatomical structure and endomembrane system. The module 2 contained 29 nodes and 230 interactions (Fig. 4B). Module 2 was linked with eukaryotic translation elongation, disease, developmental biology, metabolism of proteins, biosynthetic process, organonitrogen compound metabolic process, intracellular organelle lumen, structural molecule activity and nucleic acid binding.

Construction of the miRNA-hub gene regulatory network

The miRNA-hub gene regulatory network included 2694 (miRNA: 2348; gene: 346) nodes and 22561 interactions (Fig 5). We discovered that DDX3X was targeted by 187 miRNAs (ex; hsa-mir-149-3p); DDX5 was targeted by 145 miRNAs (ex; hsa-mir-500b-5p); NCOA3 was targeted by 143 miRNAs (ex; hsa-mir-548y); EGR1 was targeted by 129 miRNAs (ex; hsa-mir-518b); HIF1A was targeted by 101 miRNAs (ex; hsa-mir-16-5p); RPS3 was targeted by 50 miRNAs (ex; hsa-mir-5699-3p); RPS4X was targeted by 40 miRNAs (ex; hsa-mir-532-3p); RPS14 was targeted by 40 miRNAs (ex; hsa-mir-503-5p); FBL was targeted by 39 miRNAs (ex; hsa-mir-31-5p); RPL3 was targeted by 32 miRNAs (ex; hsa-mir-365b-3p) and are listed in Table 5.

Construction of the TF-hub gene regulatory network

The TF-hub gene regulatory network included 535 (TF: 181; gene: 354) nodes and 9293 interactions (Fig 6). We discovered that that EGR1 was targeted by 53 TFs (ex; LMO2); DDX5 was targeted by 51 TFs (ex; MYCN); NCOA3 was targeted by 48 TFs (ex; SIN3B); STAT1 was targeted by 42 TFs (ex; IRF8); HIF1A was targeted by 40 TFs (ex; GATA1); RPS14 was targeted by 45 TFs (ex; RCOR3); RPL3 was targeted by 44 TFs (ex; DMRT1); RPS19 was targeted by 42 TFs (ex;

SREBF1); RPL18 was targeted by 36 TFs (ex; FOXP3); RPS5 was targeted by 35 TFs (ex; POU5F1) and are listed in Table 5.

Receiver operating characteristic curve (ROC) analysis

ROC curve analyses were performed to verify the hub genes, and area under the curve (AUC) values was calculated. Fig 7 shows the AUC for EGR1 was 0.958, AUC for SIRT1 was 0.917, AUC for STAT1 was 0.932, AUC for LRRK2 was 0.922, AUC for HIF1A was 0.912, AUC for CSNK2B was 0.910, AUC for RPS3 was 0.935, AUC for RPS2 was 0.953, AUC for RPS4X was 0.940 and AUC for HDAC11 was 0.907, indicating that the hub genes had high prognostic ability.

Discussion

CAD is a highly frequent disease around world, which remains a dominant cause of cardiovascular death. Therefore, timely and appropriate diagnosis of CAD is essential to enhance the prognosis. In this investigation, we collected NGS dataset from the GEO database, and a total of 958 DEGs, including 479 up regulated genes and 479 down regulated genes, were found. SERPING1 [47] might play an important role in occurrence of development CAD. IFITM3 [48] were a novel key gene in obesity. IFITM3 [49] gene might be related to the pathophysiology of diabetes mellitus. IFITM3 [49] expression is related to the patients with hypercholesterolemia and its progression. Previous studies have shown that IFIT3 [50] might influence the prognosis in myocardial infarction. IFIT1 [51] might be involved in the pathogenesis of atherosclerosis. HBG1 [52] is important in the development of atrial fibrillation. RAP1GAP [53] was associated with cardiac hypertrophy. The results of this investigation suggest that DEGs might play a key role in the pathogenesis of CAD and CAD related complications.

The key DEGs and their relevant GO terms and signaling pathways were screened out based on a bioinformatic analysis. Signaling pathways include immune system [54], metabolism of lipids [55], phospholipid metabolism [56] and disease [57] plays an important role in CAD. DOCK4 [58], CEACAM1 [59], STAT1 [60], ARG1 [61], TLR4 [62], ADAM9 [63], VNN1 [64], ABCA1 [65], STAT2 [66], TLR5 [67], PTGS2 [68], RNF213 [69], ZDHHC17 [70], JAK2 [71], TLR8 [72], NOTCH2 [73], PDGFC (platelet derived growth factor C) [74], CMPK2 [75], TLR2 [76], CYP1B1 [77], CCR1 [78], HDAC9 [79], IL1RN [80],

GCH1 [81], LYST (lysosomal trafficking regulator) [82], PELI1 [83], EGR1 [84], SNX10 [85], CA2 [86], ZEB2 [87], HIF1A [88], PLA2G7 [89], CCR2 [90], GAB1 [91], IRAK3 [92], LDLR (low density lipoprotein receptor) [93], TLR6 [94], SIRT1 [95], NOD2 [96], ATP10D [97], ELOVL6 [98], VCAN (versican) [99], TET2 [100], TET3 [101], ZBTB20 [102], HS3ST1 [103], PF4 [104], DNAJC2 [105], NFIA (nuclear factor I A) [106], CCR7 [107], PRDX2 [108], ADK (adenosine kinase) [109], TCF7 [110], LGALS3 [111], OLFM2 [112], HDAC11 [113] and ARPC1B [114] are significantly related to the atherosclerosis. Studies have revealed that KCNJ2 [115], TLR4 [116], JAK2 [117], TLR2 [118], EGR1 [119], GAB1 [120], ZBTB11 [121], BIN1 [122], TCF4 [123], PPP1R13L [124], TRPM4 [125], LGALS3 [126] and SNTA1 [127] plays a key role in cardiac arrhythmia. Recently, increasing evidence demonstrated that KCNJ2 [128], TLR4 [129], CYP2D6 [130], TLR2 [129], SNX10 [131], SIRT1 [132], PF4 [133], PCYT2 [134] and LGALS3 [135] were altered expression in atrial fibrillation. Studies had shown that KCNJ2 [136], ARG1 [137], TLR4 [138], IFIH1 [139], FBN2 [140], PDK4 [141], TLR8 [142], PDGFC (platelet derived growth factor C) [143], FNIP1 [144], TLR2 [145], PTPN11 [146], LATS2 [147], GCH1 [148], ARFGEF2 [149], CA2 [150], PTPRC (protein tyrosine phosphatase receptor type C) [151], CCR2 [152], GAB1 [153], VEGFA (vascular endothelial growth factor A) [154], UBR1 [155], PHLPP1 [156], MTM1 [157], FMR1 [158], SIRT1 [159], NOD2 [160], MYOF (myoferlin) [161], OSBPL11 [162], ZBTB11 [121], UTRN (utrophin) [163], ZNF593 [164], CCR7 [165], PRDX2 [166], BIN1 [167], NFIC (nuclear factor I C) [168], TCF4 [169], PPP1R13L [124], NDUFB11 [170], TAX1BP3 [171], TRPM4 [172], NMRAL1 [173], LGALS3 [126] and NAA10 [174] were associated with cardiomyopathy. CD274 [175], CEACAM1 [176], STAT1 [177], ARG1 [178], TLR4 [179], LRRK2 [180], ABCA1 [181], IFIH1 [182], TLR5 [183], PTGS2 [184], CYP2D6 [185], RNF213 [186], C9ORF72 [187], JAK2 [188], TLR8 [189], NOTCH2 [190], PDGFC (platelet derived growth factor C) [191], TLR2 [192], PRKAB2 [193], HDAC9 [194], NCOA4 [195], LATS2 [196], DICER1 [197], IL1RN [198], GCH1 [148], EGR1 [199], HIPK3 [200], ZEB2 [201], HIF1A [202], PLA2G7 [203], DOCK8 [204], CCR2 [205], PPP1R15B [206], GCLC (glutamate-cysteine ligase catalytic subunit) [207], VEGFA (vascular endothelial growth factor A) [208], SORL1 [209], OGT (O-linked N-acetylglucosamine (GlcNAc) transferase) [210], EIF2AK3 [211], SLC40A1 [212], PHLPP1 [213], IGF2R [214], LPIN2 [215], SIRT1 [216],

VPS13C [217], ACSL4 [218], ELOVL6 [219], FGL2 [220], ERO1B [221], XAF1 [222], TET2 [223], TET3 [224], PF4 [225], POU2F1 [226], PC (pyruvate carboxylase) [227], NDUFS8 [228], PRDX2 [229], RUNX3 [230], HSPB1 [231], TCF4 [169], TCF7 [232], IGFBP4 [233], HSPG2 [234], NMRAL1 [173], AQP3 [235] and LGALS3 [236] might be a potential therapeutic target for diabetes mellitus. Studies have found that CEACAM1 [237], STAT1 [238], ARG1 [239], TLR4 [240], LRRK2 [241], ABCA1 [242], PTGS2 [243], CYP2D6 [244], JAK2 [245], TLR2 [246], DUSP6 [247], CYP1B1 [248], CCR1 [249], HDAC9 [250], LATS2 [251], IL1RN [252], GCH1 [253], PELI1 [254], EGR1 [255], HIPK3 [256], CCR2 [257], GCLC (glutamate-cysteine ligase catalytic subunit) [258], KLF3 [259], VEGFA (vascular endothelial growth factor A) [260], ITGB1 [261], RASA1 [262], PTPN12 [263], SNRK (SNF related kinase) [264], PRKAR1A [265], LDLR (low density lipoprotein receptor) [266], SIRT1 [267], NOD2 [268], VCAN (versican) [269], TET2 [270], PFKFB2 [271], ZBTB20 [272], MYBL2 [273], PF4 [274], VEGFB (vascular endothelial growth factor B) [275], CCR7 [276], PRDX2 [277], HSPB1 [278], ZNF791 [279], IGFBP4 [280], ESF1 [281], SNHG8 [282], LGALS3 [283] and LGMN (legumain) [284] are altered expression in myocardial infarction. Altered expression of CEACAM1 [176], ACSL1 [285], STAT1 [286], TLR4 [287], ABCA1 [288], TLR5 [183], F2RL1 [289], CYP2D6 [290], PDK4 [291], RNF213 [186], JAK2 [292], TLR8 [189], NOTCH2 [293], CENPJ (centromere protein J) [294], FNIP1 [295], TLR2 [296], KIDINS220 [297], DUSP6 [298], CYP1B1 [299], S1PR3 [300], NCOA2 [301], HDAC9 [302], PELI1 [303], EGR1 [304], HIF1A [305], CCR2 [306], IRAK3 [307], KLF3 [308], VEGFA (vascular endothelial growth factor A) [309], OGT (O-linked N-acetylglucosamine (GlcNAc) transferase) [310], PHLPP1 [213], FMR1 [311], IGF2R [312], PRKAR1A [313], WDR11 [314], LDLR (low density lipoprotein receptor) [315], TLR6 [316], SIRT1 [317], ALDH1A1 [318], NOD2 [319], ACSL4 [320], ELOVL6 [321], VCAN (versican) [322], CLIC5 [323], CLCN3 [324], OSBPL11 [162], HELZ2 [325], TET2 [326], KDM6A [327], PHF2 [328], PHGDH (phosphoglycerate dehydrogenase) [329], VEGFB (vascular endothelial growth factor B) [330], ZBTB7A [331], PC (pyruvate carboxylase) [332], CCR7 [333], PRDX2 [334], MAF1 [335], HSPB1 [336], ESF1 [281], LGALS3 [337], OLFM2 [338] and HDAC11 [339] had been confirmed in obesity. CEACAM1 [340], ACSL1 [341], TLR4 [342], ABCA1 [343], TLR5 [344], CYP2D6 [345], JAK2 [346], NOTCH2 [347], DDX3X [348], NCOA4 [349], EGR1 [350],

IQGAP2 [351], GCLC (glutamate-cysteine ligase catalytic subunit) [352], VEGFA (vascular endothelial growth factor A) [353], ITGB1 [354], LDLR (low density lipoprotein receptor) [355], TLR6 [316], SIRT1 [356], FGL2 [357], TET2 [358], PHF2 [328], VEGFB (vascular endothelial growth factor B) [359], SELENOM (selenoprotein M) [360], TRPM4 [361], OLFM2 [362] and ATAD3A [363] are thought to be involved in non-alcoholic fatty liver disease. Altered expression of ATOH8 [364], STAT1 [365], ARG1 [366], TLR4 [367], VNN1 [368], ABCA1 [369], IFIH1 [370], PTGS2 [371], F2RL1 [289], CYP2D6 [372], PDK4 [373], RNF213 [374], JAK2 [375], NOTCH2 [376], PDGFC (platelet derived growth factor C) [377], TLR2 [378], CYP1B1 [379], IL1RN [380], GCH1 [381], EGR1 [382], HIF1A [383], PLA2G7 [384], CCR2 [385], GAB1 [386], VEGFA (vascular endothelial growth factor A) [387], OGT (O-linked N-acetylglucosamine (GlcNAc) transferase) [388], OXR1 [389], IRF9 [390], FMR1 [391], LDLR (low density lipoprotein receptor) [392], SIRT1 [393], NOD2 [394], ATP13A3 [395], VCAN (versican) [396], FGL2 [397], TET2 [398], KDM6A [399], KLHL2 [400], CAVIN1 [401], TNFRSF4 [402], PF4 [403], VEGFB (vascular endothelial growth factor B) [330], CCR7 [404], PRDX2 [405], HSPB1 [406], TCF4 [407], MRPL4 [408], PHF14 [409], TRPM4 [410], AQP3 [411] and LGMN (legumain) [412] were observed to be associated with the progression of hypertension. Recent studies have shown that altered expression of DDX58 [413], STAT1 [414], TLR4 [415], CYP2D6 [416], JAK2 [417], TLR2 [418], DUSP6 [419], HDAC9 [420], LATS2 [421], CA2 [150], HIPK3 [422], CCR2 [423], GAB1 [120], UFL1 [424], OGT (O-linked N-acetylglucosamine (GlcNAc) transferase) [425], PRKAR1A [265], SIRT1 [426], FGL2 [427], TET2 [428], ASCC2 [429], BIN1 [430], HSPB1 [431], IGFBP4 [432], TRPM4 [433] and LGALS3 [434] might be associated with the progression of heart failure. STAT1 [435], TLR4 [436], ABCA1 [437], PTGS2 [68], CYP2D6 [438], CR1 [439], PDK4 [440], RNF213 [441], ZDHHC17 [70], TLR8 [442], PDGFC (platelet derived growth factor C) [443], TLR2 [444], CYP1B1 [445], HDAC9 [446], IL1RN [447], GCH1 [448], EGR1 [449], ZEB2 [450], PLA2G7 [451], CCR2 [452], GCLC (glutamate-cysteine ligase catalytic subunit) [258], VEGFA (vascular endothelial growth factor A) [453], CD46 [454], NFKBIZ (NFKB inhibitor zeta) [455], LDLR (low density lipoprotein receptor) [456], TLR6 [457], SIRT1 [458], NOD2 [459], FGL2 [460], IDH1 [461], TET2 [462], PFKFB2 [463], KDM6A [464], IKZF2 [465], ZNF606 [466], PF4 [467], CCR7 [468], RUNX3 [469], TCF7 [470], PPBP (pro-platelet basic protein) [471],

IGFBP4 [280], HSPG2 [472] and LGALS3 [236] expression might be regarded as an indicator of susceptibility to CAD. STAT1 [473], TLR4 [367], JAK2 [474], PDGFC (platelet derived growth factor C) [143], CYP1B1 [475], HDAC9 [476], ZEB2 [477], GAB1 [478], IRF9 [479], PHLPP1 [480], SIRT1 [481], NOD2 [482], JMJD1C [483], CLK4 [484], CAVIN1 [485], VEGFB (vascular endothelial growth factor B [486], PRDX2 [487], MAF1 [488], TCF7 [489], IGFBP4 [490], TRPM4 [491], NAA10 [174] and SNTA1 [492] had been demonstrated to participate in cardiac hypertrophy. STAT1 [493], JAK2 [494], NOTCH2 [495], PDGFC (platelet derived growth factor C) [143], RASA1 [262], TLR6 [496], NOD2 [482], JMJD1C [483], CAVIN1 [485], POU2F1 [497], RPS5 [498] and LGALS3 [499] are involved in the regulation of cardiac fibrosis. TLR4 [500], ABCA1 [501], CCR2 [502], LDLR (low density lipoprotein receptor) [503], SIRT1 [504] and NOD2 [505] might crucially contribute to the development of hypercholesterolemia. ABCA1 [506], TLR5 [507], PTGS2 [508], TGFA (transforming growth factor alpha) [509], PDK4 [510], JAK2 [511], TLR2 [512], NEK7 [513], CCR1 [514], BACH1 [515], NCOA4 [195], LATS2 [516], PELI1 [517], EGR1 [518], CYBB (cytochrome b-245 beta chain) [519], MEFV (MEFV innate immuity regulator, pyrin) [520], CLEC4E [521], GCLC (glutamate-cysteine ligase catalytic subunit) [522], KLF3 [523], TP53INP1 [524], ITGB1 [525], IRF9 [526], PHLPP1 [527], NOD2 [528], ACSL4 [529], FGL2 [530], PF4 [531], VEGFB (vascular endothelial growth factor B) [532], CCR7 [533], IGFBP4 [534], TRPM4 [535], BAG1 [536], LGALS3 [537] and ATAD3A [538] could induce ischemic heart disease. Therefore, the data suggest that the identified DEGs which enriched in GO terms and pathways might participant in the development of CAD and its associated complications, and contribute to CAD and CAD related complications treatment.

Notably, the PPI network linked to CAD and CAD related complications were composed of functional proteins that interacted with each other to participate in biological signal pathways, gene expression control, energy, and protein, lipid and carbohydrate metabolism. Key modules might strongly contribute to the occurrence and development of CAD and its associated complications, and have high diagnostic value. EGR1 [84], SIRT1 [95], STAT1 [60], HIF1A [88], HDAC11 [113], STAT2 [66] and IFIT1 [51] might play an important role in regulating the genetic network related to the occurrence, development of

atherosclerosis. Altered expression of EGR1 [119] might be associated with cardiac arrhythmia. EGR1 [199], SIRT1 [216], STAT1 [177], LRRK2 [180], HIF1A [202] and IFITM3 [49] genes might be related to the pathophysiology of diabetes mellitus and may be one of the markers for the early diagnosis of diabetes mellitus. EGR1 [255], SIRT1 [267], STAT1 [238] and LRRK2 [241] are mainly involved in myocardial infarction. EGR1 [304], SIRT1 [317], STAT1 [286], HIF1A [305], HDAC11 [339] and IFITM3 [48] genes have been demonstrated to be responsible for the progression of obesity. Studies have confirmed that EGR1 [350] and SIRT1 [356] are altered expressed in non-alcoholic fatty liver disease. Previous studies have shown that EGR1 [382], SIRT1 [393], STAT1 [365], HIF1A [383] and IRF9 [390] might influence the prognosis in hypertension. EGR1 [449], SIRT1 [458] and STAT1 [435] are a genes which plays a role in diagnosis of CAD. EGR1 [518] and IRF9 [526] have a significant prognostic potential in ischemic heart disease. SIRT1 [132] is molecular marker for the diagnosis and prognosis of atrial fibrillation. Studies had shown that SIRT1 [159] expression was associated with cardiomyopathy. Altered expression of SIRT1 [426] and STAT1 [414] are associated with clinical prognosis in heart failure. SIRT1 [481], STAT1 [473] and IRF9 [479] were a diagnostic biomarkers of cardiac hypertrophy and could be used as therapeutic targets. Studies had shown that SIRT1 [504] and IFITM3 [49] were associated with hypercholesterolemia. Studies have found that STAT1 [493] is altered expression in cardiac fibrosis, which can be used as a prognostic marker for cardiac fibrosis. Our findings suggested CSNK2B, RPS3, RPS2, RPS4X, EIF2AK2, GBP1, IFIT2, RPS14, RPS29, RPS9, RPS15, RPLP1, RPS19, RPL3, RPLP2 and RPL36 as novel diagnostic biomarkers for CAD and CAD related complications. Therefore, these biomarkers might be used as potential effective candidates for early diagnosis or prognosis of CAD and CAD related complications. Importantly, study on ribosomal proteins might be a significant new direction for the diagnosis, prognosis and treatment of CAD and CAD related complications.

Based on the miRNA-hub gene regulatory network and TF-hub gene regulatory network constructed by the online database miRNet and NetworkAnalyst, we identified hub genes, miRNAs and TFs. Previous study showed that DDX3X [348], EGR1 [350] and SREBF1 [539] were associated with non-alcoholic fatty liver disease. EGR1 [84], HIF1A [88], STAT1 [60], hsa-mir-

16-5p [540], hsa-mir-532-3p [541], hsa-mir-503-5p [542], SREBF1 [543] and FOXP3 [544] plays a pivotal role in the atherosclerosis. The results showed that EGR1 [119] expression participate in the progression of cardiac arrhythmia. EGR1 [199], HIF1A [202], STAT1 [177], hsa-mir-31-5p [545], SREBF1 [546] and FOXP3 [547] were observed to be associated with the progression of diabetes mellitus. EGR1 [255], STAT1 [238] and FOXP3 [548] regulates the development of myocardial infarction. EGR1 [304], HIF1A [305], STAT1 [286], hsa-mir-31-5p [549], hsa-mir-365b-3p [550], SREBF1 [551] and FOXP3 [552] might be associated with the prognosis of obesity. EGR1 [382], HIF1A [383], STAT1 [365] and FOXP3 [553] mainly involved in the occurrence of hypertension. Aberrant expression of EGR1 [449], STAT1 [435], hsa-mir-16-5p [554], IRF8 [555] and FOXP3 [556] have been observed in CAD. Studies have found that EGR1 [518] and hsa-mir-16-5p [557] expression is an independent predictor of prognosis in patients with ischemic heart disease. STAT1 [414] and FOXP3 [558] migt be a prognostic biomarkers and potential therapeutic targets for patients with heart failure. Studies have found that STAT1 [493] and RPS5 [498] mRNA expressions are an independent predictor of prognosis in patients with cardiac fibrosis. hsa-mir-16-5p [557] and FOXP3 [559] are associated with the prognosis of cardiomyopathy. FOXP3 [600] was identified as a candidate biomarker for the diagnosis and treatment of hypercholesterolemia. We identified DDX5, NCOA3, RPS3, RPS4X, RPS14, FBL, RPL3, RPS19, RPL18, hsa-mir-149-3p, hsa-mir-500b-5p,` hsa-mir-548y, hsa-mir-518b, hsa-mir-5699-3p, LMO2, MYCN, SIN3B, GATA1, RCOR3, DMRT1 and POU5F1 that might serve as novel biomarkers for CAD and CAD related complications.

In conclusion, a comprehensive bioinformatics analysis of DEGs and pathways involved in the occurrence and advanacement of CAD and CAD related complications was performed, and we find and obtained essential genes and pathways contributing to the progression of CAD and CAD related complications to improve prognosis. Moreover, these results migt promote the understanding of molecular mechanisms and clinically related molecular targets for prognosis in CAD and CAD related complications and provide novel insight into the occurrence and adancement of CAD and CAD related complications.

Acknowledgement

I thank Gualtiero Ivanoe Colombo, Centro Cardiologico Monzino IRCCS, Immunology and Functional Genomics, Via Carlo Parea, 4, Milano, Italy, very much, the author who deposited their NGS dataset GSE202625, into the public GEO database.

Conflict of interest

The authors declare that they have no conflict of interest.

Ethical approval

This article does not contain any studies with human participants or animals performed by any of the authors.

Informed consent

No informed consent because this study does not contain human or animals participants.

Availability of data and materials

The datasets supporting the conclusions of this article are available in the GEO (Gene Expression Omnibus) (https://www.ncbi.nlm.nih.gov/geo/) repository. [(GSE202625) https://www.ncbi.nlm.nih.gov/geo/query/acc.cgi?acc=GSE202625]

Consent for publication

Not applicable.

Competing interests

The authors declare that they have no competing interests.

Author Contributions

B. V. - Writing original draft, and review and editing

C. V. - Software and investigation

Authors

Basavaraj Vastrad ORCID ID: 0000-0003-2202-7637

Chanabasayya Vastrad ORCID ID: 0000-0003-3615-4450

References

1. Malakar AK, Choudhury D, Halder B, Paul P, Uddin A, Chakraborty S. A review on coronary artery disease, its risk factors, and therapeutics. J Cell Physiol. 2019;234(10):16812-16823. doi:10.1002/jcp.28350
2. Roger VL, Ballard DJ, Hallett JW Jr, Osmundson PJ, Puetz PA, Gersh BJ. Influence of coronary artery disease on morbidity and mortality after abdominal aortic aneurysmectomy: a population-based study, 1971-1987. J Am Coll Cardiol. 1989;14(5):1245-1252. doi:10.1016/0735-1097(89)90423-3
3. Fan Y, Li Y, Chen Y, Zhao YJ, Liu LW, Li J, Wang SL, Alolga RN, Yin Y, Wang XM, Zhao DS, et al. Comprehensive Metabolomic Characterization of Coronary Artery Diseases. J Am Coll Cardiol. 2016;68(12):1281-1293. doi:10.1016/j.jacc.2016.06.044
4. Lindahl B, Baron T, Albertucci M, Prati F. Myocardial infarction with non-obstructive coronary artery disease. EuroIntervention. 2021;17(11):e875-e887. doi:10.4244/EIJ-D-21-00426
5. Ghattas A, Griffiths HR, Devitt A, Lip GY, Shantsila E. Monocytes in coronary artery disease and atherosclerosis: where are we now?. J Am Coll Cardiol. 2013;62(17):1541-1551. doi:10.1016/j.jacc.2013.07.043
6. Agewall S. Coronary artery disease and arrhythmias. Eur Heart J Cardiovasc Pharmacother. 2017;3(2):69-70. doi:10.1093/ehjcvp/pvx005
7. Correale M, Totaro A, Ieva R, Ferraretti A, Musaico F, Di Biase M. Tissue Doppler imaging in coronary artery diseases and heart failure. Curr Cardiol Rev. 2012;8(1):43-53. doi:10.2174/157340312801215755
8. Michniewicz E, Mlodawska E, Lopatowska P, Tomaszuk-Kazberuk A, Malyszko J. Patients with atrial fibrillation and coronary artery disease - Double trouble. Adv Med Sci. 2018;63(1):30-35. doi:10.1016/j.advms.2017.06.005
9. Schaer B, Kühne M, Koller MT, Sticherling C, Osswald S. Therapy with an implantable cardioverter defibrillator (ICD) in patients with coronary artery disease and dilated cardiomyopathy: benefits and disadvantages. Swiss Med Wkly. 2009;139(45-46):647-653. doi:10.4414/smw.2009.12668

10. Skals R, Krogager ML, Appel EVR, Schnurr TM, Have CT, Gislason G, Poulsen HE, Køber L, Engstrøm T, Stender S, et al. Insulin resistance genetic risk score and burden of coronary artery disease in patients referred for coronary angiography. PLoS One. 2021;16(6):e0252855. doi:10.1371/journal.pone.0252855
11. Naito R, Miyauchi K. Coronary Artery Disease and Type 2 Diabetes Mellitus. Int Heart J. 2017;58(4):475-480. doi:10.1536/ihj.17-191
12. Devaraj SM, Miller RG, Orchard TJ, Kriska AM, Gary-Webb T, Costacou T. Data driven patterns of nutrient intake and coronary artery disease risk in adults with type 1 diabetes. J Diabetes Complications. 2021;35(10):108016. doi:10.1016/j.jdiacomp.2021.108016
13. Kirby RS, Halegoua-DeMarzio D. Coronary artery disease and non-alcoholic fatty liver disease: Clinical correlation using computed tomography coronary calcium scans. JGH Open. 2021;5(3):390-395. doi:10.1002/jgh3.12509
14. Rosendorff C. Hypertension and coronary artery disease: a summary of the American Heart Association scientific statement. J Clin Hypertens (Greenwich). 2007;9(10):790-795. doi:10.1111/j.1751-7176.2007.tb00006.x
15. Garcia-Labbé D, Ruka E, Bertrand OF, Voisine P, Costerousse O, Poirier P. Obesity and coronary artery disease: evaluation and treatment. Can J Cardiol. 2015;31(2):184-194. doi:10.1016/j.cjca.2014.12.008
16. de Gonzalo-Calvo D, Cenarro A, Garlaschelli K, Pellegatta F, Vilades D, Nasarre L, Camino-Lopez S, Crespo J, Carreras F, Leta R, Catapano AL, Norata GD, Civeira F, et al. Translating the microRNA signature of microvesicles derived from human coronary artery smooth muscle cells in patients with familial hypercholesterolemia and coronary artery disease. J Mol Cell Cardiol. 2017;106:55-67. doi:10.1016/j.yjmcc.2017.03.005
17. Libby P, Theroux P. Pathophysiology of coronary artery disease. Circulation. 2005;111(25):3481-3488. doi:10.1161/CIRCULATIONAHA.105.537878
18. Bauersachs R, Zeymer U, Brière JB, Marre C, Bowrin K, Huelsebeck M. Burden of Coronary Artery Disease and Peripheral Artery Disease: A Literature Review. Cardiovasc Ther. 2019;2019:8295054. doi:10.1155/2019/8295054

19. Guo F, Tang C, Li Y, Liu Y, Lv P, Wang W, Mu Y. The interplay of LncRNA ANRIL and miR-181b on the inflammation-relevant coronary artery disease through mediating NF-κB signalling pathway. J Cell Mol Med. 2018;22(10):5062-5075. doi:10.1111/jcmm.13790
20. Dokumacioglu E, Duzcan I, Iskender H, Sahin A. RhoA/ROCK-1 Signaling Pathway and Oxidative Stress in Coronary Artery Disease Patients. Braz J Cardiovasc Surg. 2022;37(2):212-218. doi:10.21470/1678-9741-2020-0525
21. Liu Y, Neogi A, Mani A. The role of Wnt signalling in development of coronary artery disease and its risk factors. Open Biol. 2020;10(10):200128. doi:10.1098/rsob.200128
22. Jia SJ, Niu PP, Cong JZ, Zhang BK, Zhao M. TLR4 signaling: a potential therapeutic target in ischemic coronary artery disease. Int Immunopharmacol. 2014;23(1):54-59. doi:10.1016/j.intimp.2014.08.011
23. Zeng L, Dang TA, Schunkert H. Genetics links between transforming growth factor β pathway and coronary disease. Atherosclerosis. 2016;253:237-246. doi:10.1016/j.atherosclerosis.2016.08.029
24. Ayhan H, Gormus U, Isbir S, Yilmaz SG, Isbir T. SCARB1 Gene Polymorphisms and HDL Subfractions in Coronary Artery Disease. In Vivo. 2017;31(5):873-876. doi:10.21873/invivo.11141
25. Kolovou V, Tsipis A, Mihas C, Katsiki N, Vartela V, Koutelou M, Manolopoulou D, Leondiadis E, Iakovou I, Mavrogieni S, et al. Tumor Protein p53 (TP53) Gene and Left Main Coronary Artery Disease. Angiology. 2018;69(8):730-735. doi:10.1177/0003319718760075
26. Altinkilic EM, Isbir S, Gormus U, Yilmaz SG, Dalan AB, Duman S, Isbir T. RRM1, RRM2 and ERCC2 Gene Polymorphisms in Coronary Artery Disease. In Vivo. 2016;30(5):611-615.
27. Coto E, Pascual I, Avanzas P, Cuesta-Lavona E, Lorca R, Martín M, Vázquez-Coto D, Díaz-Corte C, Morís C, Rodríguez-Reguero J, et al. IL17RA in early-onset coronary artery disease: Total leukocyte transcript analysis and promoter polymorphism (rs4819554) association. Cytokine. 2020;136:155285. doi:10.1016/j.cyto.2020.155285
28. Kim IJ, Kim SH, Cha DH, Lim SW, Moon JY, Kim JO, Ryu CS, Park HS, Sung JH, Kim NK. Association of COX2 -765G>C promoter polymorphism and coronary artery disease in Korean population. Genes Genomics. 2019;41(9):1055-1062. doi:10.1007/s13258-019-00835-5

29. Al-Allaf FA, Athar M, Abduljaleel Z, Taher MM, Khan W, Ba-Hammam FA, Abalkhail H, Alashwal A. Next generation sequencing to identify novel genetic variants causative of autosomal dominant familial hypercholesterolemia associated with increased risk of coronary heart disease. Gene. 2015;565(1):76-84. doi:10.1016/j.gene.2015.03.064
30. Andreini D, Melotti E, Vavassori C, Chiesa M, Piacentini L, Conte E, Mushtaq S, Manzoni M, Cipriani E, Ravagnani PM, et al. Whole-Blood Transcriptional Profiles Enable Early Prediction of the Presence of Coronary Atherosclerosis and High-Risk Plaque Features at Coronary CT Angiography. Biomedicines. 2022;10(6):1309. doi:10.3390/biomedicines10061309
31. Clough E, Barrett T. The Gene Expression Omnibus Database. Methods Mol Biol. 2016;1418:93-110. doi:10.1007/978-1-4939-3578-9_5
32. Love MI, Huber W, Anders S. Moderated estimation of fold change and dispersion for RNA-seq data with DESeq2. Genome Biol. 2014;15(12):550. doi:10.1186/s13059-014-0550-8
33. Solari A, Goeman JJ. Minimally adaptive BH: A tiny but uniform improvement of the procedure of Benjamini and Hochberg. Biom J. 2017;59(4):776-780. doi:10.1002/bimj.201500253
34. Thomas PD. The Gene Ontology and the Meaning of Biological Function. Methods Mol Biol. 2017;1446:15□24. doi:10.1007/978-1-4939-3743-1_2
35. Fabregat A, Jupe S, Matthews L, Sidiropoulos K, Gillespie M, Garapati P, Haw R, Jassal B, Korninger F, May B et al The Reactome Pathway Knowledgebase. Nucleic Acids Res. 2018;46(D1):D649–D655. doi:10.1093/nar/gkx1132
36. Reimand J, Kull M, Peterson H, Hansen J, Vilo J. g:Profiler--a web-based toolset for functional profiling of gene lists from large-scale experiments. Nucleic Acids Res. 2007;35(Web Server issue):W193-W200. doi:10.1093/nar/gkm226
37. Orchard S, Ammari M, Aranda B, Breuza L, Briganti L, Broackes-Carter F, Campbell NH, Chavali G, Chen C, del-Toro N, et al. The MIntAct project--IntAct as a common curation platform for 11 molecular interaction databases. Nucleic Acids Res. 2014;42(Database issue):D358-D363. doi:10.1093/nar/gkt1115

38. Shannon P, Markiel A, Ozier O, Baliga NS, Wang JT, Ramage D, Amin N, Schwikowski B, Ideker T Cytoscape: a software environment for integrated models of biomolecular interaction networks. Genome Res 2003;13(11):2498-2504. doi:10.1101/gr.1239303
39. Luo X, Guo L, Dai XJ, Wang Q, Zhu W, Miao X, Gong H. Abnormal intrinsic functional hubs in alcohol dependence: evidence from a voxelwise degree centrality analysis. Neuropsychiatr Dis Treat. 2017;13:2011-2020. doi:10.2147/NDT.S142742
40. Li Y, Li W, Tan Y, Liu F, Cao Y, Lee KY. Hierarchical Decomposition for Betweenness Centrality Measure of Complex Networks. Sci Rep. 2017;7:46491.. doi:10.1038/srep46491
41. Gilbert M, Li Z, Wu XN, Rohr L, Gombos S, Harter K, Schulze WX. Comparison of path-based centrality measures in protein-protein interaction networks revealed proteins with phenotypic relevance during adaptation to changing nitrogen environments. J Proteomics. 2021;235:104114. doi:10.1016/j.jprot.2021.104114
42. Li G, Li M, Wang J, Li Y, Pan Y. United Neighborhood Closeness Centrality and Orthology for Predicting Essential Proteins. IEEE/ACM Trans Comput Biol Bioinform. 2020;17(4):1451-1458. doi:10.1109/TCBB.2018.2889978
43. Zaki N, Efimov D, Berengueres J. Protein complex detection using interaction reliability assessment and weighted clustering coefficient. BMC Bioinformatics. 2013;14:163. doi:10.1186/1471-2105-14
44. Fan Y, Xia J (2018) miRNet-Functional Analysis and Visual Exploration of miRNA-Target Interactions in a Network Context. Methods Mol Biol 1819:215-233. doi:10.1007/978-1-4939-8618-7_10
45. Zhou G, Soufan O, Ewald J, Hancock REW, Basu N, Xia J (2019) NetworkAnalyst 3.0: a visual analytics platform for comprehensive gene expression profiling and meta-analysis. Nucleic Acids Res 47:W234-W241. doi:10.1093/nar/gkz240
46. Robin X, Turck N, Hainard A, Tiberti N, Lisacek F, Sanchez JC, Müller M. pROC: an open-source package for R and S+ to analyze and compare ROC curves. BMC Bioinformatics 2011;12:77. doi:10.1186/1471-2105-12-77
47. Chen S, Li LY, Wu ZM, Liu Y, Li FF, Huang K, Wang YX, Chen QJ, Wang XQ, Shen WF, et al. SerpinG1: A Novel Biomarker Associated With Poor

Coronary Collateral in Patients With Stable Coronary Disease and Chronic Total Occlusion. J Am Heart Assoc. 2022;11(24):e027614. doi:10.1161/JAHA.122.027614

48. Pomar CA, Bonet ML, Ferre-Beltrán A, Fraile-Ribot PA, García-Gasalla M, Riera M, Picó C, Palou A. Increased mRNA Levels of ADAM17, IFITM3, and IFNE in Peripheral Blood Cells Are Present in Patients with Obesity and May Predict Severe COVID-19 Evolution. Biomedicines. 2022;10(8):2007. doi:10.3390/biomedicines10082007
49. Mehrbod P, Eybpoosh S, Fotouhi F, Shokouhi Targhi H, Mazaheri V, Farahmand B. Association of IFITM3 rs12252 polymorphisms, BMI, diabetes, and hypercholesterolemia with mild flu in an Iranian population. Virol J. 2017;14(1):218. doi:10.1186/s12985-017-0884-4
50. Sun J, Zhang Q, Liu X, Shang X. Downregulation of interferon-induced protein with tetratricopeptide repeats 3 relieves the inflammatory response and myocardial fibrosis of mice with myocardial infarction and improves their cardiac function. Exp Anim. 2021;70(4):522-531. doi:10.1538/expanim.21-0060
51. Zhang M, Zhu Y, Zhu J, Xie Y, Wu R, Zhong J, Qiu Z, Jiang L. circ_0086296 induced atherosclerotic lesions via the IFIT1/STAT1 feedback loop by sponging miR-576-3p. Cell Mol Biol Lett. 2022;27(1):80. doi:10.1186/s11658-022-00372-2
52. Wang X, Meng X, Meng L, Guo Y, Li Y, Yang C, Pei Z, Li J, Wang F. Joint efficacy of the three biomarkers SNCA, GYPB and HBG1 for atrial fibrillation and stroke: Analysis via the support vector machine neural network. J Cell Mol Med. 2022;26(7):2010-2022. doi:10.1111/jcmm.17224
53. Gao Y, Zhao D, Xie WZ, Meng T, Xu C, Liu Y, Zhang P, Bi X, Zhao Z. Rap1GAP Mediates Angiotensin II-Induced Cardiomyocyte Hypertrophy by Inhibiting Autophagy and Increasing Oxidative Stress. Oxid Med Cell Longev. 2021;2021:7848027. doi:10.1155/2021/7848027
54. Masafi S, Saadat SH, Tehranchi K, Olya R, Heidari M, Malihialzackerini S, Jafari M, Rajabi E. Effect of Stress, Depression and Type D Personality on Immune System in the Incidence of Coronary Artery Disease. Open Access Maced J Med Sci. 2018;6(8):1533-1544. doi:10.3889/oamjms.2018.217
55. Cohain AT, Barrington WT, Jordan DM, Beckmann ND, Argmann CA, Houten SM, Charney AW, Ermel R, Sukhavasi K, Franzen O, et al. An

integrative multiomic network model links lipid metabolism to glucose regulation in coronary artery disease. Nat Commun. 2021;12(1):547. doi:10.1038/s41467-020-20750-8

56. Djekic D, Pinto R, Repsilber D, Hyotylainen T, Henein M. Serum untargeted lipidomic profiling reveals dysfunction of phospholipid metabolism in subclinical coronary artery disease. Vasc Health Risk Manag. 2019;15:123-135. doi:10.2147/VHRM.S202344
57. Boschetto P, Beghé B, Fabbri LM, Ceconi C. Link between chronic obstructive pulmonary disease and coronary artery disease: implication for clinical practice. Respirology. 2012;17(3):422-431. doi:10.1111/j.1440-1843.2011.02118.x
58. Huang L, Chambliss KL, Gao X, Yuhanna IS, Behling-Kelly E, Bergaya S, Ahmed M, Michaely P, Luby-Phelps K, Darehshouri A, et al. SR-B1 drives endothelial cell LDL transcytosis via DOCK4 to promote atherosclerosis. Nature. 2019;569(7757):565-569. doi:10.1038/s41586-019-1140-4
59. Yu J, Sun G, Chen Y, Li L, Wang H, Tu D, Li L, Meng Z, Wang Y. CEACAM1 Inhibited IκB-α/NF-κB Signal Pathway Via Targeting MMP-9/TIMP-1 Axis in Diabetic Atherosclerosis. J Cardiovasc Pharmacol. 2020;76(3):329-336. doi:10.1097/FJC.0000000000000868
60. Zhang M, Zhu Y, Zhu J, Xie Y, Wu R, Zhong J, Qiu Z, Jiang L. circ_0086296 induced atherosclerotic lesions via the IFIT1/STAT1 feedback loop by sponging miR-576-3p. Cell Mol Biol Lett. 2022;27(1):80. doi:10.1186/s11658-022-00372-2
61. Pourcet B, Pineda-Torra I. Transcriptional regulation of macrophage arginase 1 expression and its role in atherosclerosis. Trends Cardiovasc Med. 2013;23(5):143-152. doi:10.1016/j.tcm.2012.10.003
62. Tang ZH, Peng J, Ren Z, Yang J, Li TT, Li TH, Wang Z, Wei DH, Liu LS, Zheng XL, et al. New role of PCSK9 in atherosclerotic inflammation promotion involving the TLR4/NF-κB pathway. Atherosclerosis. 2017;262:113-122. doi:10.1016/j.atherosclerosis.2017.04.023
63. Oksala N, Levula M, Airla N, Pelto-Huikko M, Ortiz RM, Järvinen O, Salenius JP, Ozsait B, Komurcu-Bayrak E, Erginel-Unaltuna N, et al. ADAM-9, ADAM-15, and ADAM-17 are upregulated in macrophages in advanced human atherosclerotic plaques in aorta and carotid and femoral

arteries--Tampere vascular study. Ann Med. 2009;41(4):279-290. doi:10.1080/07853890802649738
64. Hu YW, Wu SG, Zhao JJ, Ma X, Lu JB, Xiu JC, Zhang Y, Huang C, Qiu YR, Sha YH, et al. VNN1 promotes atherosclerosis progression in apoE-/- mice fed a high-fat/high-cholesterol diet. J Lipid Res. 2016;57(8):1398-1411. doi:10.1194/jlr.M065565
65. Brunham LR, Singaraja RR, Duong M, Timmins JM, Fievet C, Bissada N, Kang MH, Samra A, Fruchart JC, McManus B, et al. Tissue-specific roles of ABCA1 influence susceptibility to atherosclerosis. Arterioscler Thromb Vasc Biol. 2009;29(4):548-554. doi:10.1161/ATVBAHA.108.182303
66. Lagor WR, Fields DW, Bauer RC, Crawford A, Abt MC, Artis D, Wherry EJ, Rader DJ. Genetic manipulation of the ApoF/Stat2 locus supports an important role for type I interferon signaling in atherosclerosis. Atherosclerosis. 2014;233(1):234-241. doi:10.1016/j.atherosclerosis.2013.12.043
67. Kim J, Yoo JY, Suh JM, Park S, Kang D, Jo H, Bae YS. The flagellin-TLR5-Nox4 axis promotes the migration of smooth muscle cells in atherosclerosis. Exp Mol Med. 2019;51(7):1-13. doi:10.1038/s12276-019-0275-6
68. Zhou Y, Zhou H, Hua L, Hou C, Jia Q, Chen J, Zhang S, Wang Y, He S, Jia E. Verification of ferroptosis and pyroptosis and identification of PTGS2 as the hub gene in human coronary artery atherosclerosis. Free Radic Biol Med. 2021;171:55-68. doi:10.1016/j.freeradbiomed.2021.05.009
69. Kim HJ, Choi EH, Chung JW, Kim JH, Kim YS, Seo WK, Kim GM, Bang OY. Role of the RNF213 Variant in Vascular Outcomes in Patients With Intracranial Atherosclerosis. J Am Heart Assoc. 2021;10(1):e017660. doi:10.1161/JAHA.120.017660
70. Zhang X, Sun R, Liu L. Potentially critical roles of TNPO1, RAP1B, ZDHHC17, and PPM1B in the progression of coronary atherosclerosis through microarray data analysis. J Cell Biochem. 2019;120(3):4301-4311. doi:10.1002/jcb.27715
71. Liu W, Östberg N, Yalcinkaya M, Dou H, Endo-Umeda K, Tang Y, Hou X, Xiao T, Fidler TP, Abramowicz S, et al. Erythroid lineage Jak2V617F expression promotes atherosclerosis through erythrophagocytosis and

macrophage ferroptosis. J Clin Invest. 2022;132(13):e155724. doi:10.1172/JCI155724
72. Allen RM, Michell DL, Cavnar AB, Zhu W, Makhijani N, Contreras DM, Raby CA, Semler EM, DeJulius C, Castleberry M, et al. LDL delivery of microbial small RNAs drives atherosclerosis through macrophage TLR8. Nat Cell Biol. 2022;24(12):1701-1713. doi:10.1038/s41556-022-01030-7
73. Davis-Knowlton J, Turner JE, Harrington A, Liaw L. Smooth Muscle Cell Notch2 Is Not Required for Atherosclerotic Plaque Formation in ApoE Null Mice. J Vasc Res. 2022;59(5):261-274. doi:10.1159/000525258
74. Karvinen H, Rutanen J, Leppänen O, Lach R, Levonen AL, Eriksson U, Ylä-Herttuala S. PDGF-C and -D and their receptors PDGFR-alpha and PDGFR-beta in atherosclerotic human arteries. Eur J Clin Invest. 2009;39(4):320-327. doi:10.1111/j.1365-2362.2009.02095.x
75. Lai JH, Hung LF, Huang CY, Wu DW, Wu CH, Ho LJ. Mitochondrial protein CMPK2 regulates IFN alpha-enhanced foam cell formation, potentially contributing to premature atherosclerosis in SLE. Arthritis Res Ther. 2021;23(1):120. doi:10.1186/s13075-021-02470-6
76. Miao G, Zhao X, Wang B, Zhang L, Wang G, Zheng N, Liu J, Xu Z, Zhang L. TLR2/CXCR4 coassociation facilitates Chlamydia pneumoniae infection-induced atherosclerosis. Am J Physiol Heart Circ Physiol. 2020;318(6):H1420-H1435. doi:10.1152/ajpheart.00011.2020
77. De Caterina R, Madonna R. Cytochromes CYP1A1 and CYP1B1: new pieces in the puzzle to understand the biomechanical paradigm of atherosclerosis. Cardiovasc Res. 2009;81(4):629-632. doi:10.1093/cvr/cvp013
78. Yan S, Meng L, Guo X, Chen Z, Zhang Y, Li Y. Identification of ITGAX and CCR1 as potential biomarkers of atherosclerosis via Gene Set Enrichment Analysis. J Int Med Res. 2022;50(3):3000605211039480. doi:10.1177/03000605211039480
79. Das S, Natarajan R. HDAC9: An Inflammatory Link in Atherosclerosis. Circ Res. 2020;127(6):824-826. doi:10.1161/CIRCRESAHA.120.317723
80. Dewberry R, Holden H, Crossman D, Francis S. Interleukin-1 receptor antagonist expression in human endothelial cells and atherosclerosis. Arterioscler Thromb Vasc Biol. 2000;20(11):2394-2400. doi:10.1161/01.atv.20.11.2394

81. Douglas G, Hale AB, Patel J, Chuaiphichai S, Al Haj Zen A, Rashbrook VS, Trelfa L, Crabtree MJ, McNeill E, Channon KM. Roles for endothelial cell and macrophage Gch1 and tetrahydrobiopterin in atherosclerosis progression. Cardiovasc Res. 2018;114(10):1385-1399. doi:10.1093/cvr/cvy078
82. Schiller NK, Boisvert WA, Curtiss LK. Inflammation in atherosclerosis: lesion formation in LDL receptor-deficient mice with perforin and Lyst(beige) mutations. Arterioscler Thromb Vasc Biol. 2002;22(8):1341-1346. doi:10.1161/01.atv.0000024082.46387.38
83. Burger F, Baptista D, Roth A, Brandt KJ, Miteva K. The E3 Ubiquitin Ligase Peli1 Deficiency Promotes Atherosclerosis Progression. Cells. 2022;11(13):2014. doi:10.3390/cells11132014
84. Blaschke F, Bruemmer D, Law RE. Egr-1 is a major vascular pathogenic transcription factor in atherosclerosis and restenosis. Rev Endocr Metab Disord. 2004;5(3):249-254. doi:10.1023/B:REMD.0000032413.88756.ee
85. You Y, Bao WL, Zhang SL, Li HD, Li H, Dang WZ, Zou SL, Cao XY, Wang X, Liu LX, et al. Sorting Nexin 10 Mediates Metabolic Reprogramming of Macrophages in Atherosclerosis Through the Lyn-Dependent TFEB Signaling Pathway. Circ Res. 2020;127(4):534-549. doi:10.1161/CIRCRESAHA.119.315516
86. Oksala N, Levula M, Pelto-Huikko M, Kytömäki L, Soini JT, Salenius J, Kähönen M, Karhunen PJ, Laaksonen R, Parkkila S, et al. Carbonic anhydrases II and XII are up-regulated in osteoclast-like cells in advanced human atherosclerotic plaques-Tampere Vascular Study. Ann Med. 2010;42(5):360-370. doi:10.3109/07853890.2010.486408
87. Cheng P, Wirka RC, Shoa Clarke L, Zhao Q, Kundu R, Nguyen T, Nair S, Sharma D, Kim HJ, Shi H, et al. ZEB2 Shapes the Epigenetic Landscape of Atherosclerosis. Circulation. 2022;145(6):469-485. doi:10.1161/CIRCULATIONAHA.121.057789
88. Li P, Xing J, Zhang J, Jiang J, Liu X, Zhao D, Zhang Y. Inhibition of long noncoding RNA HIF1A-AS2 confers protection against atherosclerosis via ATF2 downregulation. J Adv Res. 2020;26:123-135. doi:10.1016/j.jare.2020.07.015
89. Santoso A, Maulana R, Alzahra F, Maghfirah I, Putrinarita AD, Heriansyah T. Associations between four types of single-nucleotide polymorphisms in

PLA2G7 gene and clinical atherosclerosis: a meta-analysis. Am J Cardiovasc Dis. 2017;7(6):122-133.
90. Hüsing AM, Wulfmeyer VC, Gaedcke S, Fleig SV, Rong S, DeLuca D, Haller H, Schmitt R, von Vietinghoff S. Myeloid CCR2 Promotes Atherosclerosis after AKI. J Am Soc Nephrol. 2022;33(8):1487-1500. doi:10.1681/ASN.2022010048
91. Qian X, Wang H, Wang Y, Chen J, Guo X, Deng H. Enhanced Autophagy in GAB1-Deficient Vascular Endothelial Cells Is Responsible for Atherosclerosis Progression. Front Physiol. 2021;11:559396. doi:10.3389/fphys.2020.559396
92. Hulsmans M, Geeraert B, Arnould T, Tsatsanis C, Holvoet P. PPAR agonist-induced reduction of Mcp1 in atherosclerotic plaques of obese, insulin-resistant mice depends on adiponectin-induced Irak3 expression. PLoS One. 2013;8(4):e62253. doi:10.1371/journal.pone.0062253
93. Burke AC, Telford DE, Sutherland BG, Edwards JY, Sawyez CG, Barrett PHR, Newton RS, Pickering JG, Huff MW. Bempedoic Acid Lowers Low-Density Lipoprotein Cholesterol and Attenuates Atherosclerosis in Low-Density Lipoprotein Receptor-Deficient (LDLR+/- and LDLR-/-) Yucatan Miniature Pigs. Arterioscler Thromb Vasc Biol. 2018;38(5):1178-1190. doi:10.1161/ATVBAHA.117.310676
94. Curtiss LK, Black AS, Bonnet DJ, Tobias PS. Atherosclerosis induced by endogenous and exogenous toll-like receptor (TLR)1 or TLR6 agonists. J Lipid Res. 2012;53(10):2126-2132. doi:10.1194/jlr.M028431
95. Yang X, Wei J, He Y, Jing T, Li Y, Xiao Y, Wang B, Wang W, Zhang J, Lin R. SIRT1 inhibition promotes atherosclerosis through impaired autophagy. Oncotarget. 2017;8(31):51447-51461. doi:10.18632/oncotarget.17691
96. Vlacil AK, Schuett J, Ruppert V, Soufi M, Oberoi R, Shahin K, Wächter C, Tschernig T, Lei Y, Liu F, et al. Deficiency of Nucleotide-binding oligomerization domain-containing proteins (NOD) 1 and 2 reduces atherosclerosis. Basic Res Cardiol. 2020;115(4):47. doi:10.1007/s00395-020-0806-2
97. Kengia JT, Ko KC, Ikeda S, Hiraishi A, Mieno-Naka M, Arai T, Sato N, Muramatsu M, Sawabe M. A gene variant in the Atp10d gene associates with atherosclerotic indices in Japanese elderly population. Atherosclerosis. 2013;231(1):158-162. doi:10.1016/j.atherosclerosis.2013.08.034

98. Saito R, Matsuzaka T, Karasawa T, Sekiya M, Okada N, Igarashi M, Matsumori R, Ishii K, Nakagawa Y, Iwasaki H, et al. Macrophage Elovl6 deficiency ameliorates foam cell formation and reduces atherosclerosis in low-density lipoprotein receptor-deficient mice. Arterioscler Thromb Vasc Biol. 2011;31(9):1973-1979. doi:10.1161/ATVBAHA.110.221663
99. Barascuk N, Genovese F, Larsen L, Byrjalsen I, Zheng Q, Sun S, Hosbond S, Poulsen TS, Diederichsen A, Jensen JM, et al. A MMP derived versican neo-epitope is elevated in plasma from patients with atherosclerotic heart disease. Int J Clin Exp Med. 2013;6(3):174-184.
100. Cobo I, Tanaka T, Glass CK, Yeang C. Clonal hematopoiesis driven by DNMT3A and TET2 mutations: role in monocyte and macrophage biology and atherosclerotic cardiovascular disease. Curr Opin Hematol. 2022;29(1):1-7. doi:10.1097/MOH.0000000000000688
101. Zhang P, Chen X, Zhang Y, Su H, Zhang Y, Zhou X, Sun M, Li L, Xu Z. Tet3 enhances IL-6 expression through up-regulation of 5-hmC in IL-6 promoter in chronic hypoxia induced atherosclerosis in offspring rats. Life Sci. 2019;232:116601. doi:10.1016/j.lfs.2019.116601
102. Tao J, Qiu J, Lu L, Zhang L, Fu Y, Wang M, Han J, Shi M, Li L, Zhao Z, et al. ZBTB20 Positively Regulates Oxidative Stress, Mitochondrial Fission, and Inflammatory Responses of ox-LDL-Induced Macrophages in Atherosclerosis. Oxid Med Cell Longev. 2021;2021:5590855. doi:10.1155/2021/5590855
103. Smits NC, Kobayashi T, Srivastava PK, Skopelja S, Ivy JA, Elwood DJ, Stan RV, Tsongalis GJ, Sellke FW, Gross PL, et al. HS3ST1 genotype regulates antithrombin's inflammomodulatory tone and associates with atherosclerosis. Matrix Biol. 2017;63:69-90. doi:10.1016/j.matbio.2017.01.003
104. Sachais BS, Turrentine T, Dawicki McKenna JM, Rux AH, Rader D, Kowalska MA. Elimination of platelet factor 4 (PF4) from platelets reduces atherosclerosis in C57Bl/6 and apoE-/- mice. Thromb Haemost. 2007;98(5):1108-1113.
105. Yoshida Y, Zhang XM, Wang H, Machida T, Mine S, Kobayashi E, Adachi A, Matsutani T, Kamitsukasa I, Wada T, et al. Elevated levels of autoantibodies against DNAJC2 in sera of patients with atherosclerotic diseases. Heliyon. 2020;6(8):e04661. doi:10.1016/j.heliyon.2020.e04661

106. Holdt LM, Teupser D. Long noncoding RNA-MicroRNA pathway controlling nuclear factor IA, a novel atherosclerosis modifier gene. Arterioscler Thromb Vasc Biol. 2015;35(1):7-8. doi:10.1161/ATVBAHA.114.304485
107. Halvorsen B, Dahl TB, Smedbakken LM, Singh A, Michelsen AE, Skjelland M, Krohg-Sørensen K, Russell D, Höpken UE, Lipp M, et al. Increased levels of CCR7 ligands in carotid atherosclerosis: different effects in macrophages and smooth muscle cells. Cardiovasc Res. 2014;102(1):148-156. doi:10.1093/cvr/cvu036
108. Li J, Wang C, Wang W, Liu L, Zhang Q, Zhang J, Wang B, Wang S, Hou L, Gao C, et al. PRDX2 Protects Against Atherosclerosis by Regulating the Phenotype and Function of the Vascular Smooth Muscle Cell. Front Cardiovasc Med. 2021;8:624796. doi:10.3389/fcvm.2021.624796
109. Zhang M, Zeng X, Yang Q, Xu J, Liu Z, Zhou Y, Cao Y, Zhang X, An X, Xu Y, et al. Ablation of Myeloid ADK (Adenosine Kinase) Epigenetically Suppresses Atherosclerosis in ApoE-/- (Apolipoprotein E Deficient) Mice. Arterioscler Thromb Vasc Biol. 2018;38(12):2780-2792. doi:10.1161/ATVBAHA.118.311806
110. Ma Z, Wang C, Bai X, Wang L, Wu Q, Cai Z, Wang W, Ma Z, Liu X, Feng J, et al. TCF7 is highly expressed in immune cells on the atherosclerotic plaques, and regulating inflammatory signaling via NFκB/AKT/STAT1 signaling. Biosci Rep. 2022;42(7):BSR20212064. doi:10.1042/BSR20212064
111. Lu S, Weiser-Evans MCM. Lgals3-Transitioned Inflammatory Smooth Muscle Cells: Major Regulators of Atherosclerosis Progression and Inflammatory Cell Recruitment. Arterioscler Thromb Vasc Biol. 2022;42(8):957-959. doi:10.1161/ATVBAHA.122.318009
112. Li H, Gui H, Yuan G, Zheng X, Gao C, Yuan H. Increased plasma olfactomedin 2 after interventional therapy is a predictor for restenosis in lower extremity arteriosclerosis obliterans patients. Scand J Clin Lab Invest. 2018;78(4):269-274. doi:10.1080/00365513.2018.1452287
113. Li L, Xie W. LncRNA HDAC11-AS1 Suppresses Atherosclerosis by Inhibiting HDAC11-Mediated Adropin Histone Deacetylation. J Cardiovasc Transl Res. 2022;15(6):1256-1269. doi:10.1007/s12265-022-10248-7

114. Li J, Chen Y, Gao J, Chen Y, Zhou C, Lin X, Liu C, Zhao M, Xu Y, Ji L, et al. Eva1a ameliorates atherosclerosis by promoting re-endothelialization of injured arteries via Rac1/Cdc42/Arpc1b. Cardiovasc Res. 2021;117(2):450-461. doi:10.1093/cvr/cvaa011
115. Eckhardt LL, Farley AL, Rodriguez E, Ruwaldt K, Hammill D, Tester DJ, Ackerman MJ, Makielski JC. KCNJ2 mutations in arrhythmia patients referred for LQT testing: a mutation T305A with novel effect on rectification properties. Heart Rhythm. 2007;4(3):323-329. doi:10.1016/j.hrthm.2006.10.025
116. Yang F, Jiang X, Cao H, Shuai W, Zhang L, Wang G, Quan D, Jiang X. Daphnetin Preconditioning Decreases Cardiac Injury and Susceptibility to Ventricular Arrhythmia following Ischaemia-Reperfusion through the TLR4/MyD88/NF-Kb Signalling Pathway. Pharmacology. 2021;106(7-8):369-383. doi:10.1159/000513631
117. Wang W, Ye S, Zhang L, Jiang Q, Chen J, Chen X, Zhang F, Wu H. Granulocyte colony-stimulating factor attenuates myocardial remodeling and ventricular arrhythmia susceptibility via the JAK2-STAT3 pathway in a rabbit model of coronary microembolization. BMC Cardiovasc Disord. 2020;20(1):85. doi:10.1186/s12872-020-01385-5
118. Mersmann J, Koch A, Tran N, Zimmermann R, Granja TF, Larmann J, Herzog C, Theilmeier G, Bornstein SR, Kirschning CJ, et al. Toll-like receptor 2 signaling triggers fatal arrhythmias upon myocardial ischemia-reperfusion. Crit Care Med. 2010;38(10):1927-1932. doi:10.1097/CCM.0b013e3181ef455b
119. Li J, Xu C, Liu Y, Li Y, Du S, Zhang R, Sun Y, Zhang R, Wang Y, Xue H, et al. Fibroblast growth factor 21 inhibited ischemic arrhythmias via targeting miR-143/EGR1 axis. Basic Res Cardiol. 2020;115(2):9. doi:10.1007/s00395-019-0768-4
120. Liu M, Zhao J, Lu Y, Chen Z, Feng X, Pan G. Gab1 Overexpression Attenuates Susceptibility to Ventricular Arrhythmias in Pressure Overloaded Heart Failure Mouse Hearts Cardiovasc Drugs Ther. 2022;10.1007/s10557-022-07394-0. doi:10.1007/s10557-022-07394-0
121. Boogerd CJ, Lacraz GPA, Vértesy Á, van Kampen SJ, Perini I, de Ruiter H, Versteeg D, Brodehl A, van der Kraak P, Giacca M, et al. Spatial transcriptomics unveils ZBTB11 as a regulator of cardiomyocyte

degeneration in arrhythmogenic cardiomyopathy. Cardiovasc Res. 2022;cvac072. doi:10.1093/cvr/cvac072

122. Hong T, Yang H, Zhang SS, Cho HC, Kalashnikova M, Sun B, Zhang H, Bhargava A, Grabe M, Olgin J, et al. Cardiac BIN1 folds T-tubule membrane, controlling ion flux and limiting arrhythmia. Nat Med. 2014;20(6):624-632. doi:10.1038/nm.3543

123. Huo R, Hu C, Zhao L, Sun L, Wang N, Lu Y, Ye B, Deb A, Li F, Xu H. Enhancement of β-catenin/T-cell factor 4 signaling causes susceptibility to cardiac arrhythmia by suppressing NaV1.5 expression in mice. Heart Rhythm. 2019;16(11):1720-1728. doi:10.1016/j.hrthm.2019.05.015

124. Kalayinia S, Mahdavi M, Houshmand G, Hesami M, Pourirahim M, Maleki M. Novel homozygous stop-gain pathogenic variant of PPP1R13L gene leads to arrhythmogenic cardiomyopathy. BMC Cardiovasc Disord. 2022;22(1):359. doi:10.1186/s12872-022-02802-7

125. Amarouch MY, El Hilaly J. Inherited Cardiac Arrhythmia Syndromes: Focus on Molecular Mechanisms Underlying TRPM4 Channelopathies. Cardiovasc Ther. 2020;2020:6615038. doi:10.1155/2020/6615038

126. Cason M, Celeghin R, Marinas MB, Beffagna G, Della Barbera M, Rizzo S, Remme CA, Bezzina CR, Tiso N, Bauce B, et al. Novel pathogenic role for galectin-3 in early disease stages of arrhythmogenic cardiomyopathy. Heart Rhythm. 2021;18(8):1394-1403. doi:10.1016/j.hrthm.2021.04.006

127. Jimenez-Vazquez EN, Arad M, Macías Á, Vera-Pedrosa ML, Cruz FM, Gutierrez LK, Cuttita AJ, Monteiro da Rocha A, Herron TJ, Ponce-Balbuena D, et al. SNTA1 gene rescues ion channel function and is antiarrhythmic in cardiomyocytes derived from induced pluripotent stem cells from muscular dystrophy patients. Elife. 2022;11:e76576. doi:10.7554/eLife.76576

128. Du J, Li Z, Wang X, Li J, Liu D, Wang X, Wei J, Ma S, Zhang Y, Hou Y. Long noncoding RNA TCONS-00106987 promotes atrial electrical remodelling during atrial fibrillation by sponging miR-26 to regulate KCNJ2. J Cell Mol Med. 2020;24(21):12777-12788. doi:10.1111/jcmm.15869

129. Zhang P, Shao L, Ma J. Toll-Like Receptors 2 and 4 Predict New-Onset Atrial Fibrillation in Acute Myocardial Infarction Patients. Int Heart J. 2018;59(1):64-70. doi:10.1536/ihj.17-084
130. Chow MS, White CM, Lau CP, Fan C, Tang MO. Evaluation of CYP2D6 oxidation of dextromethorphan and propafenone in a Chinese population with atrial fibrillation. J Clin Pharmacol. 2001;41(1):92-96. doi:10.1177/00912700122009737
131. Yao J, Hou J, Lv L, Song C, Zhang M, Wu Z. Does Decreased SNX10 Serve as a Novel Risk Factor in Atrial Fibrillation of the Valvular Heart Disease? - A Case-Control Study. Braz J Cardiovasc Surg. 2021;36(1):71-77. doi:10.21470/1678-9741-2019-0413
132. Yamac AH, Kucukbuzcu S, Ozansoy M, Gok O, Oz K, Erturk M, Yilmaz E, Ersoy B, Zeybek R, Goktekin O, et al. Altered expression of micro-RNA 199a and increased levels of cardiac SIRT1 protein are associated with the occurrence of atrial fibrillation after coronary artery bypass graft surgery. Cardiovasc Pathol. 2016;25(3):232-236. doi:10.1016/j.carpath.2016.02.002
133. Yamauchi K, Furui H, Taniguchi N, Sotobata I. Plasma beta-thromboglobulin and platelet factor 4 concentrations in patients with atrial fibrillation. Jpn Heart J. 1986;27(4):481-487. doi:10.1536/ihj.27.481
134. Basu P, Alibhai FJ, Tsimakouridze EV, Singh RK, Paglialunga S, Holloway GP, Martino TA, Bakovic M. Male-Specific Cardiac Dysfunction in CTP:Phosphoethanolamine Cytidylyltransferase (Pcyt2)-Deficient Mice. Mol Cell Biol. 2015;35(15):2641-2657. doi:10.1128/MCB.00380-15
135. Clementy N, Piver E, Bisson A, Andre C, Bernard A, Pierre B, Fauchier L, Babuty D. Galectin-3 in Atrial Fibrillation: Mechanisms and Therapeutic Implications. Int J Mol Sci. 2018;19(4):976. doi:10.3390/ijms19040976
136. Ortega A, Tarazón E, Roselló-Lletí E, Gil-Cayuela C, Lago F, González-Juanatey JR, Cinca J, Jorge E, Martínez-Dolz L, Portolés M, et al. Patients with Dilated Cardiomyopathy and Sustained Monomorphic Ventricular Tachycardia Show Up-Regulation of KCNN3 and KCNJ2 Genes and CACNG8-Linked Left Ventricular Dysfunction. PLoS One. 2015;10(12):e0145518. doi:10.1371/journal.pone.0145518

137. Li C, Wang L, Li Y, Feng Z, Wang Q, Luo W. Common Variants in the ARG1 Gene Contribute to the Risk of Dilated Cardiomyopathy in the Han Chinese Population. Genet Test Mol Biomarkers. 2020;24(9):584-591. doi:10.1089/gtmb.2020.0080
138. Wu B, Li J, Ni H, Zhuang X, Qi Z, Chen Q, Wen Z, Shi H, Luo X, Jin B. TLR4 Activation Promotes the Progression of Experimental Autoimmune Myocarditis to Dilated Cardiomyopathy by Inducing Mitochondrial Dynamic Imbalance. Oxid Med Cell Longev. 2018;2018:3181278. doi:10.1155/2018/3181278
139. Dou Q, Peng Y, Zhou B, Lin J, Li Y, Yang H, Xie Q, Li C, Zhang L, Rao L. Association of innate immune IFIH1 gene polymorphisms with dilated cardiomyopathy in a Chinese population. Immunol Invest. 2014;43(7):627-637. doi:10.3109/08820139.2014.909455
140. Yagi H, Hatano M, Takeda N, Harada S, Suzuki Y, Taniguchi Y, Shintani Y, Morita H, Kanamori N, Aoyama T, et al. Congenital Contractural Arachnodactyly without FBN1 or FBN2 Gene Mutations Complicated by Dilated Cardiomyopathy. Intern Med. 2015;54(10):1237-1241. doi:10.2169/internalmedicine.54.4280
141. Meurs KM, Stern JA, Adin D, Keene BW, De Francesco TC, Tou SP. Assessment of PDK4 and TTN gene variants in 48 Doberman Pinschers with dilated cardiomyopathy. J Am Vet Med Assoc. 2020;257(10):1041-1044. doi:10.2460/javma.2020.257.10.1041
142. Satoh M, Akatsu T, Ishikawa Y, Minami Y, Takahashi Y, Nakamura M. Association between toll-like receptor 8 expression and adverse clinical outcomes in patients with enterovirus-associated dilated cardiomyopathy. Am Heart J. 2007;154(3):581-588. doi:10.1016/j.ahj.2007.05.010
143. Pontén A, Li X, Thorén P, Aase K, Sjöblom T, Ostman A, Eriksson U. Transgenic overexpression of platelet-derived growth factor-C in the mouse heart induces cardiac fibrosis, hypertrophy, and dilated cardiomyopathy. Am J Pathol. 2003;163(2):673-682. doi:10.1016/S0002-9440(10)63694-2
144. Siggs OM, Stockenhuber A, Deobagkar-Lele M, Bull KR, Crockford TL, Kingston BL, Crawford G, Anzilotti C, Steeples V, Ghaffari S, et al. Mutation of Fnip1 is associated with B-cell deficiency, cardiomyopathy, and

elevated AMPK activity. Proc Natl Acad Sci U S A. 2016;113(26):E3706-E3715. doi:10.1073/pnas.1607592113

145. Ye S, Su L, Shan P, Ye B, Wu S, Liang G, Huang W. LCZ696 Attenuated Doxorubicin-Induced Chronic Cardiomyopathy Through the TLR2-MyD88 Complex Formation. Front Cell Dev Biol. 2021;9:654051. doi:10.3389/fcell.2021.654051

146. Schramm C, Fine DM, Edwards MA, Reeb AN, Krenz M. The PTPN11 loss-of-function mutation Q510E-Shp2 causes hypertrophic cardiomyopathy by dysregulating mTOR signaling. Am J Physiol Heart Circ Physiol. 2012;302(1):H231-H243. doi:10.1152/ajpheart.00665.2011

147. Tan Y, Ouyang H, Xiao X, Zhong J, Dong M. Irisin ameliorates septic cardiomyopathy via inhibiting DRP1-related mitochondrial fission and normalizing the JNK-LATS2 signaling pathway. Cell Stress Chaperones. 2019;24(3):595-608. doi:10.1007/s12192-019-00992-2

148. Wu HE, Baumgardt SL, Fang J, Paterson M, Liu Y, Du J, Shi Y, Qiao S, Bosnjak ZJ, Warltier DC, et al. Cardiomyocyte GTP Cyclohydrolase 1 Protects the Heart Against Diabetic Cardiomyopathy. Sci Rep. 2016;6:27925. doi:10.1038/srep27925

149. Yilmaz S, Gokben S, Serdaroglu G, Eraslan C, Mancini GM, Tekin H, Tekgul H. The expanding phenotypic spectrum of ARFGEF2 gene mutation: Cardiomyopathy and movement disorder. Brain Dev. 2016;38(1):124-127. doi:10.1016/j.braindev.2015.06.004

150. Su H, Hu K, Liu Z, Chen K, Xu J. Carbonic anhydrase 2 and 3 as risk biomarkers for dilated cardiomyopathy associated heart failure. Ann Palliat Med. 2021;10(12):12554-12565. doi:10.21037/apm-21-3561

151. Thude H, Gerlach K, Richartz B, Krack A, Brenke B, Pethig K, Figulla HR, Barz D. No association between transmembrane protein-tyrosine phosphatase receptor type C (CD45) exon A point mutation (77C>G) and idiopathic dilated cardiomyopathy. Hum Immunol. 2005;66(9):1008-1012. doi:10.1016/j.humimm.2005.07.004

152. Machuca MA, Suárez EU, Echeverría LE, Martín J, González CI. SNP/haplotype associations of CCR2 and CCR5 genes with severity of chagasic cardiomyopathy. Hum Immunol. 2014;75(12):1210-1215. doi:10.1016/j.humimm.2014.09.023

153. Zhao J, Yin M, Deng H, Jin FQ, Xu S, Lu Y, Mastrangelo MA, Luo H, Jin ZG. Cardiac Gab1 deletion leads to dilated cardiomyopathy associated with mitochondrial damage and cardiomyocyte apoptosis. Cell Death Differ. 2016;23(4):695-706. doi:10.1038/cdd.2015.143
154. Zhou YL, Li XL, Zhang HF, Yao WM, Tong M, Xu Q, Cao KJ, Huang J. Decreased small arterial compliance with increased serum vascular endothelial growth factor-A and circulating endothelial progenitor cell in dilated cardiomyopathy. Chin Med J (Engl). 2008;121(4):316-320.
155. Elting M, Kariminejad A, de Sonnaville ML, Ottenkamp J, Bauhuber S, Bozorgmehr B, Zenker M, Cobben JM. Johanson-Blizzard syndrome caused by identical UBR1 mutations in two unrelated girls, one with a cardiomyopathy. Am J Med Genet A. 2008;146A(23):3058-3061. doi:10.1002/ajmg.a.32566
156. Zhang M, Wang X, Liu M, Liu D, Pan J, Tian J, Jin T, Xu Y, An F. Inhibition of PHLPP1 ameliorates cardiac dysfunction via activation of the PI3K/Akt/mTOR signalling pathway in diabetic cardiomyopathy. J Cell Mol Med. 2020;24(8):4612-4623. doi:10.1111/jcmm.15123
157. García-García J, Fernández-García MA, Blanco-Arias P, Díaz-Maroto-Cicuendez MI, Salmerón-Martínez F, Hidalgo-Olivares VM, Olivé M. Non-compaction cardiomyopathy and early respiratory failure in an adult symptomatic female carrier of centronuclear myopathy caused by a MTM1 mutation. Neuromuscul Disord. 2018;28(11):952-955. doi:10.1016/j.nmd.2018.08.003
158. Kleinfeldt T, Schneider H, Akin I, Kische S, Gökmen Turan R, Nienaber CA, Ince H. Detection of FMR1-gene in Takotsubo cardiomyopathy: a new piece in the puzzle. Int J Cardiol. 2009;137(3):e81-e83. doi:10.1016/j.ijcard.2009.06.016
159. Chen Q, Zeng Y, Yang X, Wu Y, Zhang S, Huang S, Zhong Y, Chen M. Resveratrol ameliorates myocardial fibrosis by regulating Sirt1/Smad3 deacetylation pathway in rat model with dilated cardiomyopathy. BMC Cardiovasc Disord. 2022;22(1):17. doi:10.1186/s12872-021-02401-y
160. Shen L, Li L, Li M, Wang W, Yin W, Liu W, Hu Y. Silencing of NOD2 protects against diabetic cardiomyopathy in a murine diabetes model. Int J Mol Med. 2018;42(6):3017-3026. doi:10.3892/ijmm.2018.3880

161. Kiselev A, Vaz R, Knyazeva A, Sergushichev A, Dmitrieva R, Khudiakov A, Jorholt J, Smolina N, Sukhareva K, Fomicheva Y, et al. Truncating Variant in Myof Gene Is Associated With Limb-Girdle Type Muscular Dystrophy and Cardiomyopathy. Front Genet. 2019;10:608. doi:10.3389/fgene.2019.00608
162. Bouchard L, Faucher G, Tchernof A, Deshaies Y, Marceau S, Lescelleur O, Biron S, Bouchard C, Pérusse L, Vohl MC. Association of OSBPL11 gene polymorphisms with cardiovascular disease risk factors in obesity. Obesity (Silver Spring). 2009;17(7):1466-1472. doi:10.1038/oby.2009.71
163. Chun JL, O'Brien R, Berry SE. Cardiac dysfunction and pathology in the dystrophin and utrophin-deficient mouse during development of dilated cardiomyopathy. Neuromuscul Disord. 2012;22(4):368-379. doi:10.1016/j.nmd.2011.07.003
164. Fan J, Li H, Xie R, Zhang X, Nie X, Shi X, Zhan J, Yin Z, Zhao Y, Dai B, et al. LncRNA ZNF593-AS Alleviates Contractile Dysfunction in Dilated Cardiomyopathy. Circ Res. 2021;128(11):1708-1723. doi:10.1161/CIRCRESAHA.120.318437
165. Jin Q, Gong Q, Le X, He J, Zhuang L. Bioinformatics and Experimental Analyses Reveal Immune-Related LncRNA-mRNA Pair AC011483.1-CCR7 as a Biomarker and Therapeutic Target for Ischemic Cardiomyopathy. Int J Mol Sci. 2022;23(19):11994. doi:10.3390/ijms231911994
166. Kuzuya K, Ichihara S, Suzuki Y, Inoue C, Ichihara G, Kurimoto S, Oikawa S. Proteomics analysis identified peroxiredoxin 2 involved in early-phase left ventricular impairment in hamsters with cardiomyopathy. PLoS One. 2018;13(2):e0192624. doi:10.1371/journal.pone.0192624
167. Díaz-Vesga MC, Flores-Vergara R, Riquelme JA, Llancaqueo M, Sánchez G, Vergara C, Michea L, Donoso P, Quest AFG, Olmedo I, et al. Polycystin-1 Is a Crucial Regulator of BIN1 Expression and T-Tubule Remodeling Associated with the Development of Dilated Cardiomyopathy. Int J Mol Sci. 2022;24(1):667. doi:10.3390/ijms24010667
168. Ye Y, Jin Q, Gong Q, Li A, Sun M, Jiang S, Jin Y, Zhang Z, He J, Zhuang L. Bioinformatics and Experimental Analyses Reveal NFIC as an

Upstream Transcriptional Regulator for Ischemic Cardiomyopathy. Genes (Basel). 2022;13(6):1051. doi:10.3390/genes13061051

169. Wei H, Qu H, Wang H, Ji B, Ding Y, Liu D, Duan Y, Liang H, Peng C, Xiao X, et al. 1,25-Dihydroxyvitamin-D3 prevents the development of diabetic cardiomyopathy in type 1 diabetic rats by enhancing autophagy via inhibiting the β-catenin/TCF4/GSK-3β/mTOR pathway. J Steroid Biochem Mol Biol. 2017;168:71-90. doi:10.1016/j.jsbmb.2017.02.007

170. Amate-García G, Ballesta-Martínez MJ, Serrano-Lorenzo P, Garrido-Moraga R, González-Quintana A, Blázquez A, Rubio JC, García-Consuegra I, Arenas J, Ugalde C, et al. A Novel Mutation Associated with Neonatal Lethal Cardiomyopathy Leads to an Alternative Transcript Expression in the X-Linked Complex I NDUFB11 Gene. Int J Mol Sci. 2023;24(2):1743. doi:10.3390/ijms24021743

171. Reinstein E, Orvin K, Tayeb-Fligelman E, Stiebel-Kalish H, Tzur S, Pimienta AL, Bazak L, Bengal T, Cohen L, Gaton DD, et al. Mutations in TAX1BP3 cause dilated cardiomyopathy with septo-optic dysplasia. Hum Mutat. 2015;36(4):439-442. doi:10.1002/humu.22759

172. Kovacs B, Winnik S, Medeiros-Domingo A, Costa S, Fu G, Biskup S, Ruschitzka F, Flammer AJ, Tanner FC, Duru F, et al. The novel TRPM4 c.448G>T variant is associated with familial conduction disorders, cardiomyopathy, and sudden cardiac death. Cardiol J. 2022;29(3):514-516. doi:10.5603/CJ.a2021.0157

173. Gao Z, Ti Y, Lu B, Song FQ, Zhang L, Hu BA, Xie JY, Zhang W, Han L, Zhong M. STAMP2 Attenuates Cardiac Dysfunction and Insulin Resistance in Diabetic Cardiomyopathy via NMRAL1-Mediated NF-κB Inhibition in Type 2 Diabetic Rats. Diabetes Metab Syndr Obes. 2022;15:3219-3229. doi:10.2147/DMSO.S374784

174. Shishido A, Morisada N, Tominaga K, Uemura H, Haruna A, Hanafusa H, Nozu K, Iijima K. A Japanese boy with NAA10-related syndrome and hypertrophic cardiomyopathy. Hum Genome Var. 2020;7:23. doi:10.1038/s41439-020-00110-0

175. Fang C, Huang Y, Pei Y, Zhang HH, Chen X, Guo H, Li S, Ji X, Hu J.Genome-wide gene expression profiling reveals that CD274 is up-regulated new-onset type 1 diabetes mellitus. Acta Diabetol. 2017;54(8):757-767. doi:10.1007/s00592-017-1005-y

176. Lee W. The CEACAM1 expression is decreased in the liver of severely obese patients with or without diabetes. Diagn Pathol. 2011;6:40. doi:10.1186/1746-1596-6-40
177. Chaimowitz NS, Ebenezer SJ, Hanson IC, Anderson M, Forbes LR. STAT1 Gain of Function, Type 1 Diabetes, and Reversal with JAK Inhibition. N Engl J Med. 2020;383(15):1494-1496. doi:10.1056/NEJMc2022226
178. Fawad Ali Shah S, Iqbal T, Naveed N, Akram S, Arshad Rafiq M, Hussain S. ARG1 single nucleotide polymorphisms rs2781666 and rs2781665 confer risk of Type 2 diabetes mellitus. EXCLI J. 2018;17:847-855. doi:10.17179/excli2018-1178
179. Korneev KV, Sviriaeva EN, Mitkin NA, Gorbacheva AM, Uvarova AN, Ustiugova AS, Polanovsky OL, Kulakovskiy IV, Afanasyeva MA, Schwartz AM, et al. Minor C allele of the SNP rs7873784 associated with rheumatoid arthritis and type-2 diabetes mellitus binds PU.1 and enhances TLR4 expression. Biochim Biophys Acta Mol Basis Dis. 2020;1866(3):165626. doi:10.1016/j.bbadis.2019.165626
180. Huang MH, Liu YF, Nfor ON, Hsu SY, Lin WY, Chang YS, Liaw YP. Interactive Association Between Intronic Polymorphism (rs10506151) of the LRRK2 Gene and Type 2 Diabetes on Neurodegenerative Diseases. Pharmgenomics Pers Med. 2021;14:839-847. doi:10.2147/PGPM.S316158
181. Yoon HY, Lee MH, Song Y, Yee J, Song G, Gwak HS. ABCA1 69C>T Polymorphism and the Risk of Type 2 Diabetes Mellitus: A Systematic Review and Updated Meta-Analysis. Front Endocrinol (Lausanne). 2021;12:639524. doi:10.3389/fendo.2021.639524
182. Jermendy Á, Szatmári I, Körner A, Szabó AJ, Tóth-Heyn P, Hermann R. Association between interferon-induced helicase (IFIH1) rs1990760 polymorphism and seasonal variation in the onset of type 1 diabetes mellitus. Pediatr Diabetes. 2018;19(2):300-304. doi:10.1111/pedi.12569
183. Al-Daghri NM, Clerici M, Al-Attas O, Forni D, Alokail MS, Alkharfy KM, Sabico S, Mohammed AK, Cagliani R, Sironi M. A nonsense polymorphism (R392X) in TLR5 protects from obesity but predisposes to diabetes. J Immunol. 2013;190(7):3716-3720. doi:10.4049/jimmunol.1202936

184. Chen Q, He Y, Wang X, Zhu Y, Huang Y, Cao J, Yan R. LncRNA PTGS2 regulates islet β-cell function through the miR-146a-5p/RBP4 axis and its diagnostic value in type 2 diabetes mellitus. Am J Transl Res. 2021;13(10):11316-11328.
185. Austin-Zimmerman I, Wronska M, Wang B, Irizar H, Thygesen JH, Bhat A, Denaxas S, Fatemifar G, Finan C, Harju-Seppänen J, et al. The Influence of CYP2D6 and CYP2C19 Genetic Variation on Diabetes Mellitus Risk in People Taking Antidepressants and Antipsychotics. Genes (Basel). 2021;12(11):1758. doi:10.3390/genes12111758
186. Sarkar P, Thirumurugan K. New insights into TNFα/PTP1B and PPARγ pathway through RNF213- a link between inflammation, obesity, insulin resistance, and Moyamoya disease. Gene. 2021;771:145340. doi:10.1016/j.gene.2020.145340
187. Cang X, Wang Y, Zeng J, Gao J, Yu Q, Lu C, Xu F, Lin J, Zhu J, Wang X. C9orf72 knockdown alleviates hepatic insulin resistance by promoting lipophagy. Biochem Biophys Res Commun. 2022;588:15-22. doi:10.1016/j.bbrc.2021.12.018
188. Zhang Y, Lin C, Chen R, Luo L, Huang J, Liu H, Chen W, Xu J, Yu H, Ding Y. Association analysis of SOCS3, JAK2 and STAT3 gene polymorphisms and genetic susceptibility to type 2 diabetes mellitus in Chinese population. Diabetol Metab Syndr. 2022;14(1):4. doi:10.1186/s13098-021-00774-w
189. Ahmad R, Kochumon S, Thomas R, Atizado V, Sindhu S. Increased adipose tissue expression of TLR8 in obese individuals with or without type-2 diabetes: significance in metabolic inflammation. J Inflamm (Lond). 2016;13:38. doi:10.1186/s12950-016-0147-y
190. Sharaf SA, Kantoush NA, Ayoub DF, Ibrahim AA, Abdelaal AA, Aziz RA, ElHefnawi MM, Ahmed AN. Altered expression of WFS1 and NOTCH2 genes associated with diabetic nephropathy in T2DM patients. Diabetes Res Clin Pract. 2018;140:304-313. doi:10.1016/j.diabres.2018.03.053
191. Moriya J, Ferrara N. Inhibition of protein kinase C enhances angiogenesis induced by platelet-derived growth factor C in hyperglycemic endothelial cells. Cardiovasc Diabetol. 2015;14:19. doi:10.1186/s12933-015-0180-9

192. Demirci M, Bahar Tokman H, Taner Z, Keskin FE, Çağatay P, Ozturk Bakar Y, Özyazar M, Kiraz N, Kocazeybek BS. Bacteroidetes and Firmicutes levels in gut microbiota and effects of hosts TLR2/TLR4 gene expression levels in adult type 1 diabetes patients in Istanbul, Turkey. J Diabetes Complications. 2020;34(2):107449. doi:10.1016/j.jdiacomp.2019.107449
193. Sun MW, Lee JY, de Bakker PI, Burtt NP, Almgren P, Råstam L, Tuomi T, Gaudet D, Daly MJ, Hirschhorn JN, et al. Haplotype structures and large-scale association testing of the 5' AMP-activated protein kinase genes PRKAA2, PRKAB1, and PRKAB2 with type 2 diabetes. Diabetes. 2006;55(3):849-855. doi:10.2337/diabetes.55.03.06.db05-1418
194. Chiou HY, Bai CH, Lien LM, Hu CJ, Jeng JS, Tang SC, Lin HJ, Hsieh YC.Interactive Effects of a Combination of the HDAC3 and HDAC9 Genes with Diabetes Mellitus on the Risk of Ischemic Stroke. Thromb Haemost. 2021;121(3):396-404. doi:10.1055/s-0040-1717116
195. Li W, Li W, Wang Y, Leng Y, Xia Z. Inhibition of DNMT-1 alleviates ferroptosis through NCOA4 mediated ferritinophagy during diabetes myocardial ischemia/reperfusion injury. Cell Death Discov. 2021;7(1):267. doi:10.1038/s41420-021-00656-0
196. Yuan T, Annamalai K, Naik S, Lupse B, Geravandi S, Pal A, Dobrowolski A, Ghawali J, Ruhlandt M, Gorrepati KDD, et al. The Hippo kinase LATS2 impairs pancreatic β-cell survival in diabetes through the mTORC1-autophagy axis. Nat Commun. 2021;12(1):4928. doi:10.1038/s41467-021-25145-x
197. Kalis M, Bolmeson C, Esguerra JL, Gupta S, Edlund A, Tormo-Badia N, Speidel D, Holmberg D, Mayans S, Khoo NK, et al. Beta-cell specific deletion of Dicer1 leads to defective insulin secretion and diabetes mellitus. PLoS One. 2011;6(12):e29166. doi:10.1371/journal.pone.0029166
198. Jiao J, Wang Z, Guo Y, Liu J, Huang X, Ni X, Gao D, Sun L, Zhu X, Zhou Q, et al. Association between IL-1B (-511)/IL-1RN (VNTR) polymorphisms and type 2 diabetes: a systematic review and meta-analysis. PeerJ. 2021;9:e12384. doi:10.7717/peerj.12384
199. Ao H, Liu B, Li H, Lu L. Egr1 mediates retinal vascular dysfunction in diabetes mellitus via promoting p53 transcription. J Cell Mol Med. 2019;23(5):3345-3356. doi:10.1111/jcmm.14225

200. Shan K, Liu C, Liu BH, Chen X, Dong R, Liu X, Zhang YY, Liu B, Zhang SJ, Wang JJ, et al. Circular Noncoding RNA HIPK3 Mediates Retinal Vascular Dysfunction in Diabetes Mellitus. Circulation. 2017;136(17):1629-1642. doi:10.1161/CIRCULATIONAHA.117.029004
201. de Jesus DS, Mak TCS, Wang YF, von Ohlen Y, Bai Y, Kane E, Chabosseau P, Chahrour CM, Distaso W, Salem V, et al. Dysregulation of the Pdx1/Ovol2/Zeb2 axis in dedifferentiated β-cells triggers the induction of genes associated with epithelial-mesenchymal transition in diabetes. Mol Metab. 2021;53:101248. doi:10.1016/j.molmet.2021.101248
202. Huang Y, Jin L, Yu H, Jiang G, Tam CHT, Jiang S, Zheng C, Jiang F, Zhang R, Zhang H, et al. SNPs in PRKCA-HIF1A-GLUT1 are associated with diabetic kidney disease in a Chinese Han population with type 2 diabetes. Eur J Clin Invest. 2020;50(9):e13264. doi:10.1111/eci.13264
203. Wootton PT, Stephens JW, Hurel SJ, Durand H, Cooper J, Ninio E, Humphries SE, Talmud PJ. Lp-PLA2 activity and PLA2G7 A379V genotype in patients with diabetes mellitus. Atherosclerosis. 2006;189(1):149-156. doi:10.1016/j.atherosclerosis.2005.12.009
204. Arndt T, Wedekind D, Jörns A, Tsiavaliaris G, Cuppen E, Hedrich HJ, Lenzen S. A novel Dock8 gene mutation confers diabetogenic susceptibility in the LEW.1AR1/Ztm-iddm rat, an animal model of human type 1 diabetes. Diabetologia. 2015;58(12):2800-2809. doi:10.1007/s00125-015-3757-7
205. Di Prospero NA, Artis E, Andrade-Gordon P, Johnson DL, Vaccaro N, Xi L, Rothenberg P. CCR2 antagonism in patients with type 2 diabetes mellitus: a randomized, placebo-controlled study. Diabetes Obes Metab. 2014;16(11):1055-1064. doi:10.1111/dom.12309
206. Khan R, Kadamkode V, Kesharwani D, Purkayastha S, Banerjee G, Datta M. Circulatory miR-98-5p levels are deregulated during diabetes and it inhibits proliferation and promotes apoptosis by targeting PPP1R15B in keratinocytes. RNA Biol. 2020;17(2):188-201. doi:10.1080/15476286.2019.1673117
207. Vieira SM, Monteiro MB, Marques T, Luna AM, Fortes MA, Nery M, Queiroz M, Dib SA, Vendramini MF, Azevedo MJ, et al. Association of genetic variants in the promoter region of genes encoding p22phox (CYBA) and glutamate cysteine ligase catalytic subunit (GCLC) and renal disease in

patients with type 1 diabetes mellitus. BMC Med Genet. 2011;12:129. doi:10.1186/1471-2350-12-129

208. Al-Kateb H, Mirea L, Xie X, Sun L, Liu M, Chen H, Bull SB, Boright AP, Paterson AD. Multiple variants in vascular endothelial growth factor (VEGFA) are risk factors for time to severe retinopathy in type 1 diabetes: the DCCT/EDIC genetics study. Diabetes. 2007;56(8):2161-2168. doi:10.2337/db07-0376

209. Yu Y, Mingjiao W, Yang X, Sui M, Zhang T, Liang J, Gu X, Wang X. Association between DNA methylation of SORL1 5'-flanking region and mild cognitive impairment in type 2 diabetes mellitus. Ann Endocrinol (Paris). 2016;77(6):625-632. doi:10.1016/j.ando.2016.02.008

210. Majumdar G, Wright J, Markowitz P, Martinez-Hernandez A, Raghow R, Solomon SS. Insulin stimulates and diabetes inhibits O-linked N-acetylglucosamine transferase and O-glycosylation of Sp1. Diabetes. 2004;53(12):3184-3192. doi:10.2337/diabetes.53.12.3184

211. Fatani TH. EIF2AK3 novel mutation in a child with early-onset diabetes mellitus, a case report. BMC Pediatr. 2019;19(1):85. doi:10.1186/s12887-019-1432-8

212. Huang B, Wen W, Ye S. Dapagliflozin Ameliorates Renal Tubular Ferroptosis in Diabetes via SLC40A1 Stabilization. Oxid Med Cell Longev. 2022;2022:9735555. doi:10.1155/2022/9735555

213. Lupse B, Heise N, Maedler K, Ardestani A. PHLPP1 deletion restores pancreatic β-cell survival and normoglycemia in the db/db mouse model of obesity-associated diabetes. Cell Death Discov. 2022;8(1):57. doi:10.1038/s41420-022-00853-5

214. Chanprasertyothin S, Jongjaroenprasert W, Ongphiphadhanakul B. The association of soluble IGF2R and IGF2R gene polymorphism with type 2 diabetes. J Diabetes Res. 2015;2015:216383. doi:10.1155/2015/216383

215. Aulchenko YS, Pullen J, Kloosterman WP, Yazdanpanah M, Hofman A, Vaessen N, Snijders PJ, Zubakov D, Mackay I, Olavesen M, et al. LPIN2 is associated with type 2 diabetes, glucose metabolism, and body composition. Diabetes. 2007;56(12):3020-3026. doi:10.2337/db07-0338

216. Mihanfar A, Akbarzadeh M, Ghazizadeh Darband S, Sadighparvar S, Majidinia M. SIRT1: a promising therapeutic target in type 2 diabetes

mellitus. Arch Physiol Biochem. 2021;1-16. doi:10.1080/13813455.2021.1956976

217. Holstein JD, Patzer O, Körner A, Stumvoll M, Kovacs P, Holstein A. Genetic variants in GCKR, GIPR, ADCY5 and VPS13C and the risk of severe sulfonylurea-induced hypoglycaemia in patients with type 2 diabetes. Exp Clin Endocrinol Diabetes. 2013;121(1):54-57. doi:10.1055/s-0032-1321834

218. Chen Y, Li S, Yin M, Li Y, Chen C, Zhang J, Sun K, Kong X, Chen Z, Qian J. Isorhapontigenin Attenuates Cardiac Microvascular Injury in Diabetes Mellitus via the Inhibition of Mitochondrial-Derived Ferroptosis Through PRDX2-MFN2-ACSL4 Pathways. Diabetes. 2022;db220553. doi:10.2337/db22-0553

219. Matsuzaka T. Role of fatty acid elongase Elovl6 in the regulation of energy metabolism and pathophysiological significance in diabetes. Diabetol Int. 2020;12(1):68-73. doi:10.1007/s13340-020-00481-3

220. Ding Y, Liu K, Wang Y, Su G, Deng H, Zeng Q, Liao Y, Wang Z. Expression and significance of fgl2 prothrombinase in cardiac microvascular endothelial cells of rats with type 2 diabetes. J Huazhong Univ Sci Technolog Med Sci. 2010;30(5):575-581. doi:10.1007/s11596-010-0545-y

221. Awazawa M, Futami T, Sakada M, Kaneko K, Ohsugi M, Nakaya K, Terai A, Suzuki R, Koike M, Uchiyama Y, et al. Deregulation of pancreas-specific oxidoreductin ERO1β in the pathogenesis of diabetes mellitus. Mol Cell Biol. 2014;34(7):1290-1299. doi:10.1128/MCB.01647-13

222. Nishimura Y, Iwashita M, Hayashi M, Shinjo T, Watanabe Y, Zeze T, Yamashita A, Fukuda T, Sanui T, Sano T, et al. XAF1 overexpression exacerbates diabetes by promoting pancreatic β-cell apoptosis. Acta Diabetol. 2022;59(10):1275-1286. doi:10.1007/s00592-022-01930-y

223. Scherm MG, Serr I, Zahm AM, Schug J, Bellusci S, Manfredini R, Salb VK, Gerlach K, Weigmann B, Ziegler AG, et al. miRNA142-3p targets Tet2 and impairs Treg differentiation and stability in models of type 1 diabetes. Nat Commun. 2019;10(1):5697. doi:10.1038/s41467-019-13587-3

224. Da Li, Cao T, Sun X, Jin S, Di Xie, Huang X, Yang X, Carmichael GG, Taylor HS, Diano S, et al. Hepatic TET3 contributes to type-2 diabetes by inducing the HNF4α fetal isoform. Nat Commun. 2020;11(1):342. doi:10.1038/s41467-019-14185-z

225. Bayraktar M, Dündar S, Kirazli S, Teletar F. Platelet factor 4, beta-thromboglobulin and thrombospondin levels in type I diabetes mellitus patients. J Int Med Res. 1994;22(2):90-94. doi:10.1177/030006059402200204
226. Batool A, Jahan N, Sun Y, Hanif A, Xue H. Genetic association of IDE, POU2F1, PON1, IL1α and IL1β with type 2 diabetes in Pakistani population. Mol Biol Rep. 2014;41(5):3063-3069. doi:10.1007/s11033-014-3165-y
227. Han J, Liu YQ. Reduction of islet pyruvate carboxylase activity might be related to the development of type 2 diabetes mellitus in Agouti-K mice. J Endocrinol. 2010;204(2):143-152. doi:10.1677/JOE-09-0391
228. Flotyńska J, Klause D, Kulecki M, Cieluch A, Chomicka-Pawlak R, Zozulińska-Ziółkiewicz D, Uruska A. Higher NADH Dehydrogenase [Ubiquinone] Iron-Sulfur Protein 8 (NDUFS8) Serum Levels Correlate with Better Insulin Sensitivity in Type 1 Diabetes. Curr Issues Mol Biol. 2022;44(9):3872-3883. doi:10.3390/cimb44090266
229. Moghaddam DA, Heber A, Capin D, Kreutz T, Opitz D, Lenzen E, Bloch W, Brixius K, Brinkmann C. Training increases peroxiredoxin 2 contents in the erythrocytes of overweight/obese men suffering from type 2 diabetes. Wien Med Wochenschr. 2011;161(21-22):511-518. doi:10.1007/s10354-011-0037-0
230. Meng S, Cao J, Zhang X, Fan Y, Fang L, Wang C, Lv Z, Fu D, Li Y. Downregulation of microRNA-130a contributes to endothelial progenitor cell dysfunction in diabetic patients via its target Runx3. PLoS One. 2013;8(7):e68611. doi:10.1371/journal.pone.0068611
231. Tokuda H, Kuroyanagi G, Tsujimoto M, Enomoto Y, Matsushima-Nishiwaki R, Onuma T, Kojima A, Doi T, Tanabe K, Akamatsu S, et al. Release of Phosphorylated HSP27 (HSPB1) from Platelets Is Accompanied with the Acceleration of Aggregation in Diabetic Patients. PLoS One. 2015;10(6):e0128977. doi:10.1371/journal.pone.0128977
232. Rouskas K, Cauchi S, Raverdy V, Yengo L, Froguel P, Pattou F. Weight loss independent association of TCF7 L2 gene polymorphism with fasting blood glucose after Roux-en-Y gastric bypass in type 2 diabetic patients. Surg Obes Relat Dis. 2014;10(4):679-683. doi:10.1016/j.soard.2013.12.016

233. Hjortebjerg R, Tarnow L, Jorsal A, Parving HH, Rossing P, Bjerre M, Frystyk J. IGFBP-4 Fragments as Markers of Cardiovascular Mortality in Type 1 Diabetes Patients With and Without Nephropathy. J Clin Endocrinol Metab. 2015;100(8):3032-3040. doi:10.1210/jc.2015-2196
234. Kurnaz-Gömleksiz Ö, Tokat B, Aslan EI, Yanar F, Ermiş-Karaali Z, Öztürk O, Yilmaz-Aydoğan H. Can rs3767140 SNP of the perlecan (HSPG2) gene affect the diabetes mellitus through the dyslipidemia?. Cell Mol Biol (Noisy-le-grand). 2016;62(8):35-39.
235. Satake M, Ikarashi N, Kagami M, Ogiue N, Toda T, Kobayashi Y, Ochiai W, Sugiyama K. Increases in the expression levels of aquaporin-2 and aquaporin-3 in the renal collecting tubules alleviate dehydration associated with polyuria in diabetes mellitus. Biol Pharm Bull. 2010;33(12):1965-1970. doi:10.1248/bpb.33.1965
236. Ibrahim BA, Mohamed SH, Hassaan MMM, Sabbah NA. Associations of galectin-3 expression and LGALS-3 (rs4652) gene variant with coronary artery disease risk in diabetics. J Med Biochem. 2021;40(4):395-406. doi:10.5937/jomb0-30424
237. Wang Y, Chen Y, Yan Y, Li X, Chen G, He N, Shen S, Chen G, Zhang C, Liao W, et al. Loss of CEACAM1, a Tumor-Associated Factor, Attenuates Post-infarction Cardiac Remodeling by Inhibiting Apoptosis. Sci Rep. 2016;6:21972. doi:10.1038/srep21972
238. Liu S, He Y, Shi J, Liu L, Ma H, He L, Guo Y. STAT1-avtiviated LINC00961 regulates myocardial infarction by the PI3K/AKT/GSK3β signaling pathway. J Cell Biochem. 2019;120(8):13226-13236. doi:10.1002/jcb.28596
239. Zhang R, Ji Z, Qu Y, Yang M, Su Y, Zuo W, Zhao Q, Ma G, Li Y. Clinical value of ARG1 in acute myocardial infarction patients: Bioinformatics-based approach. Biomed Pharmacother. 2020;121:109590. doi:10.1016/j.biopha.2019.109590
240. Shi H, Zhou P, Gao G, Liu PP, Wang SS, Song R, Zou YY, Yin G, Wang L. Astragaloside IV prevents acute myocardial infarction by inhibiting the TLR4/MyD88/NF-κB signaling pathway. J Food Biochem. 2021;45(7):e13757. doi:10.1111/jfbc.13757
241. Liu Y, Chen L, Gao L, Pei X, Tao Z, Xu Y, Li R. LRRK2 deficiency protects the heart against myocardial infarction injury in mice via the

P53/HMGB1 pathway. Free Radic Biol Med. 2022;191:119-127. doi:10.1016/j.freeradbiomed.2022.08.035

242. Louwe MC, Lammers B, Frias MA, Foks AC, de Leeuw LR, Hildebrand RB, Kuiper J, Smit JWA, Van Berkel TJC, James RW, et al. Abca1 deficiency protects the heart against myocardial infarction-induced injury. Atherosclerosis. 2016;251:159-163. doi:10.1016/j.atherosclerosis.2016.06.023

243. Gao F, Zhao Y, Zhang B, Xiao C, Sun Z, Gao Y, Dou X. Suppression of lncRNA Gm47283 attenuates myocardial infarction via miR-706/ Ptgs2/ferroptosis axis. Bioengineered. 2022;13(4):10786-10802. doi:10.1080/21655979.2022.2065743

244. Anstensrud AK, Molden E, Haug HJ, Qazi R, Muriq H, Fosshaug LE, Spigset O, Øie E. Impact of genotype-predicted CYP2D6 metabolism on clinical effects and tolerability of metoprolol in patients after myocardial infarction - a prospective observational study. Eur J Clin Pharmacol. 2020;76(5):673-683. doi:10.1007/s00228-020-02832-0

245. Zhao C, Ren Y, Zhang Y. NDRG4 Alleviates Myocardial Infarction-Induced Apoptosis through the JAK2/STAT3 Pathway. Comput Math Methods Med. 2022;2022:4869470. doi:10.1155/2022/4869470

246. Li MJ, Yan SB, Dong H, Huang ZG, Li DM, Tang YL, Pan YF, Yang Z, Pan HB, Chen G. Clinical assessment and molecular mechanism of the upregulation of Toll-like receptor 2 (TLR2) in myocardial infarction. BMC Cardiovasc Disord. 2022;22(1):314. doi:10.1186/s12872-022-02754-y

247. Zhou X, Zhang C, Wu X, Hu X, Zhang Y, Wang X, Zheng L, Gao P, Du J, Zheng W, et al. Dusp6 deficiency attenuates neutrophil-mediated cardiac damage in the acute inflammatory phase of myocardial infarction. Nat Commun. 2022;13(1):6672. doi:10.1038/s41467-022-33631-z

248. Han Y, Dong B, Chen M, Yao C. LncRNA H19 suppresses pyroptosis of cardiomyocytes to attenuate myocardial infarction in a PBX3/CYP1B1-dependent manner. Mol Cell Biochem. 2021;476(3):1387-1400. doi:10.1007/s11010-020-03998-y

249. Liehn EA, Merx MW, Postea O, Becher S, Djalali-Talab Y, Shagdarsuren E, Kelm M, Zernecke A, Weber C. Ccr1 deficiency reduces inflammatory remodelling and preserves left ventricular function after

myocardial infarction. J Cell Mol Med. 2008;12(2):496-506. doi:10.1111/j.1582-4934.2007.00194.x

250. Liu F, Di Y, Ma W, Kang X, Li X, Ji Z. HDAC9 exacerbates myocardial infarction via inactivating Nrf2 pathways. J Pharm Pharmacol. 2022;74(4):565-572. doi:10.1093/jpp/rgab065

251. Ma C, Peng P, Zhou Y, Liu T, Wang L, Lu C. MicroRNA□93 promotes angiogenesis and attenuates remodeling via inactivation of the Hippo/Yap pathway by targeting Lats2 after myocardial infarctionω. Mol Med Rep. 2020;22(1):483-493. doi:10.3892/mmr.2020.11085

252. van Minkelen R, Wettinger SB, de Visser MC, Vos HL, Reitsma PH, Rosendaal FR, Bertina RM, Doggen CJ. Haplotypes of the interleukin-1 receptor antagonist gene, interleukin-1 receptor antagonist mRNA levels and the risk of myocardial infarction. Atherosclerosis. 2009;203(1):201-205. doi:10.1016/j.atherosclerosis.2008.06.029

253. Liu Y, Baumgardt SL, Fang J, Shi Y, Qiao S, Bosnjak ZJ, Vásquez-Vivar J, Xia Z, Warltier DC, Kersten JR, et al. Transgenic overexpression of GTP cyclohydrolase 1 in cardiomyocytes ameliorates post-infarction cardiac remodeling. Sci Rep. 2017;7(1):3093. doi:10.1038/s41598-017-03234-6

254. Thirunavukkarasu M, Selvaraju V, Joshi M, Coca-Soliz V, Tapias L, Saad I, Fournier C, Husain A, Campbell J, Yee SP, et al. Disruption of VEGF Mediated Flk-1 Signaling Leads to a Gradual Loss of Vessel Health and Cardiac Function During Myocardial Infarction: Potential Therapy With Pellino-1. J Am Heart Assoc. 2018;7(18):e007601. doi:10.1161/JAHA.117.007601

255. Fan K, Huang W, Qi H, Song C, He C, Liu Y, Zhang Q, Wang L, Sun H. The Egr-1/miR-15a-5p/GPX4 axis regulates ferroptosis in acute myocardial infarction. Eur J Pharmacol. 2021;909:174403. doi:10.1016/j.ejphar.2021.174403

256. Ma ZF, Wang N, Zhang J, Wan YF, Xiao N, Chen C. Overexpression of miR-431 inhibits cardiomyocyte apoptosis following myocardial infarction via targeting HIPK3. Eur Rev Med Pharmacol Sci. 2021;25(4):2056-2064. doi:10.26355/eurrev_202102_25110

257. Wang J, Seo MJ, Deci MB, Weil BR, Canty JM, Nguyen J. Effect of CCR2 inhibitor-loaded lipid micelles on inflammatory cell migration and

cardiac function after myocardial infarction. Int J Nanomedicine. 2018;13:6441-6451. doi:10.2147/IJN.S178650

258. Koide S, Kugiyama K, Sugiyama S, Nakamura S, Fukushima H, Honda O, Yoshimura M, Ogawa H. Association of polymorphism in glutamate-cysteine ligase catalytic subunit gene with coronary vasomotor dysfunction and myocardial infarction. J Am Coll Cardiol. 2003;41(4):539-545. doi:10.1016/s0735-1097(02)02866-8

259. Mao Q, Liang XL, Zhang CL, Pang YH, Lu YX. LncRNA KLF3-AS1 in human mesenchymal stem cell-derived exosomes ameliorates pyroptosis of cardiomyocytes and myocardial infarction through miR-138-5p/Sirt1 axis. Stem Cell Res Ther. 2019;10(1):393. doi:10.1186/s13287-019-1522-4

260. Iribarren C, Phelps BH, Darbinian JA, McCluskey ER, Quesenberry CP, Hytopoulos E, Vogelman JH, Orentreich N. Circulating angiopoietins-1 and -2, angiopoietin receptor Tie-2 and vascular endothelial growth factor-A as biomarkers of acute myocardial infarction: a prospective nested case-control study. BMC Cardiovasc Disord. 2011;11:31. doi:10.1186/1471-2261-11-31

261. Li L, Guan Q, Dai S, Wei W, Zhang Y. Integrin β1 Increases Stem Cell Survival and Cardiac Function after Myocardial Infarction. Front Pharmacol. 2017;8:135. doi:10.3389/fphar.2017.00135

262. Liu X, Xu Y, Deng Y, Li H. MicroRNA-223 Regulates Cardiac Fibrosis After Myocardial Infarction by Targeting RASA1. Cell Physiol Biochem. 2018;46(4):1439-1454. doi:10.1159/000489185

263. Yang CF, Chen YY, Singh JP, Hsu SF, Liu YW, Yang CY, Chang CW, Chen SN, Shih RH, Hsu SD, et al. Targeting protein tyrosine phosphatase PTP-PEST (PTPN12) for therapeutic intervention in acute myocardial infarction. Cardiovasc Res. 2020;116(5):1032-1046. doi:10.1093/cvr/cvz165

264. Wang ZY, Liu XX, Deng YF. Negative feedback of SNRK to circ-SNRK regulates cardiac function post-myocardial infarction. Cell Death Differ. 2022;29(4):709-721. doi:10.1038/s41418-021-00885-x

265. Chen Q, Su L, Liu C, Gao F, Chen H, Yin Q, Li S. PRKAR1A and SDCBP Serve as Potential Predictors of Heart Failure Following Acute Myocardial Infarction. Front Immunol. 2022;13:878876. doi:10.3389/fimmu.2022.878876

266. Rimbert A, Dalila N, Wolters JC, Huijkman N, Smit M, Kloosterhuis N, Riemsma M, van der Veen Y, Singla A, van Dijk F, et al.A common variant in CCDC93 protects against myocardial infarction and cardiovascular mortality by regulating endosomal trafficking of low-density lipoprotein receptor. Eur Heart J. 2020;41(9):1040-1053. doi:10.1093/eurheartj/ehz727
267. Chen L, Li S, Zhu J, You A, Huang X, Yi X, Xue M. Mangiferin prevents myocardial infarction-induced apoptosis and heart failure in mice by activating the Sirt1/FoxO3a pathway. J Cell Mol Med. 2021;25(6):2944-2955. doi:10.1111/jcmm.16329
268. Li X, Li F, Chu Y, Wang X, Zhang H, Hu Y, Zhang Y, Wang Z, Wei X, Jian W, et al. NOD2 deficiency protects against cardiac remodeling after myocardial infarction in mice. Cell Physiol Biochem. 2013;32(6):1857-1866. doi:10.1159/000356618
269. Chabior A, Gąsecka A, Marchel M, Gozdowska R, Makowska A, Maciak K, Góra M, Filipiak KJ, Burzyńska B, Opolski G. Expression of versican mRNA transcript to predict cardiac remodelling after myocardial infarction. Kardiol Pol. 2021;79(7-8):833-840. doi:10.33963/KP.a2021.0042
270. Wang S, Hu S, Luo X, Bao X, Li J, Liu M, Lv Y, Zhao C, Zeng M, Chen X, et al. Prevalence and prognostic significance of DNMT3A- and TET2- clonal haematopoiesis-driver mutations in patients presenting with ST-segment elevation myocardial infarction. EBioMedicine. 2022;78:103964. doi:10.1016/j.ebiom.2022.103964
271. Yang X, Li J, Hu X, Zhang Y, Kuang Y, Liu Y, Liu C, Gao H, Ma L, Tang J, et al. Identification of PFKFB2 as a key gene for the transition from acute to old myocardial infarction in peripheral blood. Front Cardiovasc Med. 2022;9:993579. doi:10.3389/fcvm.2022.993579
272. Li F, Yang Y, Xue C, Tan M, Xu L, Gao J, Xu L, Zong J, Qian W. Zinc Finger Protein ZBTB20 protects against cardiac remodelling post-myocardial infarction via ROS-TNFα/ASK1/JNK pathway regulation. J Cell Mol Med. 2020;24(22):13383-13396. doi:10.1111/jcmm.15961
273. Rafatian G, Kamkar M, Parent S, Michie C, Risha Y, Molgat ASD, Seymour R, Suuronen EJ, Davis DR. Mybl2 rejuvenates heart explant-derived cells from aged donors after myocardial infarction. Aging Cell. 2020;19(7):e13174. doi:10.1111/acel.13174

274. Kuijpers PM, Hamulyak K, Strik JJ, Wellens HJ, Honig A. Beta-thromboglobulin and platelet factor 4 levels in post-myocardial infarction patients with major depression. Psychiatry Res. 2002;109(2):207-210. doi:10.1016/s0165-1781(02)00017-3
275. Devaux Y, Vausort M, Azuaje F, Vaillant M, Lair ML, Gayat E, Lassus J, Ng LL, Kelly D, Wagner DR, et al. Low levels of vascular endothelial growth factor B predict left ventricular remodeling after acute myocardial infarction. J Card Fail. 2012;18(4):330-337. doi:10.1016/j.cardfail.2012.01.010
276. Wołkow PP, Drabik L, Totoń-Żurańska J, Kuś K, Foryś J, Słowik A, Pera J, Godlewski J, Tomala M, Żmudka K, et al. Polymorphism in the chemokine receptor 7 gene (CCR7) is associated with previous myocardial infarction in patients undergoing elective coronary angiography. Int J Immunogenet. 2016;43(4):218-225. doi:10.1111/iji.12270
277. Li H, Yang H, Wang D, Zhang L, Ma T. Peroxiredoxin2 (Prdx2) Reduces Oxidative Stress and Apoptosis of Myocardial Cells Induced by Acute Myocardial Infarction by Inhibiting the TLR4/Nuclear Factor kappa B (NF-κB) Signaling Pathway. Med Sci Monit. 2020;26:e926281. doi:10.12659/MSM.926281
278. Wang Y, Liu J, Kong Q, Cheng H, Tu F, Yu P, Liu Y, Zhang X, Li C, Li Y, et al. Cardiomyocyte-specific deficiency of HSPB1 worsens cardiac dysfunction by activating NFκB-mediated leucocyte recruitment after myocardial infarction. Cardiovasc Res. 2019;115(1):154-167. doi:10.1093/cvr/cvy163
279. Zheng HF, Sun J, Zou ZY, Zhang Y, Hou GY. MiRNA-488-3p suppresses acute myocardial infarction-induced cardiomyocyte apoptosis via targeting ZNF791. Eur Rev Med Pharmacol Sci. 2019;23(11):4932-4939. doi:10.26355/eurrev_201906_18083
280. Anastasilakis AD, Koulaxis D, Upadhyay J, Pagkalidou E, Kefala N, Perakakis N, Polyzos SA, Economou F, Mantzoros CS. Free IGF-1, Intact IGFBP-4, and PicoPAPP-A are Altered in Acute Myocardial Infarction Compared to Stable Coronary Artery Disease and Healthy Controls. Horm Metab Res. 2019;51(2):112-119. doi:10.1055/a-0794-6163
281. Pan X, Chen S, Chen X, Ren Q, Yue L, Niu S, Li Z, Zhu R, Chen X, Jia Z, et al. UTP14A, DKC1, DDX10, PinX1, and ESF1 Modulate Cardiac

Angiogenesis Leading to Obesity-Induced Cardiac Injury. J Diabetes Res. 2022;2022:2923291. doi:10.1155/2022/2923291

282. Tang J, Tang QX, Liu S. METTL3-modified lncRNA-SNHG8 binds to PTBP1 to regulate ALAS2 expression to increase oxidative stress and promote myocardial infarction. Mol Cell Biochem. 2022;10.1007/s11010-022-04570-6. doi:10.1007/s11010-022-04570-6

283. Djordjevic A, Zivkovic M, Boskovic M, Dekleva M, Stankovic G, Stankovic A, Djuric T. Variants Tagging LGALS-3 Haplotype Block in Association with First Myocardial Infarction and Plasma Galectin-3 Six Months after the Acute Event. Genes (Basel). 2022;14(1):109. doi:10.3390/genes14010109

284. Jia D, Chen S, Bai P, Luo C, Liu J, Sun A, Ge J. Cardiac Resident Macrophage-Derived Legumain Improves Cardiac Repair by Promoting Clearance and Degradation of Apoptotic Cardiomyocytes After Myocardial Infarction. Circulation. 2022;145(20):1542-1556. doi:10.1161/CIRCULATIONAHA.121.057549

285. Chen Y, He L, Yang Y, Chen Y, Song Y, Lu X, Liang Y. he inhibition of Nrf2 accelerates renal lipid deposition through suppressing the ACSL1 expression in obesity-related nephropathy. Ren Fail. 2019;41(1):821-831. doi:10.1080/0886022X.2019.1655450

286. Cox AR, Chernis N, Bader DA, Saha PK, Masschelin PM, Felix JB, Sharp R, Lian Z, Putluri V, Rajapakshe K, et al. STAT1 Dissociates Adipose Tissue Inflammation From Insulin Sensitivity in Obesity. Diabetes. 2020;69(12):2630-2641. doi:10.2337/db20-038

287. Benomar Y, Taouis M. Molecular Mechanisms Underlying Obesity-Induced Hypothalamic Inflammation and Insulin Resistance: Pivotal Role of Resistin/TLR4 Pathways. Front Endocrinol (Lausanne). 2019;10:140. doi:10.3389/fendo.2019.00140

288. Velazquez-Roman J, Angulo-Zamudio UA, León-Sicairos N, Medina-Serrano J, DeLira-Bustillos N, Villamil-Ramírez H, Canizales-Quinteros S, Macías-Kauffer L, Campos-Romero A, Alcántar-Fernández J, et al. Association of FTO, ABCA1, ADRB3, and PPARG variants with obesity, type 2 diabetes, and metabolic syndrome in a Northwest Mexican adult population. J Diabetes Complications. 2021;35(11):108025. doi:10.1016/j.jdiacomp.2021.108025

289. Shetty PB, Tang H, Tayo BO, Morrison AC, Hanis CL, Rao DC, Young JH, Fox ER, Boerwinkle E, et al. Variants in CXADR and F2RL1 are associated with blood pressure and obesity in African-Americans in regions identified through admixture mapping. J Hypertens. 2012;30(10):1970-1976. doi:10.1097/HJH.0b013e3283578c80
290. Rodríguez-Morató J, Goday A, Langohr K, Pujadas M, Civit E, Pérez-Mañá C, Papaseit E, Ramon JM, Benaiges D, Castañer O, et al. Short- and medium-term impact of bariatric surgery on the activities of CYP2D6, CYP3A4, CYP2C9, and CYP1A2 in morbid obesity. Sci Rep. 2019;9(1):20405. doi:10.1038/s41598-019-57002-9
291. Thoudam T, Ha CM, Leem J, Chanda D, Park JS, Kim HJ, Jeon JH, Choi YK, Liangpunsakul S, Huh YH, et al. PDK4 Augments ER-Mitochondria Contact to Dampen Skeletal Muscle Insulin Signaling During Obesity. Diabetes. 2019;68(3):571-586. doi:10.2337/db18-0363
292. Jiang M, He J, Sun Y, Dong X, Yao J, Gu H, Liu L. Leptin Induced TLR4 Expression via the JAK2-STAT3 Pathway in Obesity-Related Osteoarthritis. Oxid Med Cell Longev. 2021;2021:7385160. doi:10.1155/2021/7385160
293. Grarup N, Andersen G, Krarup NT, Albrechtsen A, Schmitz O, Jørgensen T, Borch-Johnsen K, Hansen T, Pedersen O. Association testing of novel type 2 diabetes risk alleles in the JAZF1, CDC123/CAMK1D, TSPAN8, THADA, ADAMTS9, and NOTCH2 loci with insulin release, insulin sensitivity, and obesity in a population-based sample of 4,516 glucose-tolerant middle-aged Danes. Diabetes. 2008;57(9):2534-2540. doi:10.2337/db08-0436
294. Ding W, Zhang C, Wang B, Zhou X, Sun L, Zhong S, Liu J, Zhang J, Wang X, Wu Q. Loss of the centrosomal protein Cenpj leads to dysfunction of the hypothalamus and obesity in mice. Sci China Life Sci. 2021;64(3):419-433. doi:10.1007/s11427-020-1767-5
295. Zhou Q, Gu Y, Lang H, Wang X, Chen K, Gong X, Zhou M, Ran L, Zhu J, Mi M. Dihydromyricetin prevents obesity-induced slow-twitch-fiber reduction partially via FLCN/FNIP1/AMPK pathway. Biochim Biophys Acta Mol Basis Dis. 2017;1863(6):1282-1291. doi:10.1016/j.bbadis.2017.03.019

296. Martínez-García MÁ, Ojeda-Ojeda M, Rodríguez-Martín E, Insenser M, Moncayo S, Álvarez-Blasco F, Luque-Ramírez M, Escobar-Morreale HF. TLR2 and TLR4 Surface and Gene Expression in White Blood Cells after Fasting and Oral Glucose, Lipid and Protein Challenges: Influence of Obesity and Sex Hormones. Biomolecules. 2020;10(1):111. doi:10.3390/biom10010111
297. Josifova DJ, Monroe GR, Tessadori F, de Graaff E, van der Zwaag B, Mehta SG; DDD Study; Harakalova M, Duran KJ, Savelberg SM, et al. Heterozygous KIDINS220/ARMS nonsense variants cause spastic paraplegia, intellectual disability, nystagmus, and obesity. Hum Mol Genet. 2016;25(11):2158-2167. doi:10.1093/hmg/ddw082
298. Liu R, Peters M, Urban N, Knowlton J, Napierala T, Gabrysiak J. Mice lacking DUSP6/8 have enhanced ERK1/2 activity and resistance to diet-induced obesity. Biochem Biophys Res Commun. 2020;533(1):17-22. doi:10.1016/j.bbrc.2020.08.106
299. Rojas IY, Moyer BJ, Ringelberg CS, Tomlinson CR. Reversal of obesity and liver steatosis in mice via inhibition of aryl hydrocarbon receptor and altered gene expression of CYP1B1, PPARα, SCD1, and osteopontin. Int J Obes (Lond). 2020;44(4):948-963. doi:10.1038/s41366-019-0512-z
300. Chakrabarty S, Bui Q, Badeanlou L, Hester K, Chun J, Ruf W, Ciaraldi TP, Samad F. S1P/S1PR3 signalling axis protects against obesity-induced metabolic dysfunction. Adipocyte. 2022;11(1):69-83. doi:10.1080/21623945.2021.2021700
301. Lu Y, Habtetsion TG, Li Y, Zhang H, Qiao Y, Yu M, Tang Y, Zhen Q, Cheng Y, et al. Association of NCOA2 gene polymorphisms with obesity and dyslipidemia in the Chinese Han population. Int J Clin Exp Pathol. 2015;8(6):7341-7349.
302. Goo B, Ahmadieh S, Zarzour A, Yiew NKH, Kim D, Shi H, Greenway J, Cave S, Nguyen J, Aribindi S, et al. Sex-Dependent Role of Adipose Tissue HDAC9 in Diet-Induced Obesity and Metabolic Dysfunction. Cells. 2022;11(17):2698. doi:10.3390/cells11172698
303. Kim D, Lee H, Koh J, Ko JS, Yoon BR, Jeon YK, Cho YM, Kim TH, Suh YS, Lee HJ, et al. Cytosolic Pellino-1-Mediated K63-Linked Ubiquitination of IRF5 in M1 Macrophages Regulates Glucose Intolerance in Obesity. Cell Rep. 2017;20(4):832-845. doi:10.1016/j.celrep.2017.06.088

304. Zhang J, Zhang Y, Sun T, Guo F, Huang S, Chandalia M, Abate N, Fan D, Xin HB, Chen YE, et al. Dietary obesity-induced Egr-1 in adipocytes facilitates energy storage via suppression of FOXC2. Sci Rep. 2013;3:1476. doi:10.1038/srep01476
305. Drareni K, Ballaire R, Barilla S, Mathew MJ, Toubal A, Fan R, Liang N, Chollet C, Huang Z, Kondili M, et al. GPS2 Deficiency Triggers Maladaptive White Adipose Tissue Expansion in Obesity via HIF1A Activation. Cell Rep. 2018;24(11):2957-2971.e6. doi:10.1016/j.celrep.2018.08.032
306. Lee SJ, Kang JS, Kim HM, Lee ES, Lee JH, Chung CH, Lee EY. CCR2 knockout ameliorates obesity-induced kidney injury through inhibiting oxidative stress and ER stress. PLoS One. 2019;14(9):e0222352. doi:10.1371/journal.pone.0222352
307. Hulsmans M, Geeraert B, Arnould T, Tsatsanis C, Holvoet P. PPAR agonist-induced reduction of Mcp1 in atherosclerotic plaques of obese, insulin-resistant mice depends on adiponectin-induced Irak3 expression. PLoS One. 2013;8(4):e62253. doi:10.1371/journal.pone.0062253
308. Shan HJ, Gu WX, Duan G, Chen HL. Fat mass and obesity associated (FTO)-mediated N6-methyladenosine modification of Krüppel-like factor 3 (KLF3) promotes osteosarcoma progression. Bioengineered. 2022;13(4):8038-8050. doi:10.1080/21655979.2022.2051785
309. Elias I, Franckhauser S, Bosch F. New insights into adipose tissue VEGF-A actions in the control of obesity and insulin resistance. Adipocyte. 2013;2(2):109-112. doi:10.4161/adip.22880
310. Yang Y, Fu M, Li MD, Zhang K, Zhang B, Wang S, Liu Y, Ni W, Ong Q, Mi J, et al. O-GlcNAc transferase inhibits visceral fat lipolysis and promotes diet-induced obesity. Nat Commun. 2020;11(1):181. doi:10.1038/s41467-019-13914-8
311. Hickey SE, Walters-Sen L, Mosher TM, Pfau RB, Pyatt R, Snyder PJ, Sotos JF, Prior TW. Duplication of the Xq27.3-q28 region, including the FMR1 gene, in an X-linked hypogonadism, gynecomastia, intellectual disability, short stature, and obesity syndrome. Am J Med Genet A. 2013;161A(9):2294-2299. doi:10.1002/ajmg.a.36034
312. Choi YJ, Lee YA, Hong YC, Cho J, Lee KS, Shin CH, Kim BN, Kim JI, Park SJ, Bisgaard H, et al.Effect of prenatal bisphenol A exposure on

early childhood body mass index through epigenetic influence on the insulin-like growth factor 2 receptor (IGF2R) gene. Environ Int. 2020;143:105929. doi:10.1016/j.envint.2020.105929

313. Loid P, Pekkinen M, Reyes M, Mustila T, Viljakainen H, Jüppner H, Mäkitie O. GNAS, PDE4D, and PRKAR1A Mutations and GNAS Methylation Changes Are Not a Common Cause of Isolated Early-Onset Severe Obesity Among Finnish Children. Front Pediatr. 2020;8:145. doi:10.3389/fped.2020.00145

314. Lu D, Yang J, Zhang J, Guo X. Severe obesity, hypogonadotropic hypogonadism and a WDR11 gene mutation. QJM. 2022;115(3):160-161. doi:10.1093/qjmed/hcab279

315. Du Y, Li S, Cui CJ, Zhang Y, Yang SH, Li JJ. Leptin decreases the expression of low-density lipoprotein receptor via PCSK9 pathway: linking dyslipidemia with obesity. J Transl Med. 2016;14(1):276. doi:10.1186/s12967-016-1032-4

316. Arias-Loste MT, Iruzubieta P, Puente Á, Ramos D, Santa Cruz C, Estébanez Á, Llerena S, Alonso-Martín C, San Segundo D, Álvarez L, et al. Increased Expression Profile and Functionality of TLR6 in Peripheral Blood Mononuclear Cells and Hepatocytes of Morbidly Obese Patients with Non-Alcoholic Fatty Liver Disease. Int J Mol Sci. 2016;17(11):1878. doi:10.3390/ijms17111878

317. Abduraman MA, Azizan NA, Teoh SH, Tan ML. Ketogenesis and SIRT1 as a tool in managing obesity. Obes Res Clin Pract. 2021;15(1):10-18. doi:10.1016/j.orcp.2020.12.001

318. Haenisch M, Nguyen T, Fihn CA, Goldstein AS, Amory JK, Treuting P, Brabb T, Paik J. Investigation of an ALDH1A1-specific inhibitor for suppression of weight gain in a diet-induced mouse model of obesity. Int J Obes (Lond). 2021;45(7):1542-1552. doi:10.1038/s41366-021-00818-1

319. Rodriguez-Nunez I, Caluag T, Kirby K, Rudick CN, Dziarski R, Gupta D. Nod2 and Nod2-regulated microbiota protect BALB/c mice from diet-induced obesity and metabolic dysfunction. Sci Rep. 2017;7(1):548. doi:10.1038/s41598-017-00484-2

320. Killion EA, Reeves AR, El Azzouny MA, Yan QW, Surujon D, Griffin JD, Bowman TA, Wang C, Matthan NR, Klett EL, et al. A role for long-chain acyl-CoA synthetase-4 (ACSL4) in diet-induced phospholipid

remodeling and obesity-associated adipocyte dysfunction. Mol Metab. 2018;9:43-56. doi:10.1016/j.molmet.2018.01.012

321. Matsuzaka T, Shimano H, Yahagi N, Kato T, Atsumi A, Yamamoto T, Inoue N, Ishikawa M, Okada S, Ishigaki N, et al. Crucial role of a long-chain fatty acid elongase, Elovl6, in obesity-induced insulin resistance. Nat Med. 2007;13(10):1193-1202. doi:10.1038/nm1662

322. Han CY, Kang I, Harten IA, Gebe JA, Chan CK, Omer M, Alonge KM, den Hartigh LJ, Gomes Kjerulf D, Goodspeed L, et al. Adipocyte-Derived Versican and Macrophage-Derived Biglycan Control Adipose Tissue Inflammation in Obesity. Cell Rep. 2020;31(13):107818. doi:10.1016/j.celrep.2020.107818

323. Bradford EM, Miller ML, Prasad V, Nieman ML, Gawenis LR, Berryman M, Lorenz JN, Tso P, Shull GE. CLIC5 mutant mice are resistant to diet-induced obesity and exhibit gastric hemorrhaging and increased susceptibility to torpor. Am J Physiol Regul Integr Comp Physiol. 2010;298(6):R1531-R1542. doi:10.1152/ajpregu.00849.2009

324. Ma MM, Jin CC, Huang XL, Sun L, Zhou H, Wen XJ, Huang XQ, Du JY, Sun HS, Ren ZX, et al. Clcn3 deficiency ameliorates high-fat diet-induced obesity and adipose tissue macrophage inflammation in mice. Acta Pharmacol Sin. 2019;40(12):1532-1543. doi:10.1038/s41401-019-0229-5

325. Yoshino S, Satoh T, Yamada M, Hashimoto K, Tomaru T, Katano-Toki A, Kakizaki S, Okada S, Shimizu H, Ozawa A, et al. Protection against high-fat diet-induced obesity in Helz2-deficient male mice due to enhanced expression of hepatic leptin receptor. Endocrinology. 2014;155(9):3459-3472. doi:10.1210/en.2013-2160

326. Salah N, Salem L, Taha S, Youssef M, Annaka L, Hassan S, Mahmoud R. DNMT3A and TET2; Potential Estimates of Generic DNA Methylation in Children and Adolescents with Obesity; Relation to Metabolic Dysregulation. Horm Res Paediatr. 2022;95(1):25-34. doi:10.1159/000521701

327. Chen J, Xu X, Li Y, Li F, Zhang J, Xu Q, Chen W, Wei Y, Wang X. Kdm6a suppresses the alternative activation of macrophages and impairs energy expenditure in obesity. Cell Death Differ. 2021;28(5):1688-1704. doi:10.1038/s41418-020-00694-8

328. Bricambert J, Alves-Guerra MC, Esteves P, Prip-Buus C, Bertrand-Michel J, Guillou H, Chang CJ, Vander Wal MN, Canonne-Hergaux F, Mathurin P, et al. The histone demethylase Phf2 acts as a molecular checkpoint to prevent NAFLD progression during obesity. Nat Commun. 2018;9(1):2092. doi:10.1038/s41467-018-04361-y
329. Hamano M, Esaki K, Moriyasu K, Yasuda T, Mohri S, Tashiro K, Hirabayashi Y, Furuya S. Hepatocyte-Specific Phgdh-Deficient Mice Culminate in Mild Obesity, Insulin Resistance, and Enhanced Vulnerability to Protein Starvation. Nutrients. 2021;13(10):3468. doi:10.3390/nu13103468
330. Zhu X, Wang Y, Zhu L, Zhu Y, Zhang K, Wang L, Bai H, Yang Q, Ben J, Zhang H, et al. Class A1 scavenger receptor prevents obesity-associated blood pressure elevation through suppressing overproduction of vascular endothelial growth factor B in macrophages. Cardiovasc Res. 2021;117(2):547-560. doi:10.1093/cvr/cvaa030
331. Zhou JP, Ren YD, Xu QY, Song Y, Zhou F, Chen MY, Liu JJ, Chen LG, Pan JS. Obesity-Induced Upregulation of ZBTB7A Promotes Lipid Accumulation through SREBP1. Biomed Res Int. 2020;2020:4087928. doi:10.1155/2020/4087928
332. Lynch CJ, McCall KM, Billingsley ML, Bohlen LM, Hreniuk SP, Martin LF, Witters LA, Vannucci SJ. Pyruvate carboxylase in genetic obesity. Am J Physiol. 1992;262(5 Pt 1):E608-E618. doi:10.1152/ajpendo.1992.262.5.E608
333. Sano T, Sanada T, Sotomaru Y, Shinjo T, Iwashita M, Yamashita A, Fukuda T, Sanui T, Asano T, Kanematsu T, et al. Ccr7 null mice are protected against diet-induced obesity via Ucp1 upregulation and enhanced energy expenditure. Nutr Metab (Lond). 2019;16:43. doi:10.1186/s12986-019-0372-5
334. Nunoue T, Yamaguchi S, Teshigawara S, Katayama A, Nakatsuka A, Eguchi J, Niki T, Wada J. Lgals9 deficiency ameliorates obesity by modulating redox state of PRDX2. Sci Rep. 2021;11(1):5991. doi:10.1038/s41598-021-85080-1
335. Bonhoure N, Byrnes A, Moir RD, Hodroj W, Preitner F, Praz V, Marcelin G, Chua SC Jr, Martinez-Lopez N, Singh R, et al. Loss of the RNA polymerase III repressor MAF1 confers obesity resistance. Genes Dev. 2015;29(9):934-947. doi:10.1101/gad.258350.115

336. Pilch W, Wyrostek J, Major P, Zuziak R, Piotrowska A, Czerwińska-Ledwig O, Grzybkowska A, Zasada M, Ziemann E, Żychowska M. The effect of whole-body cryostimulation on body composition and leukocyte expression of HSPA1A, HSPB1, and CRP in obese men. Cryobiology. 2020;94:100-106. doi:10.1016/j.cryobiol.2020.04.002
337. Baek JH, Kim SJ, Kang HG, Lee HW, Kim JH, Hwang KA, Song J, Chun KH. Galectin-3 activates PPARγ and supports white adipose tissue formation and high-fat diet-induced obesity. Endocrinology. 2015;156(1):147-156. doi:10.1210/en.2014-1374
338. González-García I, Freire-Agulleiro Ó, Nakaya N, Ortega FJ, Garrido-Gil P, Liñares-Pose L, Fernø J, Labandeira-Garcia JL, Diéguez C, Sultana A, et al. Olfactomedin 2 deficiency protects against diet-induced obesity. Metabolism. 2022;129:155122. doi:10.1016/j.metabol.2021.155122
339. Yang H, Chen L, Sun Q, Yao F, Muhammad S, Sun C. The role of HDAC11 in obesity-related metabolic disorders: A critical review. J Cell Physiol. 2021;236(8):5582-5591. doi:10.1002/jcp.30286
340. Heinrich G, Ghadieh HE, Ghanem SS, Muturi HT, Rezaei K, Al-Share QY, Bowman TA, Zhang D, Garofalo RS, Yin L, et al. Loss of Hepatic CEACAM1: A Unifying Mechanism Linking Insulin Resistance to Obesity and Non-Alcoholic Fatty Liver Disease. Front Endocrinol (Lausanne). 2017;8:8. doi:10.3389/fendo.2017.00008
341. Omanovic Kolaric T, Kizivat T, Mihaljevic V, Zjalic M, Bilic-Curcic I, Kuna L, Smolic R, Vcev A, Wu GY, Smolic M. Liraglutide Exerts Protective Effects by Downregulation of PPARγ, ACSL1 and SREBP-1c in Huh7 Cell Culture Models of Non-Alcoholic Steatosis and Drug-Induced Steatosis. Curr Issues Mol Biol. 2022;44(8):3465-3480. doi:10.3390/cimb44080239
342. Si MD, Wu M, Cheng XZ, Ma ZH, Zheng YG, Li J, Li S, Song YX, Ma D. Swertia mussotii prevents high-fat diet-induced non-alcoholic fatty liver disease in rats by inhibiting expression the TLR4/MyD88 and the phosphorylation of NF-κB. Pharm Biol. 2022;60(1):1960-1968. doi:10.1080/13880209.2022.2127153
343. Li J, Qi J, Tang Y, Liu H, Zhou K, Dai Z, Yuan L, Sun C. A nanodrug system overexpressed circRNA_0001805 alleviates nonalcoholic fatty liver

disease via miR-106a-5p/miR-320a and ABCA1/CPT1 axis. J Nanobiotechnology. 2021;19(1):363. doi:10.1186/s12951-021-01108-8

344. Kanuri G, Ladurner R, Skibovskaya J, Spruss A, Königsrainer A, Bischoff SC, Bergheim I. Expression of toll-like receptors 1-5 but not TLR 6-10 is elevated in livers of patients with non-alcoholic fatty liver disease. Liver Int. 2015;35(2):562-568. doi:10.1111/liv.12442

345. Müller P, Messmer M, Bayer M, Pfeilschifter JM, Hintermann E, Christen U. Non-alcoholic fatty liver disease (NAFLD) potentiates autoimmune hepatitis in the CYP2D6 mouse model. J Autoimmun. 2016;69:51-58. doi:10.1016/j.jaut.2016.02.007

346. Kaltenecker D, Themanns M, Mueller KM, Spirk K, Suske T, Merkel O, Kenner L, Luís A, Kozlov A, Haybaeck J, et al. Hepatic growth hormone - JAK2 - STAT5 signalling: Metabolic function, non-alcoholic fatty liver disease and hepatocellular carcinoma progression. Cytokine. 2019;124:154569. doi:10.1016/j.cyto.2018.10.010

347. Cui J, Wang Y, Xue H. Long non-coding RNA GAS5 contributes to the progression of nonalcoholic fatty liver disease by targeting the microRNA-29a-3p/NOTCH2 axis. Bioengineered. 2022;13(4):8370-8381. doi:10.1080/21655979.2022.2026858

348. Liu P, Zhang Y, Tang C, Cen L, Chen Y, Li S, Chen X, Yu M, Zhang J, Zhang X, et al. The DEAD-box helicase DDX3x ameliorates non-alcoholic fatty liver disease via mTORC1 signalling pathway. Liver Int. 2022;42(8):1793-1802. doi:10.1111/liv.15278

349. Qi X, Song A, Ma M, Wang P, Zhang X, Lu C, Zhang J, Zheng S, Jin H. Curcumol inhibits ferritinophagy to restrain hepatocyte senescence through YAP/NCOA4 in non-alcoholic fatty liver disease. Cell Prolif. 2021;54(9):e13107. doi:10.1111/cpr.13107

350. Li Z, Yu P, Wu J, Tao F, Zhou J. Transcriptional Regulation of Early Growth Response Gene-1 (EGR1) is Associated with Progression of Nonalcoholic Fatty Liver Disease (NAFLD) in Patients with Insulin Resistance. Med Sci Monit. 2019;25:2293-3004. doi:10.12659/MSM.914044

351. Zhang L, Yang SY, Qi-Li FR, Liu XX, Zhang WT, Peng C, Wu P, Li P, Li P, Xu X. Administration of isoliquiritigenin prevents nonalcoholic

fatty liver disease through a novel IQGAP2-CREB-SIRT1 axis. Phytother Res. 2021;35(7):3898-3915. doi:10.1002/ptr.7101

352. Hashemi M, Hoseini H, Yaghmaei P, Moazeni-Roodi A, Bahari A, Hashemzehi N, Shafieipour S. Association of polymorphisms in glutamate-cysteine ligase catalytic subunit and microsomal triglyceride transfer protein genes with nonalcoholic fatty liver disease. DNA Cell Biol. 2011;30(8):569-575. doi:10.1089/dna.2010.1162

353. Shen H, Yu H, Li QY, Wei YT, Fu J, Dong H, Cao D, Guo LN, Chen L, Yang Y, et al. Hepatocyte-derived VEGFA accelerates the progression of non-alcoholic fatty liver disease to hepatocellular carcinoma via activating hepatic stellate cells. Acta Pharmacol Sin. 2022;43(11):2917-2928. doi:10.1038/s41401-022-00907-5

354. Albadawy R, Agwa SHA, Khairy E, Saad M, El Touchy N, Othman M, Matboli M. Clinical Significance of HSPD1/MMP14/ITGB1/miR-6881-5P/Lnc-SPARCL1-1:2 RNA Panel in NAFLD/NASH Diagnosis: Egyptian Pilot Study. Biomedicines. 2021;9(9):1248. doi:10.3390/biomedicines9091248

355. Xin P, Han H, Gao D, Cui W, Yang X, Ying C, Sun X, Hao L. Alleviative effects of resveratrol on nonalcoholic fatty liver disease are associated with up regulation of hepatic low density lipoprotein receptor and scavenger receptor class B type I gene expressions in rats. Food Chem Toxicol. 2013;52:12-18. doi:10.1016/j.fct.2012.10.026

356. Mei Y, Hu H, Deng L, Sun X, Tan W. Therapeutic effects of isosteviol sodium on non-alcoholic fatty liver disease by regulating autophagy via Sirt1/AMPK pathway. Sci Rep. 2022;12(1):12857. doi:10.1038/s41598-022-16119-0

357. Colak Y, Senates E, Ozturk O, Yilmaz Y, Coskunpinar E, Kahraman OT, Sahin O, Zemheri E, Enc FY, Ulasoglu C, et al. Plasma fibrinogen-like protein 2 levels in patients with non-alcoholic fatty liver disease. Hepatogastroenterology. 2011;58(112):2087-2090. doi:10.5754/hge11248

358. Lee J, Song JH, Park JH, Chung MY, Lee SH, Jeon SB, Park SH, Hwang JT, Choi HK. Dnmt1/Tet2-mediated changes in Cmip methylation regulate the development of nonalcoholic fatty liver disease by controlling the Gbp2-Pparγ-CD36 axis. Exp Mol Med. 2023;10.1038/s12276-022-00919-5. doi:10.1038/s12276-022-00919-5

359. Falkevall A, Mehlem A, Folestad E, Ning FC, Osorio-Conles Ó, Radmann R, de Hollanda A, Wright SD, Scotney P, Nash A, et al. Inhibition of VEGF-B signaling prevents non-alcoholic fatty liver disease development by targeting lipolysis in the white adipose tissue. J Hepatol. 2023;S0168-8278(23)00026-0. doi:10.1016/j.jhep.2023.01.014
360. Cai J, Huang J, Yang J, Chen X, Zhang H, Zhu Y, Liu Q, Zhang Z. The protective effect of selenoprotein M on non-alcoholic fatty liver disease: the role of the AMPKα1-MFN2 pathway and Parkin mitophagy. Cell Mol Life Sci. 2022;79(7):354. doi:10.1007/s00018-022-04385-0
361. Zhao YW, Yang J, Niu J, Wang T, Liang XD, Ren Y, Wang R. Pharmacodynamic Evaluation of the Gexia Zhuyu Decoction in the Treatment of NAFLD and the Molecular Mechanism Underlying the TRPM4 Pathway Regulation. Evid Based Complement Alternat Med. 2021;2021:3364579. doi:10.1155/2021/3364579
362. Bertran L, Jorba-Martin R, Barrientos-Riosalido A, Portillo-Carrasquer M, Aguilar C, Riesco D, Martínez S, Vives M, Sabench F, Castillo DD, et al. New Insights of OLFM2 and OLFM4 in Gut-Liver Axis and Their Potential Involvement in Nonalcoholic Fatty Liver Disease. Int J Mol Sci. 2022;23(13):7442. doi:10.3390/ijms23137442
363. Chen L, Li Y, Sottas C, Lazaris A, Petrillo SK, Metrakos P, Li L, Ishida Y, Saito T, Garza S, Papadopoulos V. Loss of mitochondrial ATPase ATAD3A contributes to nonalcoholic fatty liver disease through accumulation of lipids and damaged mitochondria. J Biol Chem. 2022;298(6):102008. doi:10.1016/j.jbc.2022.102008
364. Morikawa M, Mitani Y, Holmborn K, Kato T, Koinuma D, Maruyama J, Vasilaki E, Sawada H, Kobayashi M, Ozawa T, et al. The ALK-1/SMAD/ATOH8 axis attenuates hypoxic responses and protects against the development of pulmonary arterial hypertension. Sci Signal. 2019;12(607):eaay4430. doi:10.1126/scisignal.aay4430
365. Jandl K, Marsh LM, Mutgan AC, Crnkovic S, Valzano F, Zabini D, Hoffmann J, Foris V, Gschwandtner E, Klepetko W, et al. Impairment of the NKT-STAT1-CXCL9 Axis Contributes to Vessel Fibrosis in Pulmonary Hypertension Caused by Lung Fibrosis. Am J Respir Crit Care Med. 2022;206(8):981-998. doi:10.1164/rccm.202201-0142OC

366. Shah SFA, Iqbal T, Qamar R, Rafiq MA, Hussain S. ARG1 Gene Polymorphisms and Their Association in Individuals with Essential Hypertension: A Case-Control Study. DNA Cell Biol. 2018;37(7):609-616. doi:10.1089/dna.2018.4222
367. Mehta JL, Ding Z, Liu S, Wang X, Khaidakov M. Hypertension, TLR4 activation in brain and cardiac hypertrophy. Cardiovasc Res. 2014;103(1):3-4. doi:10.1093/cvr/cvu128
368. Fava C, Montagnana M, Danese E, Sjögren M, Almgren P, Engström G, Hedblad B, Guidi GC, Minuz P, Melander O. Vanin-1 T26I polymorphism, hypertension and cardiovascular events in two large urban-based prospective studies in Swedes. Nutr Metab Cardiovasc Dis. 2013;23(1):53-60. doi:10.1016/j.numecd.2011.01.012
369. Dong Y, Lin Y, Liu W, Zhang W, Jiang Y, Song W. Atrial Natriuretic Peptide Inhibited ABCA1/G1-dependent Cholesterol Efflux Related to Low HDL-C in Hypertensive Pregnant Patients. Front Pharmacol. 2021;12:715302. doi:10.3389/fphar.2021.715302
370. Bouças AP, Brondani LA, Souza BM, Lemos NE, de Oliveira FS, Canani LH, Crispim D. The A allele of the rs1990760 polymorphism in the IFIH1 gene is associated with protection for arterial hypertension in type 1 diabetic patients and with expression of this gene in human mononuclear cells. PLoS One. 2013;8(12):e83451. doi:10.1371/journal.pone.0083451
371. Xing Y, Zhao S, Wei Q, Gong S, Zhao X, Zhou F, Ai-Lamki R, Ortmann D, Du M, Pedersen R, et al. A novel piperidine identified by stem cell-based screening attenuates pulmonary arterial hypertension by regulating BMP2 and PTGS2 levels. Eur Respir J. 2018;51(4):1702229. doi:10.1183/13993003.02229-201
372. Chen L, Xiao T, Chen L, Xie S, Deng M, Wu D. The Association of ADRB1 and CYP2D6 Polymorphisms With Antihypertensive Effects and Analysis of Their Contribution to Hypertension Risk. Am J Med Sci. 2018;355(3):235-239. doi:10.1016/j.amjms.2017.11.002
373. Yuan K, Shao NY, Hennigs JK, Discipulo M, Orcholski ME, Shamskhou E, Richter A, Hu X, Wu JC, de Jesus Perez VA. Increased Pyruvate Dehydrogenase Kinase 4 Expression in Lung Pericytes Is Associated with Reduced Endothelial-Pericyte Interactions and Small Vessel

Loss in Pulmonary Arterial Hypertension. Am J Pathol. 2016;186(9):2500-2514. doi:10.1016/j.ajpath.2016.05.016

374. Hiraide T, Kataoka M, Suzuki H, Aimi Y, Chiba T, Isobe S, Katsumata Y, Goto S, Kanekura K, Yamada Y, et al. Poor outcomes in carriers of the RNF213 variant (p.Arg4810Lys) with pulmonary arterial hypertension. J Heart Lung Transplant. 2020;39(2):103-112. doi:10.1016/j.healun.2019.08.022

375. Zhang L, Wang Y, Wu G, Rao L, Wei Y, Yue H, Yuan T, Yang P, Xiong F, Zhang S, et al. Blockade of JAK2 protects mice against hypoxia-induced pulmonary arterial hypertension by repressing pulmonary arterial smooth muscle cell proliferation. Cell Prolif. 2020;53(2):e12742. doi:10.1111/cpr.12742

376. Sahoo S, Li Y, de Jesus D, Sembrat J, Rojas MM, Goncharova E, Cifuentes-Pagano E, Straub AC, Pagano PJ. Notch2 suppression mimicking changes in human pulmonary hypertension modulates Notch1 and promotes endothelial cell proliferation. Am J Physiol Heart Circ Physiol. 2021;321(3):H542-H557. doi:10.1152/ajpheart.00125.2021

377. van Roeyen CRC, Martin IV, Drescher A, Schuett KA, Hermert D, Raffetseder U, Otten S, Buhl EM, Braun GS, Kuppe C, et al. Identification of platelet-derived growth factor C as a mediator of both renal fibrosis and hypertension. Kidney Int. 2019;95(5):1103-1119. doi:10.1016/j.kint.2018.11.031

378. Holmes L Jr, Lim A, Comeaux CR, Dabney KW, Okundaye O. DNA Methylation of Candidate Genes (ACE II, IFN-γ, AGTR 1, CKG, ADD1, SCNN1B and TLR2) in Essential Hypertension: A Systematic Review and Quantitative Evidence Synthesis. Int J Environ Res Public Health. 2019;16(23):4829. doi:10.3390/ijerph16234829

379. Zaabalawi A, Renshall L, Beards F, Lightfoot AP, Degens H, Alexander Y, Hasan R, Bilal H, Graf BA, Harris LK, et al. Internal Mammary Arteries as a Model to Demonstrate Restoration of the Impaired Vasodilation in Hypertension, Using Liposomal Delivery of the CYP1B1 Inhibitor, 2,3',4,5'-Tetramethoxystilbene. Pharmaceutics. 2022;14(10):2046. doi:10.3390/pharmaceutics14102046

380. Yang SA. Exonic polymorphism (rs315952, Ser133Ser) of interleukin 1 receptor antagonist (IL1RN) is related to overweigh/obese with

hypertension. J Exerc Rehabil. 2014;10(5):332-336. doi:10.12965/jer.140155

381. Wang Z, Cheng C, Yang X, Zhang C. L-phenylalanine attenuates high salt-induced hypertension in Dahl SS rats through activation of GCH1-BH4. PLoS One. 2021;16(4):e0250126. doi:10.1371/journal.pone.0250126

382. Laggner M, Oberndorfer F, Golabi B, Bauer J, Zuckermann A, Hacker P, Lang I, Skoro-Sajer N, Gerges C, Taghavi S, et al. EGR1 Is Implicated in Right Ventricular Cardiac Remodeling Associated with Pulmonary Hypertension. Biology (Basel). 2022;11(5):677. doi:10.3390/biology11050677

383. Li Z, Hu X, Wan J, Yang J, Jia Z, Tian L, Wu X, Song C, Yan C. The alleles of AGT and HIF1A gene affect the risk of hypertension in plateau residents. Exp Biol Med (Maywood). 2022;247(3):237-245. doi:10.1177/15353702211055838

384. Miwa Y, Kamide K, Takiuchi S, Yoshii M, Horio T, Tanaka C, Banno M, Miyata T, Kawano Y. Association of PLA2G7 polymorphisms with carotid atherosclerosis in hypertensive Japanese. Hypertens Res. 2009;32(12):1112-1118. doi:10.1038/hr.2009.151

385. Abid S, Marcos E, Parpaleix A, Amsellem V, Breau M, Houssaini A, Vienney N, Lefevre M, Derumeaux G, Evans S, et al. CCR2/CCR5-mediated macrophage-smooth muscle cell crosstalk in pulmonary hypertension. Eur Respir J. 2019;54(4):1802308. doi:10.1183/13993003.02308-2018

386. Jiang B, Deng Q, Huo Y, Li W, Shibuya M, Luo J. Endothelial Gab1 deficiency aggravates splenomegaly in portal hypertension independent of angiogenesis. Am J Physiol Gastrointest Liver Physiol. 2015;308(5):G416-G426. doi:10.1152/ajpgi.00292.2014

387. Patel N, Moenkemeyer F, Germano S, Cheung MM. Plasma vascular endothelial growth factor A and placental growth factor: novel biomarkers of pulmonary hypertension in congenital diaphragmatic hernia. Am J Physiol Lung Cell Mol Physiol. 2015;308(4):L378-L383. doi:10.1152/ajplung.00261.2014

388. Barnes JW, Tian L, Heresi GA, Farver CF, Asosingh K, Comhair SA, Aulak KS, Dweik RA. O-linked β-N-acetylglucosamine transferase directs

cell proliferation in idiopathic pulmonary arterial hypertension. Circulation. 2015;131(14):1260-1268. doi:10.1161/CIRCULATIONAHA.114.0138

389. Dianat M, Radan M, Mard SA, Sohrabi F, Saryazdi SSN. Contribution of reactive oxygen species via the OXR1 signaling pathway in the pathogenesis of monocrotaline-induced pulmonary arterial hypertension: The protective role of Crocin. Life Sci. 2020;256:117848. doi:10.1016/j.lfs.2020.117848

390. Chen YJ, Li Y, Guo X, Huo B, Chen Y, He Y, Xiao R, Zhu XH, Jiang DS, Wei X. Upregulation of IRF9 Contributes to Pulmonary Artery Smooth Muscle Cell Proliferation During Pulmonary Arterial Hypertension. Front Pharmacol. 2021;12:773235. doi:10.3389/fphar.2021.773235

391. Hamlin AA, Sukharev D, Campos L, Mu Y, Tassone F, Hessl D, Nguyen DV, Loesch D, Hagerman RJ. Hypertension in FMR1 premutation males with and without fragile X-associated tremor/ataxia syndrome (FXTAS). Am J Med Genet A. 2012;158A(6):1304-1309. doi:10.1002/ajmg.a.35323

392. Calvier L, Herz J, Hansmann G. Interplay of Low-Density Lipoprotein Receptors, LRPs, and Lipoproteins in Pulmonary Hypertension. JACC Basic Transl Sci. 2022;7(2):164-180. doi:10.1016/j.jacbts.2021.09.011

393. Yeganeh-Hajahmadi M, Najafipour H, Rostamzadeh F, Naghibzadeh-Tahami A. Klotho and SIRT1 changes from pre-diabetes to diabetes and pre-hypertension to hypertension. Diabetol Metab Syndr. 2021;13(1):115. doi:10.1186/s13098-021-00736-2

394. Kwon MY, Hwang N, Park YJ, Perrella MA, Chung SW. NOD2 deficiency exacerbates hypoxia-induced pulmonary hypertension and enhances pulmonary vascular smooth muscle cell proliferation. Oncotarget. 2018;9(16):12671-12681. doi:10.18632/oncotarget.23912

395. Machado RD, Welch CL, Haimel M, Bleda M, Colglazier E, Coulson JD, Debeljak M, Ekstein J, Fineman JR, Golden WC, et al. Biallelic variants of ATP13A3 cause dose-dependent childhood-onset pulmonary arterial hypertension characterised by extreme morbidity and mortality. J Med Genet. 2022;59(9):906-911. doi:10.1136/jmedgenet-2021-107831

396. Chang YT, Chan CK, Eriksson I, Johnson PY, Cao X, Westöö C, Norvik C, Andersson-Sjöland A, Westergren-Thorsson G, Johansson S, et

al. Versican accumulates in vascular lesions in pulmonary arterial hypertension. Pulm Circ. 2016;6(3):347-359. doi:10.1086/686994

397. Fan C, Wang J, Mao C, Li W, Liu K, Wang Z. The FGL2 prothrombinase contributes to the pathological process of experimental pulmonary hypertension. J Appl Physiol (1985). 2019;127(6):1677-1687. doi:10.1152/japplphysiol.00396.2019

398. Hiraide T, Suzuki H, Shinya Y, Momoi M, Inami T, Katsumata Y, Fukuda K, Kosaki K, Kataoka M. TET2 Variants in Japanese Patients With Pulmonary Arterial Hypertension. CJC Open. 2021;4(4):416-419. doi:10.1016/j.cjco.2021.11.008

399. Salguero MV, Chan K, Greeley SAW, Dyamenahalli U, Waggoner D, Del Gaudio D, Rajiyah T, Lemelman M. Novel KDM6A Kabuki Syndrome Mutation With Hyperinsulinemic Hypoglycemia and Pulmonary Hypertension Requiring ECMO. J Endocr Soc. 2022;6(4):bvac015. doi:10.1210/jendso/bvac015

400. Zhang C, Meermeier NP, Terker AS, Blankenstein KI, Singer JD, Hadchouel J, Ellison DH, Yang CL. Degradation by Cullin 3 and effect on WNK kinases suggest a role of KLHL2 in the pathogenesis of Familial Hyperkalemic Hypertension. Biochem Biophys Res Commun. 2016;469(1):44-48. doi:10.1016/j.bbrc.2015.11.067

401. Liu J, Ke X, Wang L, Zhang Y, Yang J. Deficiency of cold-inducible RNA-binding protein exacerbated monocrotaline-induced pulmonary artery hypertension through Caveolin1 and CAVIN1. J Cell Mol Med. 2021;25(10):4732-4743. doi:10.1111/jcmm.16437

402. Mashimo Y, Suzuki Y, Hatori K, Tabara Y, Miki T, Tokunaga K, Katsuya T, Ogihara T, Yamada M, Takahashi N, et al. Association of TNFRSF4 gene polymorphisms with essential hypertension. J Hypertens. 2008;26(5):902-913. doi:10.1097/HJH.0b013e3282f6a65e

403. Kurrek MM, Winkler M, Robinson DR, Zapol WM. Platelet factor 4 injection produces acute pulmonary hypertension in the awake lamb. Anesthesiology. 1995;82(1):183-31A. doi:10.1097/00000542-199501000-00023

404. Cai M, Li X, Dong H, Wang Y, Huang X. CCR7 and its related molecules may be potential biomarkers of pulmonary arterial hypertension. FEBS Open Bio. 2021;11(6):1565-1578. doi:10.1002/2211-5463.13130

405. Mahal Z, Fujikawa K, Matsuo H, Zahid HM, Koike M, Misumi M, Kaneko T, Mashimo T, Ohara H, Nabika T. Effects of the Prdx2 depletion on blood pressure and life span in spontaneously hypertensive rats. Hypertens Res. 2019;42(5):610-617. doi:10.1038/s41440-019-0207-9
406. Nam MH, Nahomi RB, Pantcheva MB, Dhillon A, Chiodo VA, Smith WC, Nagaraj RH. AAV2-Mediated Expression of HspB1 in RGCs Prevents Somal Damage and Axonal Transport Deficits in a Mouse Model of Ocular Hypertension. Transl Vis Sci Technol. 2022;11(11):8. doi:10.1167/tvst.11.11.8
407. Huang CX, Jiang ZX, Du DY, Zhang ZM, Liu Y, Li YT. Hsa_circ_0016070/micro-340-5p Axis Accelerates Pulmonary Arterial Hypertension Progression by Upregulating TWIST1 Transcription Via TCF4/β-Catenin Complex. J Am Heart Assoc. 2022;11(14):e024147. doi:10.1161/JAHA.121.024147
408. Zhao Q, Sun H, Yin L, Wang L. miR□126a□5p□Dbp and miR□31a□Crot/Mrpl4 interaction pairs crucial for the development of hypertension and stroke. Mol Med Rep. 2019;20(5):4151-4167. doi:10.3892/mmr.2019.10679
409. Schinagl C, Melum GR, Rødningen OK, Bjørgo K, Andresen JH. Severe persistent pulmonary hypertension of the newborn and dysmorphic features in neonate with a deletion involving TWIST1 and PHF14: a case report. J Med Case Rep. 2017;11(1):226. doi:10.1186/s13256-017-1402-4
410. Mathar I, Vennekens R, Meissner M, Kees F, Van der Mieren G, Camacho Londoño JE, Uhl S, Voets T, Hummel B, van den Bergh A, et al. Increased catecholamine secretion contributes to hypertension in TRPM4-deficient mice. J Clin Invest. 2010;120(9):3267-3279. doi:10.1172/JCI41348
411. da Silva IV, Santos AC, Matos A, Pereira da Silva A, Soveral G, Rebelo I, Bicho M. Association of Aquaporin-3, Aquaporin-7, NOS3 and CYBA polymorphisms with hypertensive disorders in women. Pregnancy Hypertens. 2021;24:44-49. doi:10.1016/j.preghy.2021.02.008
412. Bai P, Lyu L, Yu T, Zuo C, Fu J, He Y, Wan Q, Wan N, Jia D, Lyu A. Macrophage-Derived Legumain Promotes Pulmonary Hypertension by Activating the MMP (Matrix Metalloproteinase)-2/TGF (Transforming Growth Factor)-β1 Signaling. Arterioscler Thromb Vasc Biol. 2019;39(4):e130-e145. doi:10.1161/ATVBAHA.118.312254

413. Yu P, Liang P, Pang S, Yuan W, Zhao Y, Huang Q. The Function, Role and Process of DDX58 in Heart Failure and Human Cancers. Front Oncol. 2022;12:911309. doi:10.3389/fonc.2022.911309
414. Wu L, Archacki SR, Zhang T, Wang QK. Induction of high STAT1 expression in transgenic mice with LQTS and heart failure. Biochem Biophys Res Commun. 2007;358(2):449-454. doi:10.1016/j.bbrc.2007.04.119
415. Liao M, Xie Q, Zhao Y, Yang C, Lin C, Wang G, Liu B, Zhu L. Main active components of Si-Miao-Yong-An decoction (SMYAD) attenuate autophagy and apoptosis via the PDE5A-AKT and TLR4-NOX4 pathways in isoproterenol (ISO)-induced heart failure models. Pharmacol Res. 2022;176:106077. doi:10.1016/j.phrs.2022.106077
416. Luzum JA, Sweet KM, Binkley PF, Schmidlen TJ, Jarvis JP, Christman MF, Sadee W, Kitzmiller JP. CYP2D6 Genetic Variation and Beta-Blocker Maintenance Dose in Patients with Heart Failure. Pharm Res. 2017;34(8):1615-1625. doi:10.1007/s11095-017-2104-8
417. Sano S, Wang Y, Yura Y, Sano M, Oshima K, Yang Y, Katanasaka Y, Min KD, Matsuura S, Ravid K, et al. JAK2V617F -Mediated Clonal Hematopoiesis Accelerates Pathological Remodeling in Murine Heart Failure. JACC Basic Transl Sci. 2019;4(6):684-697. doi:10.1016/j.jacbts.2019.05.013
418. Liang S, Xinyong C, Hongmin Z, Jing W, Lang H, Ping Z. TLR2 and TLR3 expression as a biomarker for the risk of doxorubicin-induced heart failure. Toxicol Lett. 2018;295:205-211. doi:10.1016/j.toxlet.2018.06.1219
419. Maillet M, Purcell NH, Sargent MA, York AJ, Bueno OF, Molkentin JD. DUSP6 (MKP3) null mice show enhanced ERK1/2 phosphorylation at baseline and increased myocyte proliferation in the heart affecting disease susceptibility. J Biol Chem. 2008;283(45):31246-31255. doi:10.1074/jbc.M806085200
420. Liao PP, Liu LH, Wang B, Fang X, Zhou SQ, Li W, Zhang YQ, Guan SM. Correlation between Histone Deacetylase 9 and Regulatory T Cell in Patients with Chronic Heart Failure. Curr Med Sci. 2018;38(2):199-203. doi:10.1007/s11596-018-1866-5
421. Shao D, Zhai P, Hu C, Mukai R, Sciarretta S, Del Re D, Sadoshima J.Lats2 promotes heart failure by stimulating p53-mediated apoptosis during

pressure overload. Sci Rep. 2021;11(1):23469. doi:10.1038/s41598-021-02846-3

422. Deng Y, Wang J, Xie G, Zeng X, Li H. Circ-HIPK3 Strengthens the Effects of Adrenaline in Heart Failure by MiR-17-3p - ADCY6 Axis. Int J Biol Sci. 2019;15(11):2484-2496. doi:10.7150/ijbs.36149

423. Ortlepp JR, Vesper K, Mevissen V, Schmitz F, Janssens U, Franke A, Hanrath P, Weber C, Zerres K, Hoffmann R. Chemokine receptor (CCR2) genotype is associated with myocardial infarction and heart failure in patients under 65 years of age. J Mol Med (Berl). 2003;81(6):363-367. doi:10.1007/s00109-003-0435-x

424. Li J, Yue G, Ma W, Zhang A, Zou J, Cai Y, Tang X, Wang J, Liu J, Li H, et al. Ufm1-Specific Ligase Ufl1 Regulates Endoplasmic Reticulum Homeostasis and Protects Against Heart Failure. Circ Heart Fail. 2018;11(10):e004917. doi:10.1161/CIRCHEARTFAILURE.118.004917

425. Watson LJ, Facundo HT, Ngoh GA, Ameen M, Brainard RE, Lemma KM, Long BW, Prabhu SD, Xuan YT, Jones SP. O-linked β-N-acetylglucosamine transferase is indispensable in the failing heart. Proc Natl Acad Sci U S A. 2010;107(41):17797-17802. doi:10.1073/pnas.1001907107

426. Lin B, Zhao H, Li L, Zhang Z, Jiang N, Yang X, Zhang T, Lian B, Liu Y, Zhang C, et al. Sirt1 improves heart failure through modulating the NF-κB p65/microRNA-155/BNDF signaling cascade. Aging (Albany NY). 2020;13(10):14482-14498. doi:10.18632/aging.103640

427. You Y, Huang S, Liu H, Fan C, Liu K, Wang Z. Soluble fibrinogen□like protein 2 levels are decreased in patients with ischemic heart failure and associated with cardiac function. Mol Med Rep. 2021;24(2):559. doi:10.3892/mmr.2021.12198

428. Assmus B, Cremer S, Kirschbaum K, Culmann D, Kiefer K, Dorsheimer L, Rasper T, Abou-El-Ardat K, Herrmann E, Berkowitsch A, et al. Clonal haematopoiesis in chronic ischaemic heart failure: prognostic role of clone size for DNMT3A- and TET2-driver gene mutations. Eur Heart J. 2021;42(3):257-265. doi:10.1093/eurheartj/ehaa845

429. Cao Y, Pan C, Wang YC, Zhou Z, Jedian V, Meng Y, Campbell G, Guardino K, Li C, Wang J, et al. Identification of DNA Damage Repair Enzyme Ascc2 as Causal for Heart Failure With Preserved Ejection

Fraction. Circulation. 2022;145(14):1102-1104. doi:10.1161/CIRCULATIONAHA.121.055857
430. Gambardella J, Wang XJ, Ferrara J, Morelli MB, Santulli G. Cardiac BIN1 Replacement Therapy Ameliorates Inotropy and Lusitropy in Heart Failure by Regulating Calcium Handling. JACC Basic Transl Sci. 2020;5(6):579-581. doi:10.1016/j.jacbts.2020.03.018
431. Marunouchi T, Abe Y, Murata M, et al. Changes in small heat shock proteins HSPB1, HSPB5 and HSPB8 in mitochondria of the failing heart following myocardial infarction in rats. Biol Pharm Bull. 2013;36(4):529-539. doi:10.1248/bpb.b12-00796
432. Konev AA, Kharitonov AV, Rozov FN, Altshuler EP, Serebryanaya DV, Lassus J, Harjola VP, Katrukha AG, Postnikov AB. CT-IGFBP-4 as a novel prognostic biomarker in acute heart failure. ESC Heart Fail. 2020;7(2):434-444. doi:10.1002/ehf2.12590
433. Feng J, Zong P, Yan J, Yue Z, Li X, Smith C, Ai X, Yue L. Upregulation of transient receptor potential melastatin 4 (TRPM4) in ventricular fibroblasts from heart failure patients. Pflugers Arch. 2021;473(3):521-531. doi:10.1007/s00424-021-02525-2
434. Vlachou F, Varela A, Stathopoulou K, Ntatsoulis K, Synolaki E, Pratsinis H, Kletsas D, Sideras P, Davos CH, Capetanaki Y, et al. Galectin-3 interferes with tissue repair and promotes cardiac dysfunction and comorbidities in a genetic heart failure model. Cell Mol Life Sci. 2022;79(5):250. doi:10.1007/s00018-022-04266-6
435. Saadatian Z, Nariman-Saleh-Fam Z, Bastami M, Mansoori Y, Khaheshi I, Parsa SA, Daraei A, Vahed SZ, Yousefi B, Kafil HS, et al. Dysregulated expression of STAT1, miR-150, and miR-223 in peripheral blood mononuclear cells of coronary artery disease patients with significant or insignificant stenosis. J Cell Biochem. 2019;120(12):19810-19824. doi:10.1002/jcb.29286
436. Du P, Gao K, Cao Y, Yang S, Wang Y, Guo R, Zhao M, Jia S. RFX1 downregulation contributes to TLR4 overexpression in CD14+ monocytes via epigenetic mechanisms in coronary artery disease. Clin Epigenetics. 2019;11(1):44. doi:10.1186/s13148-019-0646-9
437. Fan Q, Zhu Y, Zhao F. Association of rs2230806 in ABCA1 with coronary artery disease: An updated meta-analysis based on 43 research

studies. Medicine (Baltimore). 2020;99(4):e18662. doi:10.1097/MD.0000000000018662
438. Bhat MA, Gandhi G. CYP2D6 (C2850T, G1846A, C100T) polymorphisms, haplotypes and MDR analysis in predicting coronary artery disease risk in north-west Indian population: A case-control study. Gene. 2018;663:17-24. doi:10.1016/j.gene.2018.04.008
439. de Vries MA, Trompet S, Mooijaart SP, Smit RA, Böhringer S, Castro Cabezas M, Jukema JW. Complement receptor 1 gene polymorphisms are associated with cardiovascular risk. Atherosclerosis. 2017;257:16-21. doi:10.1016/j.atherosclerosis.2016.12.017
440. Du P, Guo R, Gao K, Yang S, Yao B, Cui H, Zhao M, Jia S. Identification of differentially expressed genes and the role of PDK4 in CD14+ monocytes of coronary artery disease. Biosci Rep. 2021;41(4):BSR20204124. doi:10.1042/BSR20204124
441. Morimoto T, Mineharu Y, Ono K, Nakatochi M, Ichihara S, Kabata R, Takagi Y, Cao Y, Zhao L, Kobayashi H, et al. Significant association of RNF213 p.R4810K, a moyamoya susceptibility variant, with coronary artery disease. PLoS One. 2017;12(4):e0175649. doi:10.1371/journal.pone.0175649
442. Chen Z, Ma G, Qian Q, Yao Y, Feng Y, Tang C. Toll-like receptor 8 polymorphism and coronary artery disease. Mol Biol Rep. 2009;36(7):1897-1901. doi:10.1007/s11033-008-9396-z
443. Lee C, Li X. Platelet-derived growth factor-C and -D in the cardiovascular system and diseases. Mol Aspects Med. 2018;62:12-21. doi:10.1016/j.mam.2017.09.005
444. Qi B, Chen JH, Tao L, Zhu CM, Wang Y, Deng GX, Miao L. Integrated Weighted Gene Co-expression Network Analysis Identified That TLR2 and CD40 Are Related to Coronary Artery Disease. Front Genet. 2021;11:613744. doi:10.3389/fgene.2020.613744
445. Mir R, Elfaki I, Jha CK, Javid J, Babakr AT, Banu S, Mir MM, Jamwal D, Khullar N, Alzahrani KJ, et al. Biological and Clinical Implications of TNF-α Promoter and CYP1B1 Gene Variations in Coronary Artery Disease Susceptibility. Cardiovasc Hematol Disord Drug Targets. 2021;21(4):266-277. doi:10.2174/1871529X22666211221151830

446. Ma L, Bryce NS, Turner AW, Di Narzo AF, Rahman K, Xu Y, Ermel R, Sukhavasi K, d'Escamard V, Chandel N, et al. The HDAC9-associated risk locus promotes coronary artery disease by governing TWIST1. PLoS Genet. 2022;18(6):e1010261. doi:10.1371/journal.pgen.1010261
447. Arman A, Soylu O, Yildirim A, Furman A, Ercelen N, Aydogan H, Coker A, Tezel T. Interleukin-1 receptor antagonist gene VNTR polymorphism is associated with coronary artery disease. Arq Bras Cardiol. 2008;91(5):293-298. doi:10.1590/s0066-782x2008001700002
448. Antoniades C, Shirodaria C, Van Assche T, Cunnington C, Tegeder I, Lötsch J, Guzik TJ, Leeson P, Diesch J, Tousoulis D, et al. GCH1 haplotype determines vascular and plasma biopterin availability in coronary artery disease effects on vascular superoxide production and endothelial function. J Am Coll Cardiol. 2008;52(2):158-165. doi:10.1016/j.jacc.2007.12.062
449. Peng J, Xiang Y. Value analysis of CD69 combined with EGR1 in the diagnosis of coronary heart disease. Exp Ther Med. 2019;17(3):2047-2052. doi:10.3892/etm.2019.7175
450. Rafiei A, Khodabakhsh F, Cohan RA, Azadegan-Dehkordi F, Salimian M. The correlation of long non-coding RNAs IFNG-AS1 and ZEB2-AS1 with IFN-γ and ZEB-2 expression in PBMCs and clinical features of patients with coronary artery disease. Mol Biol Rep. 2022;49(5):3389-3399. doi:10.1007/s11033-022-07168-9
451. Casas JP, Ninio E, Panayiotou A, Palmen J, Cooper JA, Ricketts SL, Sofat R, Nicolaides AN, Corsetti JP, Fowkes FG, et al. PLA2G7 genotype, lipoprotein-associated phospholipase A2 activity, and coronary heart disease risk in 10 494 cases and 15 624 controls of European Ancestry. Circulation. 2010;121(21):2284-2293. doi:10.1161/CIRCULATIONAHA.109.92338
452. Golbus JR, Stitziel NO, Zhao W, Xue C, Farrall M, McPherson R, Erdmann J, Deloukas P, Watkins H, Schunkert H, et al. Common and Rare Genetic Variation in CCR2, CCR5, or CX3CR1 and Risk of Atherosclerotic Coronary Heart Disease and Glucometabolic Traits. Circ Cardiovasc Genet. 2016;9(3):250-258. doi:10.1161/CIRCGENETICS.115.001374
453. Wang Y, Huang Q, Liu J, Wang Y, Zheng G, Lin L, Yu H, Tang W, Huang Z. Vascular endothelial growth factor A polymorphisms are associated with increased risk of coronary heart disease: a meta-analysis. Oncotarget. 2017;8(18):30539-30551. doi:10.18632/oncotarget.15546

454. Mishra N, Mohata M, Narang R, Lakshmy R, Hazarika A, Pandey RM, Das N, Luthra K. Altered Expression of Complement Regulatory Proteins CD35, CD46, CD55, and CD59 on Leukocyte Subsets in Individuals Suffering From Coronary Artery Disease. Front Immunol. 2019;10:2072. doi:10.3389/fimmu.2019.02072
455. Coto E, Reguero JR, Avanzas P, Pascual I, Martín M, Hevia S, Morís C, Díaz-Molina B, Lambert JL, Alonso B, et al. Gene variants in the NF-KB pathway (NFKB1, NFKBIA, NFKBIZ) and risk for early-onset coronary artery disease. Immunol Lett. 2019;208:39-43. doi:10.1016/j.imlet.2019.02.007
456. Gretarsdottir S, Helgason H, Helgadottir A, Sigurdsson A, Thorleifsson G, Magnusdottir A, Oddsson A, Steinthorsdottir V, Rafnar T, de Graaf J, et al. A Splice Region Variant in LDLR Lowers Non-high Density Lipoprotein Cholesterol and Protects against Coronary Artery Disease. PLoS Genet. 2015;11(9):e1005379. doi:10.1371/journal.pgen.1005379
457. Wang C, Li Q, Yang H, Gao C, Du Q, Zhang C, Zhu L, Li Q. MMP9, CXCR1, TLR6, and MPO participant in the progression of coronary artery disease. J Cell Physiol. 2020;235(11):8283-8292. doi:10.1002/jcp.29485
458. Askin L, Tibilli H, Tanriverdi O, Turkmen S. The relationship between coronary artery disease and SIRT1 protein. North Clin Istanb. 2020;7(6):631-635. doi:10.14744/nci.2020.31391
459. Galluzzo S, Patti G, Dicuonzo G, Di Sciascio G, Tonini G, Ferraro E, Spoto C, Campanale R, Zoccoli A, Angeletti S. Association between NOD2/CARD15 polymorphisms and coronary artery disease: a case-control study. Hum Immunol. 2011;72(8):636-640. doi:10.1016/j.humimm.2011.04.005
460. Cheng J, Chen Y, Xu B, Wu J, He F. Association of Soluble Fibrinogen-like Protein 2 with the Severity of Coronary Artery Disease. Intern Med. 2016;55(17):2343-2350. doi:10.2169/internalmedicine.55.6149
461. Kattih B, Shirvani A, Klement P, Garrido AM, Gabdoulline R, Liebich A, Brandes M, Chaturvedi A, Seeger T, Thol F, et al. IDH1/2 mutations in acute myeloid leukemia patients and risk of coronary artery disease and cardiac dysfunction-a retrospective propensity score analysis. Leukemia. 2021;35(5):1301-1316. doi:10.1038/s41375-020-01043-x

462. Opstad TB, Solheim S, Pettersen AR, Kalstad AA, Arnesen H, Seljeflot I. TERT and TET2 Genetic Variants Affect Leukocyte Telomere Length and Clinical Outcome in Coronary Artery Disease Patients-A Possible Link to Clonal Hematopoiesis. Biomedicines. 2022;10(8):2027. doi:10.3390/biomedicines10082027
463. Gao J, Feng W, Lv W, Liu W, Fu C. HIF-1/AKT Signaling-Activated PFKFB2 Alleviates Cardiac Dysfunction and Cardiomyocyte Apoptosis in Response to Hypoxia. Int Heart J. 2021;62(2):350-358. doi:10.1536/ihj.20-315
464. Dai H, Zhao N, Zheng Y. CircLDLR Modulates the Proliferation and Apoptosis of Vascular Smooth Muscle Cells in Coronary Artery Disease Through miR-26-5p/KDM6A Axis. J Cardiovasc Pharmacol. 2022;80(1):132-139. doi:10.1097/FJC.0000000000001275
465. Ye H, Hong Q, Li Y, Xu X, Huang YI, Xu L, Zhou A, Deng Y, Duan S. lack of association between the IKZF2 rs12619285 polymorphism and coronary heart disease. Exp Ther Med. 2015;9(4):1309-1313. doi:10.3892/etm.2015.2282
466. Guo J, Wang Q, Liu Y, Lu L, Hua Y, Hu R, Wang M, Li Z, Wang X, Wang BH, et al. Association of expression of ZNF606 gene from monocytes with the risk of coronary artery disease. Clin Biochem. 2018;60:44-51. doi:10.1016/j.clinbiochem.2018.08.005
467. Sadayasu T, Nakashima Y, Yashiro A, Kawashima T, Kuroiwa A. Heparin-releasable platelet factor 4 in patients with coronary artery disease. Clin Cardiol. 1991;14(9):725-729. doi:10.1002/clc.4960140906
468. Hueso M, Mallén A, Casas Á, Guiteras J, Sbraga F, Blasco-Lucas A, Lloberas N, Torras J, Cruzado JM, Navarro E. Integrated miRNA/mRNA Counter-Expression Analysis Highlights Oxidative Stress-Related Genes CCR7 and FOXO1 as Blood Markers of Coronary Arterial Disease. Int J Mol Sci. 2020;21(6):1943. doi:10.3390/ijms21061943
469. Su Z, Lu H, Jiang H, Zhu H, Li Z, Zhang P, Ni P, Shen H, Xu W, Xu H. IFN-γ-producing Th17 cells bias by HMGB1-T-bet/RUNX3 axis might contribute to progression of coronary artery atherosclerosis. Atherosclerosis. 2015;243(2):421-428. doi:10.1016/j.atherosclerosis.2015.09.0
470. Zafar U, Khaliq S, Ali Z, Lone KP. TCF7-L2 rs7903146 polymorphism in metabolic syndrome with and without acute coronary

syndrome. J Pak Med Assoc. 2020;70(10):1774-1778. doi:10.5455/JPMA.45480
471. Mansanguan C, Maneerat Y. PPBP gene as a biomarker for coronary heart disease risk in postmenopausal Thai women. PeerJ. 2022;10:e13615. doi:10.7717/peerj.13615
472. Cai H, Wang XL, Wilcken DE. Genetic polymorphism of heparan sulfate proteoglycan (perlecan, HSPG2), lipid profiles and coronary artery disease in the Australian population. Atherosclerosis. 2000;148(1):125-129. doi:10.1016/s0021-9150(99)00213-0
473. Zhen C, Liu H, Gao L, Tong Y, He C. Signal transducer and transcriptional activation 1 protects against pressure overload-induced cardiac hypertrophy. FASEB J. 2021;35(1):e21240. doi:10.1096/fj.202000325RRR
474. Hao L, Ren M, Rong B, Xie F, Lin MJ, Zhao YC, Yue X, Han WQ, Zhong JQ. TWEAK/Fn14 mediates atrial-derived HL-1 myocytes hypertrophy via JAK2/STAT3 signalling pathway. J Cell Mol Med. 2018;22(9):4344-4353. doi:10.1111/jcmm.13724
475. Alsaad AMS. Dasatinib induces gene expression of CYP1A1, CYP1B1, and cardiac hypertrophy markers (BNP, β-MHC) in rat cardiomyocyte H9c2 cells. Toxicol Mech Methods. 2018;28(9):678-684. doi:10.1080/15376516.2018.1497746
476. Zhang J, Liang Y, Huang X, Guo X, Liu Y, Zhong J, Yuan J. STAT3-induced upregulation of lncRNA MEG3 regulates the growth of cardiac hypertrophy through miR-361-5p/HDAC9 axis. Sci Rep. 2019;9(1):460. doi:10.1038/s41598-018-36369-1
477. Cheng Z, Liu L, Li Q. lncRNA ZEB2-AS1 stimulates cardiac hypertrophy by downregulating PTEN. Exp Ther Med. 2020;20(5):92. doi:10.3892/etm.2020.9220
478. Wang Y. Fill a Gab(1) in cardiac hypertrophy signaling: search a missing link between gp130 and ERK5 in hypertrophic remodeling in heart. Circ Res. 2003;93(3):186-188. doi:10.1161/01.RES.0000087333.88497.AE
479. Jiang DS, Luo YX, Zhang R, Zhang XD, Chen HZ, Zhang Y, Chen K, Zhang SM, Fan GC, Liu PP, et al. Interferon regulatory factor 9 protects against cardiac hypertrophy by targeting myocardin. Hypertension. 2014;63(1):119-127. doi:10.1161/HYPERTENSIONAHA.113.02083

480. Moc C, Taylor AE, Chesini GP, Zambrano CM, Barlow MS, Zhang X, Gustafsson ÅB, Purcell NH. Physiological activation of Akt by PHLPP1 deletion protects against pathological hypertrophy. Cardiovasc Res. 2015;105(2):160-170. doi:10.1093/cvr/cvu243
481. Li L, Zhao L, Yi-Ming W, Yu YS, Xia CY, Duan JL, Su DF. Sirt1 hyperexpression in SHR heart related to left ventricular hypertrophy. Can J Physiol Pharmacol. 2009;87(1):56-62. doi:10.1139/Y08-099
482. Zong J, Salim M, Zhou H, Bian ZY, Dai J, Yuan Y, Deng W, Zhang JY, Zhang R, Wu QQ, et al. NOD2 deletion promotes cardiac hypertrophy and fibrosis induced by pressure overload. Lab Invest. 2013;93(10):1128-1136. doi:10.1038/labinvest.2013.99
483. Zhang S, Lu Y, Jiang C. Inhibition of histone demethylase JMJD1C attenuates cardiac hypertrophy and fibrosis induced by angiotensin II. J Recept Signal Transduct Res. 2020;40(4):339-347. doi:10.1080/10799893.2020.1734819
484. Huang J, Wang L, Shen Y, Zhang S, Zhou Y, Du J, Ma X, Liu Y, Liang D, Shi D, et al. CDC-like kinase 4 deficiency contributes to pathological cardiac hypertrophy by modulating NEXN phosphorylation. Nat Commun. 2022;13(1):4433. doi:10.1038/s41467-022-31996-9
485. Taniguchi T, Maruyama N, Ogata T, Kasahara T, Nakanishi N, Miyagawa K, Naito D, Hamaoka T, Nishi M, Matoba S, et al. PTRF/Cavin-1 Deficiency Causes Cardiac Dysfunction Accompanied by Cardiomyocyte Hypertrophy and Cardiac Fibrosis. PLoS One. 2016;11(9):e0162513. doi:10.1371/journal.pone.0162513
486. Karpanen T, Bry M, Ollila HM, Seppänen-Laakso T, Liimatta E, Leskinen H, Kivelä R, Helkamaa T, Merentie M, Jeltsch M, et al. Overexpression of vascular endothelial growth factor-B in mouse heart alters cardiac lipid metabolism and induces myocardial hypertrophy. Circ Res. 2008;103(9):1018-1026. doi:10.1161/CIRCRESAHA.108.178459
487. Liu F, Su H, Liu B, Mei Y, Ke Q, Sun X, Tan W. STVNa Attenuates Isoproterenol-Induced Cardiac Hypertrophy Response through the HDAC4 and Prdx2/ROS/Trx1 Pathways. Int J Mol Sci. 2020;21(2):682. doi:10.3390/ijms21020682
488. Sun Y, Chen C, Xue R, Wang Y, Dong B, Li J, Chen C, Jiang J, Fan W, Liang Z, et al. Maf1 ameliorates cardiac hypertrophy by inhibiting RNA

polymerase III through ERK1/2. Theranostics. 2019;9(24):7268-7281. doi:10.7150/thno.33006
489. Ren J, Qi H, Song C, Ba L, Liu R, Feng X, Wang L, Zhang M, Xie Y, Sun H. LncRNA4930473A02Rik promotes cardiac hypertrophy by regulating TCF7 via sponging miR-135a in mice. Cell Death Discov. 2021;7(1):378. doi:10.1038/s41420-021-00775-8
490. Serebryanaya DV, Adasheva DA, Konev AA, Artemieva MM, Katrukha IA, Postnikov AB, Medvedeva NA, Katrukha AG. IGFBP-4 Proteolysis by PAPP-A in a Primary Culture of Rat Neonatal Cardiomyocytes under Normal and Hypertrophic Conditions. Biochemistry (Mosc). 2021;86(11):1395-1406. doi:10.1134/S0006297921110043
491. Demion M, Thireau J, Gueffier M, Finan A, Khoueiry Z, Cassan C, Serafini N, Aimond F, Granier M, Pasquié JL, et al. Trpm4 gene invalidation leads to cardiac hypertrophy and electrophysiological alterations. PLoS One. 2014;9(12):e115256. doi:10.1371/journal.pone.0115256
492. Dong T, Zhao Y, Jin HF, Shen L, Lin Y, Si LL, Chen L, Liu JC. SNTA1-deficient human cardiomyocytes demonstrate hypertrophic phenotype and calcium handling disorder. Stem Cell Res Ther. 2022;13(1):288. doi:10.1186/s13287-022-02955-4
493. Dai B, Cui M, Zhu M, Su WL, Qiu MC, Zhang H. STAT1/3 and ERK1/2 synergistically regulate cardiac fibrosis induced by high glucose. Cell Physiol Biochem. 2013;32(4):960-971. doi:10.1159/000354499
494. Qu H, Wang Y, Wang Y, Yang T, Feng Z, Qu Y, Zhou H. Luhong formula inhibits myocardial fibrosis in a paracrine manner by activating the gp130/JAK2/STAT3 pathway in cardiomyocytes. J Ethnopharmacol. 2017;202:28-37. doi:10.1016/j.jep.2017.01.033
495. Geng H, Guan J. MiR-18a-5p inhibits endothelial-mesenchymal transition and cardiac fibrosis through the Notch2 pathway. Biochem Biophys Res Commun. 2017;491(2):329-336. doi:10.1016/j.bbrc.2017.07.101
496. Zhang Y, Zhang Y. Toll-like receptor-6 (TLR6) deficient mice are protected from myocardial fibrosis induced by high fructose feeding through anti-oxidant and inflammatory signaling pathway. Biochem Biophys Res Commun. 2016;473(2):388-395. doi:10.1016/j.bbrc.2016.02.111

497. Feng N, Yu H, Wang Y, Zhang Y, Xiao H, Gao W. Exercise training attenuates angiotensin II-induced cardiac fibrosis by reducing POU2F1 expression. J Sport Health Sci. 2022;S2095-2546(22)00104-1. doi:10.1016/j.jshs.2022.10.004
498. Zhang X, Hu C, Zhang N, Wei WY, Li LL, Wu HM, Ma ZG, Tang QZ. Matrine attenuates pathological cardiac fibrosis via RPS5/p38 in mice. Acta Pharmacol Sin. 2021;42(4):573-584. doi:10.1038/s41401-020-0473-8
499. Fu H, Nie S, Luo P, Ruan Y, Zhang Z, Miao H, Li X, Wen S, Bai R. Galectin-3 and acute heart failure: genetic polymorphisms, plasma level, myocardial fibrosis and 1-year outcomes. Biomark Med. 2020;14(11):943-954. doi:10.2217/bmm-2020-0269
500. Ji C, Pan Y, Xu S, Yu C, Ji J, Chen M, Hu F. Propolis ameliorates restenosis in hypercholesterolemia rabbits with carotid balloon injury by inhibiting lipid accumulation, oxidative stress, and TLR4/NF-κB pathway. J Food Biochem. 2021;45(4):e13577. doi:10.1111/jfbc.13577
501. Takeyama Y, Uehara Y, Anan A, Morihara D, Yokoyama K, Takata K, Tanaka T, Irie M, Iwata K, Shakado S, et al. Increased hepatic ABCA1 transporter is associated with hypercholesterolemia in a cholestatic rat model and primary biliary cholangitis patients. Med Mol Morphol. 2017;50(4):227-237. doi:10.1007/s00795-017-0166-7
502. Han KH, Han KO, Green SR, Quehenberger O. Expression of the monocyte chemoattractant protein-1 receptor CCR2 is increased in hypercholesterolemia. Differential effects of plasma lipoproteins on monocyte function. J Lipid Res. 1999;40(6):1053-1063.
503. Banerjee P, Chan KC, Tarabocchia M, Benito-Vicente A, Alves AC, Uribe KB, Bourbon M, Skiba PJ, Pordy R, Gipe DA, et al. Functional Analysis of LDLR (Low-Density Lipoprotein Receptor) Variants in Patient Lymphocytes to Assess the Effect of Evinacumab in Homozygous Familial Hypercholesterolemia Patients With a Spectrum of LDLR Activity. Arterioscler Thromb Vasc Biol. 2019;39(11):2248-2260. doi:10.1161/ATVBAHA.119.313051
504. Li X, Hu W, Li L, Chen Z, Jiang T, Zhang D, Liu K, Wang H. MiR-133a-3p/Sirt1 epigenetic programming mediates hypercholesterolemia susceptibility in female offspring induced by prenatal dexamethasone

exposure. Biochem Pharmacol. 2022;206:115306. doi:10.1016/j.bcp.2022.115306

505. Johansson ME, Zhang XY, Edfeldt K, Lundberg AM, Levin MC, Borén J, Li W, Yuan XM, Folkersen L, Eriksson P, et al. Innate immune receptor NOD2 promotes vascular inflammation and formation of lipid-rich necrotic cores in hypercholesterolemic mice. Eur J Immunol. 2014;44(10):3081-3092. doi:10.1002/eji.201444755

506. Frikke-Schmidt R, Nordestgaard BG, Stene MC, Sethi AA, Remaley AT, Schnohr P, Grande P, Tybjaerg-Hansen A. Association of loss-of-function mutations in the ABCA1 gene with high-density lipoprotein cholesterol levels and risk of ischemic heart disease. JAMA. 2008;299(21):2524-2532. doi:10.1001/jama.299.21.2524

507. Parapanov R, Lugrin J, Rosenblatt-Velin N, Feihl F, Waeber B, Milano G, Vergely C, Li N, Pacher P, Liaudet L. Toll-like receptor 5 deficiency exacerbates cardiac injury and inflammation induced by myocardial ischaemia-reperfusion in the mouse. Clin Sci (Lond). 2015;129(2):187-198. doi:10.1042/CS20140444

508. Tang WQ, Yang FR, Chen KM, Yang H, Liu Y, Dou B. CircZNF609 Aggravated Myocardial Ischemia Reperfusion Injury via Mediation of miR-214-3p/PTGS2 Axis. Korean Circ J. 2022;52(9):680-696. doi:10.4070/kcj.2021.0252

509. Herrmann JL, Abarbanell AM, Wang Y, Weil BR, Poynter JA, Manukyan MC, Meldrum DR. Transforming growth factor-α enhances stem cell-mediated postischemic myocardial protection. Ann Thorac Surg. 2011;92(5):1719-1725. doi:10.1016/j.athoracsur.2011.06.057

510. Yin Q, Wang P, Wu X. MicroRNA -148 alleviates cardiac dysfunction, immune disorders and myocardial apoptosis in myocardial ischemia-reperfusion (MI/R) injury by targeting pyruvate dehydrogenase kinase (PDK4). Bioengineered. 2021;12(1):5552-5565. doi:10.1080/21655979.2021.1965812

511. Mahdiani S, Omidkhoda N, Rezaee R, Heidari S, Karimi G. Induction of JAK2/STAT3 pathway contributes to protective effects of different therapeutics against myocardial ischemia/reperfusion. Biomed Pharmacother. 2022;155:113751. doi:10.1016/j.biopha.2022.113751

512. Arslan F, Smeets MB, O'Neill LA, Keogh B, McGuirk P, Timmers L, Tersteeg C, Hoefer IE, Doevendans PA, Pasterkamp G, et al. Myocardial ischemia/reperfusion injury is mediated by leukocytic toll-like receptor-2 and reduced by systemic administration of a novel anti-toll-like receptor-2 antibody. Circulation. 2010;121(1):80-90. doi:10.1161/CIRCULATIONAHA.109.880187
513. Li Y, Sun X, Liu X, Li J, Li X, Wang G, Liu Y, Lu X, Cui L, Shao M, et al. P2X7R-NEK7-NLRP3 Inflammasome Activation: A Novel Therapeutic Pathway of Qishen Granule in the Treatment of Acute Myocardial Ischemia. J Inflamm Res. 2022;15:5309-5326. doi:10.2147/JIR.S373962
514. Chen C, Peng H, Zeng Y, Dong G. CD14, CD163, and CCR1 are involved in heart and blood communication in ischemic cardiac diseases. J Int Med Res. 2020;48(9):300060520951649. doi:10.1177/0300060520951649
515. Sun M, Guo M, Ma G, Zhang N, Pan F, Fan X, Wang R. MicroRNA-30c-5p protects against myocardial ischemia/reperfusion injury via regulation of Bach1/Nrf2. Toxicol Appl Pharmacol. 2021;426:115637. doi:10.1016/j.taap.2021.115637
516. Chen Y, Liu C, Li J, Zhou P, Zhao X, Chen R, Song L, Zhao H, Yan H. LATS2 Deletion Attenuates Myocardial Ischemia-Reperfusion Injury by Promoting Mitochondrial Biogenesis. Oxid Med Cell Longev. 2021;2021:1058872. doi:10.1155/2021/1058872
517. Yang J, Tong T, Zhu C, Zhou M, Jiang Y, Chen H, Que L, Liu L, Zhu G, Ha T, et al. Peli1 contributes to myocardial ischemia/reperfusion injury by impairing autophagy flux via its E3 ligase mediated ubiquitination of P62. J Mol Cell Cardiol. 2022;173:30-46. doi:10.1016/j.yjmcc.2022.09.004
518. Huang C, Qu Y, Feng F, Zhang H, Shu L, Zhu X, Huang G, Xu J. Cardioprotective Effect of circ_SMG6 Knockdown against Myocardial Ischemia/Reperfusion Injury Correlates with miR-138-5p-Mediated EGR1/TLR4/TRIF Inactivation. Oxid Med Cell Longev. 2022;2022:1927260. doi:10.1155/2022/1927260
519. Gul-Kahraman K, Yilmaz-Bozoglan M, Sahna E. Physiological and pharmacological effects of melatonin on remote ischemic perconditioning after myocardial ischemia-reperfusion injury in rats: Role of Cybb, Fas,

NfκB, Irisin signaling pathway. J Pineal Res. 2019;67(2):e12589. doi:10.1111/jpi.12589
520. Hermansson C, Lundqvist A, Wasslavik C, Palmqvist L, Jeppsson A, Hultén LM. Reduced expression of NLRP3 and MEFV in human ischemic heart tissue. Biochem Biophys Res Commun. 2013;430(1):425-428. doi:10.1016/j.bbrc.2012.11.070
521. Delgobo M, Frantz S. When Sensing Goes Wrong: Role of Clec4e in Ischemic Heart Injury. JACC Basic Transl Sci. 2021;6(8):647-649. doi:10.1016/j.jacbts.2021.07.003
522. Skvortsova L, Perfelyeva A, Khussainova E, Mansharipova A, Forman HJ, Djansugurova L. Association of GCLM -588C/T and GCLC -129T/C Promoter Polymorphisms of Genes Coding the Subunits of Glutamate Cysteine Ligase with Ischemic Heart Disease Development in Kazakhstan Population. Dis Markers. 2017;2017:4209257. doi:10.1155/2017/4209257
523. Chen G, Yue A, Wang M, Ruan Z, Zhu L. The Exosomal lncRNA KLF3-AS1 From Ischemic Cardiomyocytes Mediates IGF-1 Secretion by MSCs to Rescue Myocardial Ischemia-Reperfusion Injury. Front Cardiovasc Med. 2021;8:671610. doi:10.3389/fcvm.2021.671610
524. Wang Z, Fu M, Li Y. miR-142-5p and miR-212-5p cooperatively inhibit the proliferation and collagen formation of cardiac fibroblasts by regulating c-Myc/TP53INP1. Can J Physiol Pharmacol. 2020;98(5):314-323. doi:10.1139/cjpp-2019-0495
525. Henning C, Branopolski A, Follert P, Lewandowska O, Ayhan A, Benkhoff M, Flögel U, Kelm M, Heiss C, Lammert E. Endothelial β1 Integrin-Mediated Adaptation to Myocardial Ischemia. Thromb Haemost. 2021;121(6):741-754. doi:10.1055/s-0040-1721505
526. Zhang Y, Liu X, She ZG, Jiang DS, Wan N, Xia H, Zhu XH, Wei X, Zhang XD, Li H. Interferon regulatory factor 9 is an essential mediator of heart dysfunction and cell death following myocardial ischemia/reperfusion injury. Basic Res Cardiol. 2014;109(5):434. doi:10.1007/s00395-014-0434-9
527. Li Y, Li Z, Liu J, Liu Y, Miao G. miR-190-5p Alleviates Myocardial Ischemia-Reperfusion Injury by Targeting PHLPP1. Dis Markers. 2021;2021:8709298. doi:10.1155/2021/8709298

528. Liu Y, Yang H, Liu LX, Yan W, Guo HJ, Li WJ, Tian C, Li HH, Wang HX. NOD2 contributes to myocardial ischemia/reperfusion injury by regulating cardiomyocyte apoptosis and inflammation. Life Sci. 2016;149:10-17. doi:10.1016/j.lfs.2016.02.039
529. Zhang F, Li Z, Gao P, Zou J, Cui Y, Qian Y, Gu R, Xu W, Hu J. HJ11 decoction restrains development of myocardial ischemia-reperfusion injury in rats by suppressing ACSL4-mediated ferroptosis. Front Pharmacol. 2022;13:1024292. doi:10.3389/fphar.2022.1024292
530. Shao L, Wu D, Zhang P, Li W, Wang J, Su G, Liao Y, Wang Z, Liu K. The significance of microthrombosis and fgl2 in no-reflow phenomenon of rats with acute myocardial ischemia/reperfusion. Clin Appl Thromb Hemost. 2013;19(1):19-28. doi:10.1177/1076029612437577
531. Laghrissi-Thode F, Wagner WR, Pollock BG, Johnson PC, Finkel MS. Elevated platelet factor 4 and beta-thromboglobulin plasma levels in depressed patients with ischemic heart disease. Biol Psychiatry. 1997;42(4):290-295. doi:10.1016/S0006-3223(96)00345-9
532. Bellomo D, Headrick JP, Silins GU, Paterson CA, Thomas PS, Gartside M, Mould A, Cahill MM, Tonks ID, Grimmond SM, et al. Mice lacking the vascular endothelial growth factor-B gene (Vegfb) have smaller hearts, dysfunctional coronary vasculature, and impaired recovery from cardiac ischemia. Circ Res. 2000;86(2):E29-E35. doi:10.1161/01.res.86.2.e29
533. Meng XW, Zhang M, Hu JK, Chen XY, Long YQ, Liu H, Feng XM, Ji FH, Peng K. Activation of CCL21-GPR174/CCR7 on cardiac fibroblasts underlies myocardial ischemia/reperfusion injury. Front Genet. 2022;13:946524. doi:10.3389/fgene.2022.946524
534. Bhattarai A, Singh Sunar P, Shah S, Chamlagain R, Babu Pokhrel N, Khanal P, Kumar Sah S, Poudel S, Belbase K, Chand S, et al. CT-IGFBP-4 as a Predictive Novel Biomarker of Ischemic Cardiovascular Events and Mortality: A Systematic Review. J Interv Cardiol. 2022;2022:1816504. doi:10.1155/2022/1816504
535. Jacobs G, Oosterlinck W, Dresselaers T, Geenens R, Kerselaers S, Himmelreich U, Herijgers P, Vennekens R. Enhanced β-adrenergic cardiac reserve in Trpm4□/□ mice with ischaemic heart failure. Cardiovasc Res. 2015;105(3):330-339. doi:10.1093/cvr/cvv009

536. Gurusamy N, Lekli I, Gorbunov NV, Gherghiceanu M, Popescu LM, Das DK. Cardioprotection by adaptation to ischaemia augments autophagy in association with BAG-1 protein. J Cell Mol Med. 2009;13(2):373-387. doi:10.1111/j.1582-4934.2008.00495.x
537. Rong J, Pan H, He J, Zhang Y, Hu Y, Wang C, Fu Q, Fan W, Zou Q, Zhang L, et al. Long non-coding RNA KCNQ1OT1/microRNA-204-5p/LGALS3 axis regulates myocardial ischemia/reperfusion injury in mice. Cell Signal. 2020;66:109441. doi:10.1016/j.cellsig.2019.109441
538. Bao Y, Qiao Y, Yu H, Zhang Z, Yang H, Xin X, Chen Y, Guo Y, Wu N, Jia D. miRNA-27a Transcription Activated by c-Fos Regulates Myocardial Ischemia-Reperfusion Injury by Targeting ATAD3a. Oxid Med Cell Longev. 2021;2021:2514947. doi:10.1155/2021/2514947
539. Lin Y, Ding D, Huang Q, Liu Q, Lu H, Lu Y, Chi Y, Sun X, Ye G, Zhu H, et al. Downregulation of miR-192 causes hepatic steatosis and lipid accumulation by inducing SREBF1: Novel mechanism for bisphenol A-triggered non-alcoholic fatty liver disease. Biochim Biophys Acta Mol Cell Biol Lipids. 2017;1862(9):869-882. doi:10.1016/j.bbalip.2017.05.001
540. Mahjoubin-Tehran M, Aghaee-Bakhtiari SH, Sahebkar A, Butler AE, Oskuee RK, Jalili A. In silico and in vitro analysis of microRNAs with therapeutic potential in atherosclerosis. Sci Rep. 2022;12(1):20334. doi:10.1038/s41598-022-24260-z
541. Huang R, Cao Y, Li H, Hu Z, Zhang H, Zhang L, Su W, Xu Y, Liang L, Melgiri ND, et al. miR-532-3p-CSF2RA Axis as a Key Regulator of Vulnerable Atherosclerotic Plaque Formation. Can J Cardiol. 2020;36(11):1782-1794. doi:10.1016/j.cjca.2019.12.018
542. Wang Y, Xu Z, Wang X, Zheng J, Peng L, Zhou Y, Song Y, Lu Z. Extracellular-vesicle containing miRNA-503-5p released by macrophages contributes to atherosclerosis. Aging (Albany NY). 2021;13(8):12239-12257. doi:10.18632/aging.103855
543. Pu Y, Zhao Q, Men X, Jin W, Yang M. MicroRNA-325 facilitates atherosclerosis progression by mediating the SREBF1/LXR axis via KDM1A. Life Sci. 2021;277:119464. doi:10.1016/j.lfs.2021.119464
544. Klingenberg R, Gerdes N, Badeau RM, Gisterå A, Strodthoff D, Ketelhuth DF, Lundberg AM, Rudling M, Nilsson SK, Olivecrona G, et al. Depletion of FOXP3+ regulatory T cells promotes hypercholesterolemia and

atherosclerosis. J Clin Invest. 2013;123(3):1323-1334. doi:10.1172/JCI63891

545. Heilmeier U, Hackl M, Schroeder F, Torabi S, Kapoor P, Vierlinger K, Eiriksdottir G, Gudmundsson EF, Harris TB, Gudnason V, et al. Circulating serum microRNAs including senescent miR-31-5p are associated with incident fragility fractures in older postmenopausal women with type 2 diabetes mellitus. Bone. 2022;158:116308. doi:10.1016/j.bone.2021.116308

546. Krause C, Sievert H, Geißler C, Grohs M, El Gammal AT, Wolter S, Ohlei O, Kilpert F, Krämer UM, Kasten M, et al. Critical evaluation of the DNA-methylation markers ABCG1 and SREBF1 for Type 2 diabetes stratification. Epigenomics. 2019;11(8):885-897. doi:10.2217/epi-2018-0159

547. Vorobjova T, Uibo O, Heilman K, Rägo T, Honkanen J, Vaarala O, Tillmann V, Ojakivi I, Uibo R. Increased FOXP3 expression in small-bowel mucosa of children with coeliac disease and type I diabetes mellitus. Scand J Gastroenterol. 2009;44(4):422-430. doi:10.1080/00365520802624177

548. Ghourbani Gazar S, Andalib A, Hashemi M, Rezaei A. CD4□Foxp3□ Treg and its ICOS□ subsets in patients with myocardial infarction. Iran J Immunol. 2012;9(1):53-60.

549. Lauria F, Iacomino G, Russo P, Venezia A, Marena P, Ahrens W, De Henauw S, Eiben G, Foraita R, Hebestreit A, et al. Circulating miRNAs Are Associated with Inflammation Biomarkers in Children with Overweight and Obesity: Results of the I.Family Study. Genes (Basel). 2022;13(4):632. doi:10.3390/genes13040632

550. Thompson MD, Cismowski MJ, Serpico M, Pusateri A, Brigstock DR. Elevation of circulating microRNA levels in obese children compared to healthy controls. Clin Obes. 2017;7(4):216-221. doi:10.1111/cob.12192

551. Huang XY, Chen JX, Ren Y, Fan LC, Xiang W, He XJ. Exosomal miR-122 promotes adipogenesis and aggravates obesity through the VDR/SREBF1 axis. Obesity (Silver Spring). 2022;30(3):666-679. doi:10.1002/oby.23365

552. Donma M, Karasu E, Ozdilek B, Turgut B, Topcu B, Nalbantoglu B, Donma O. CD4(+), CD25(+), FOXP3 (+) T Regulatory Cell Levels in Obese, Asthmatic, Asthmatic Obese, and Healthy Children. Inflammation. 2015;38(4):1473-1478. doi:10.1007/s10753-015-0122-4

553. Kassan M, Wecker A, Kadowitz P, Trebak M, Matrougui K. CD4+CD25+Foxp3 regulatory T cells and vascular dysfunction in hypertension. J Hypertens. 2013;31(10):1939-1943. doi:10.1097/HJH.0b013e328362feb7
554. Dégano IR, Camps-Vilaró A, Subirana I, García-Mateo N, Cidad P, Muñoz-Aguayo D, Puigdecanet E, Nonell L, Vila J, Crepaldi FM, et al. Association of Circulating microRNAs with Coronary Artery Disease and Usefulness for Reclassification of Healthy Individuals: The REGICOR Study. J Clin Med. 2020;9(5):1402. doi:10.3390/jcm9051402
555. Chmielewski S, Piaszyk-Borychowska A, Wesoly J, Bluyssen HA. STAT1 and IRF8 in Vascular Inflammation and Cardiovascular Disease: Diagnostic and Therapeutic Potential. Int Rev Immunol. 2016;35(5):434-454. doi:10.3109/08830185.2015.1087519
556. Lundberg AK, Jonasson L, Hansson GK, Mailer RKW. Activation-induced FOXP3 isoform profile in peripheral CD4+ T cells is associated with coronary artery disease. Atherosclerosis. 2017;267:27-33. doi:10.1016/j.atherosclerosis.2017.10.026
557. Calderon-Dominguez M, Mangas A, Belmonte T, Quezada-Feijoo M, Ramos M, Toro R. Ischemic dilated cardiomyopathy pathophysiology through microRNA-16-5p. Rev Esp Cardiol (Engl Ed). 2021;74(9):740-749. doi:10.1016/j.rec.2020.08.012
558. Gorzin F, Amirzargar AA, Mahmoudi MJ, Rahnemoon Z, Najmi Varzaneh F, Hedayat M, Sadati S, Eskandari V, Rahmati Z, Rezaei N. FOXP3, RORγt and IL-10 cytokine profile in chronic heart failure. Bratisl Lek Listy. 2017;118(10):637-641. doi:10.4149/BLL_2017_122
559. Nogueira LG, Santos RH, Fiorelli AI, Mairena EC, Benvenuti LA, Bocchi EA, Stolf NA, Kalil J, Cunha-Neto E. Myocardial gene expression of T-bet, GATA-3, Ror-γt, FoxP3, and hallmark cytokines in chronic Chagas disease cardiomyopathy: an essentially unopposed TH1-type response. Mediators Inflamm. 2014;2014:914326. doi:10.1155/2014/914326
560. Klingenberg R, Gerdes N, Badeau RM, Gisterå A, Strodthoff D, Ketelhuth DF, Lundberg AM, Rudling M, Nilsson SK, Olivecrona G, et al. Depletion of FOXP3+ regulatory T cells promotes hypercholesterolemia and atherosclerosis. J Clin Invest. 2013;123(3):1323-1334. doi:10.1172/JCI63891

Tables

Table 1 The statistical metrics for key differentially expressed genes (DEGs)

Gene Symbol	logFC	pValue	tvalue	Regulations	Gene Name
SERPING1	1.34737	0.00021	3.706609	Up	serpin family G member 1
BATF2	1.331407	0.000125	3.837006	Up	basic leucine zipper ATF-like transcription factor 2
IFIT2	1.272744	2.31E-05	4.233076	Up	interferon induced protein with tetratricopeptide repeats 2
IFITM3	1.215453	0.00147	3.180597	Up	interferon induced transmembrane protein 3
IFIT3	1.172875	0.000725	3.379824	Up	interferon induced protein with tetratricopeptide repeats 3
IFIT1	1.171077	0.0027	2.999944	Up	interferon induced protein with tetratricopeptide repeats 1
ETV7	1.114009	0.00184	3.11497	Up	ETS variant transcription factor 7
OAS3	1.024405	0.000376	3.556587	Up	2'-5'-oligoadenylate synthetase 3
TMTC1	0.931747	0.021112	2.305969	Up	transmembrane O-mannosyltransferase targeting cadherins 1
APOBEC3B	0.931609	0.012829	2.48849	Up	apolipoprotein B mRNA editing enzyme catalytic subunit 3B
GBP1	0.929822	0.000258	3.654382	Up	guanylate binding protein 1
EPSTI1	0.920207	0.001192	3.24085	Up	epithelial stromal interaction 1
CLEC4D	0.872703	1.01E-05	4.414765	Up	C-type lectin domain family 4 member D
DOCK4	0.8362	0.000119	3.848573	Up	dedicator of cytokinesis 4
HES4	0.835958	0.024775	2.2449	Up	hes family bHLH transcription factor 4
KCNJ2	0.835905	4.73E-06	4.576522	Up	potassium inwardly rectifying channel subfamily J member 2
CD274	0.819088	0.000473	3.49551	Up	CD274 molecule
CEACAM1	0.816987	0.005091	2.801204	Up	CEA cell adhesion molecule 1
SAMD9L	0.813642	0.000252	3.660232	Up	sterile alpha motif domain containing 9 like
P2RY14	0.813432	0.000165	3.767227	Up	purinergic receptor P2Y14
XAF1	0.808362	0.000828	3.343235	Up	XIAP associated factor 1
ATOH8	0.805311	0.038638	2.068025	Up	atonal bHLH transcription factor 8
PARP14	0.793259	8.49E-05	3.930223	Up	poly(ADP-ribose) polymerase family member 14
KLHL2	0.780556	5.91E-05	4.016415	Up	kelch like family member 2
ACSL1	0.775533	0.000219	3.696031	Up	acyl-CoA synthetase long chain family member 1
HERC5	0.7645	0.007374	2.679463	Up	HECT and RLD domain containing E3 ubiquitin protein ligase 5
CLIC2	0.730668	0.006852	2.703957	Up	chloride intracellular channel 2
CLEC12A	0.726151	0.004566	2.836188	Up	C-type lectin domain family 12 member A
DDX60	0.721343	0.000557	3.451706	Up	DExD/H-box helicase 60
GPR141	0.720453	0.010111	2.572011	Up	G protein-coupled receptor 141
PARP9	0.71404	0.000183	3.741179	Up	poly(ADP-ribose) polymerase family member 9
ABTB2	0.710111	0.001463	3.181943	Up	ankyrin repeat and BTB domain containing 2
DDX58	0.693868	0.000539	3.460647	Up	DExD/H-box helicase 58
MFAP3	0.69334	0.002632	3.007709	Up	microfibril associated protein 3
PLSCR1	0.692948	0.002953	2.972544	Up	phospholipid scramblase 1
TRIM22	0.683496	0.000817	3.346936	Up	tripartite motif containing 22
ZCCHC2	0.681019	5.70E-05	4.025055	Up	zinc finger CCHC-type containing 2
STAT1	0.674543	0.000864	3.331384	Up	signal transducer and activator of transcription 1

ARG1	0.673665	0.012455	2.498976	Up	arginase 1
RPL10P9	0.671755	0.021699	2.295599	Up	ribosomal protein L10 pseudogene 9
SIPA1L2	0.67103	0.00145	3.18447	Up	signal induced proliferation associated 1 like 2
TLR4	0.667694	2.05E-05	4.258931	Up	toll like receptor 4
LRRK2	0.665569	0.000542	3.459179	Up	leucine rich repeat kinase 2
SLC22A15	0.661911	0.00486	2.816162	Up	solute carrier family 22 member 15
OTX1	0.659532	0.03092	2.158105	Up	orthodenticlehomeobox 1
ADAM9	0.647465	0.00108	3.268682	Up	ADAM metallopeptidase domain 9
DDX60L	0.645804	0.001594	3.157072	Up	DExD/H-box 60 like
VNN1	0.641048	0.009634	2.588691	Up	vanin 1
ABCA1	0.636261	0.002882	2.980032	Up	ATP binding cassette subfamily A member 1
EIF2AK2	0.636113	0.00135	3.205214	Up	eukaryotic translation initiation factor 2 alpha kinase 2
IFIT5	0.630053	0.000416	3.529509	Up	interferon induced protein with tetratricopeptide repeats 5
IFIH1	0.618202	0.001297	3.21671	Up	interferon induced with helicase C domain 1
IFI44	0.618021	0.017235	2.381663	Up	interferon induced protein 44
STAT2	0.615677	0.000285	3.628433	Up	signal transducer and activator of transcription 2
YWHAZP3	0.608301	0.018656	2.352337	Up	tyrosine 3-monooxygenase/tryptophan 5-monooxygenase activation protein zeta pseudogene 3
TAFA2	0.595204	0.015335	2.424379	Up	TAFA chemokine like family member 2
KIAA1958	0.594388	0.002635	3.007372	Up	KIAA1958
RAPGEF2	0.593416	0.00071	3.385859	Up	Rap guanine nucleotide exchange factor 2
TNFAIP6	0.590855	0.028495	2.190403	Up	TNF alpha induced protein 6
TLR5	0.590181	0.001122	3.257947	Up	toll like receptor 5
HELZ2	0.589171	0.004159	2.865849	Up	helicase with zinc finger 2
FBXO30	0.585234	0.005649	2.767483	Up	F-box protein 30
PLAGL1	0.582807	0.000686	3.395016	Up	PLAG1 like zinc finger 1
GCA	0.575742	0.001659	3.145408	Up	grancalcin
PTGS2	0.574859	0.002986	2.969219	Up	prostaglandin-endoperoxide synthase 2
TGFA	0.572994	0.004076	2.872211	Up	transforming growth factor alpha
TASOR2	0.570514	0.000682	3.396683	Up	transcription activation suppressor family member 2
F2RL1	0.563748	0.005743	2.762104	Up	F2R like trypsin receptor 1
CYP2D6	0.56302	0.023761	2.260978	Up	cytochrome P450 family 2 subfamily D member 6
ANKRD50	0.562817	0.005971	2.749396	Up	ankyrin repeat domain 50
ZNF117	0.558817	0.029504	2.176685	Up	zinc finger protein 117
DMXL2	0.547937	0.000788	3.35708	Up	Dmx like 2
TRIM5	0.547222	0.000591	3.435614	Up	tripartite motif containing 5
RSAD2	0.547122	0.016317	2.401754	Up	radical S-adenosyl methionine domain containing 2
H2BC20P	0.546954	0.017995	2.365718	Up	H2B clustered histone 20, pseudogene
N4BP2	0.543854	0.003728	2.900335	Up	NEDD4 binding protein 2
CR1	0.541191	0.021279	2.302993	Up	complement C3b/C4b receptor 1 (Knops blood group)
ATP10D	0.537928	0.000168	3.762776	Up	ATPase phospholipid transporting 10D (putative)
OAS2	0.537738	0.003734	2.899822	Up	2'-5'-oligoadenylate synthetase 2
CMTM1	0.537572	0.041771	2.035798	Up	CKLF like MARVEL transmembrane domain containing 1

HCAR2	0.535121	0.023954	2.257862	Up	hydroxycarboxylic acid receptor 2
ITPRID2	0.533528	0.001044	3.278516	Up	ITPR interacting domain containing 2
FAS	0.531983	0.000675	3.399584	Up	Fas cell surface death receptor
SAMD9	0.528811	0.002804	2.988402	Up	sterile alpha motif domain containing 9
SHTN1	0.527115	0.002243	3.05596	Up	shootin 1
KIF16B	0.52603	0.003741	2.89924	Up	kinesin family member 16B
PMAIP1	0.524654	8.77E-05	3.92229	Up	phorbol-12-myristate-13-acetate-induced protein 1
FCHO2	0.524503	0.016081	2.40708	Up	FCH and mu domain containing endocytic adaptor 2
IL18RAP	0.519371	0.023752	2.26112	Up	interleukin 18 receptor accessory protein
NFXL1	0.516859	0.021014	2.307728	Up	nuclear transcription factor, X-box binding like 1
FBN2	0.515662	0.010761	2.55038	Up	fibrillin 2
RTP4	0.515513	0.009985	2.576349	Up	receptor transporter protein 4
RUFY4	0.514121	0.040901	2.04453	Up	RUN and FYVE domain containing 4
SRGAP2B	0.514009	0.0051	2.800679	Up	SLIT-ROBO Rho GTPase activating protein 2B
KDM1B	0.513563	0.001624	3.151566	Up	lysine demethylase 1B
IFI35	0.51341	0.029451	2.177397	Up	interferon induced protein 35
BTAF1	0.512355	0.011178	2.537083	Up	B-TFIID TATA-box binding protein associated factor 1
PDK4	0.511529	0.001808	3.120116	Up	pyruvate dehydrogenase kinase 4
NBPF8	0.510558	0.004191	2.863386	Up	NBPF member 8
FAR2	0.507732	0.003187	2.949145	Up	fatty acyl-CoA reductase 2
KIAA1109	0.50668	0.002187	3.063523	Up	KIAA1109
LPCAT2	0.504469	0.004106	2.869878	Up	lysophosphatidylcholineacyltransferase 2
C1GALT1	0.50381	0.000962	3.301451	Up	core 1 synthase, glycoprotein-N-acetylgalactosamine 3-beta-galactosyltransferase 1
KLRC1	0.502888	0.040472	2.048896	Up	killer cell lectin like receptor C1
RNF213	0.502731	0.000242	3.670472	Up	ring finger protein 213
LIG4	0.501645	0.01533	2.424478	Up	DNA ligase 4
ZNF217	0.501204	0.001226	3.232785	Up	zinc finger protein 217
PAPSS2	0.500885	0.003403	2.928771	Up	3'-phosphoadenosine 5'-phosphosulfate synthase 2
ACSL4	0.500849	0.009779	2.583538	Up	acyl-CoA synthetase long chain family member 4
ZDHHC17	0.499689	0.006198	2.73713	Up	zinc finger DHHC-type palmitoyltransferase 17
TET2	0.499416	0.007646	2.667332	Up	tetmethylcytosinedioxygenase 2
NRIP1	0.498661	0.00142	3.190569	Up	nuclear receptor interacting protein 1
ZCCHC4	0.49555	0.001692	3.139601	Up	zinc finger CCHC-type containing 4
MYSM1	0.49512	0.012473	2.498476	Up	Myb like, SWIRM and MPN domains 1
HIP1	0.494891	0.003432	2.92613	Up	huntingtin interacting protein 1
AFF1	0.494654	0.004066	2.872982	Up	AF4/FMR2 family member 1
C9orf72	0.494444	0.004389	2.84877	Up	C9orf72-SMCR8 complex subunit
ZSWIM6	0.492426	0.00165	3.146904	Up	zinc finger SWIM-type containing 6
JAK2	0.49181	0.015583	2.41854	Up	Janus kinase 2
HERC2P2	0.491808	0.032493	2.138298	Up	HERC2 pseudogene 2
APC	0.48934	0.004879	2.814919	Up	APC regulator of WNT signaling pathway
TMOD2	0.488967	0.001984	3.092564	Up	tropomodulin 2

PIK3AP1	0.488163	0.003014	2.966318	Up	phosphoinositide-3-kinase adaptor protein 1
MFSD14B	0.486134	0.001188	3.241719	Up	major facilitator superfamily domain containing 14B
NBPF3	0.485507	0.009444	2.595532	Up	NBPF member 3
RNF19A	0.484059	0.001997	3.090722	Up	ring finger protein 19A, RBR E3 ubiquitin protein ligase
NTNG2	0.483654	0.024859	2.243585	Up	netrin G2
ATP8A1	0.482522	0.003975	2.880157	Up	ATPase phospholipid transporting 8A1
SHPRH	0.481667	0.004485	2.841851	Up	SNF2 histone linker PHD RING helicase
TCP11L2	0.481393	0.014461	2.445596	Up	t-complex 11 like 2
TMLHE	0.480668	0.00015	3.790518	Up	trimethyllysine hydroxylase, epsilon
MCTP2	0.479897	0.037	2.085766	Up	multiple C2 and transmembrane domain containing 2
SAMD4A	0.479833	0.049953	1.960367	Up	sterile alpha motif domain containing 4A
HERC2P9	0.479408	0.005886	2.754053	Up	HERC2 pseudogene 9
FRY	0.478601	0.000191	3.730268	Up	FRY microtubule binding protein
TLR8	0.478578	0.006217	2.736093	Up	toll like receptor 8
RP2	0.476914	0.001886	3.10764	Up	RP2 activator of ARL3 GTPase
MX2	0.476544	0.004909	2.812922	Up	MX dynamin like GTPase 2
WDFY3	0.475723	0.029199	2.180796	Up	WD repeat and FYVE domain containing 3
MED13L	0.47572	0.004851	2.81677	Up	mediator complex subunit 13L
PKN2	0.475605	0.008086	2.648464	Up	protein kinase N2
NOTCH2	0.475537	0.001402	3.194296	Up	notch receptor 2
CENPJ	0.475401	0.013148	2.479724	Up	centromere protein J
ZBTB11	0.474157	0.005524	2.774763	Up	zinc finger and BTB domain containing 11
MIS18BP1	0.47377	0.000952	3.304325	Up	MIS18 binding protein 1
CHMP5	0.47245	0.001033	3.28135	Up	charged multivesicular body protein 5
PDGFC	0.471686	0.011648	2.522644	Up	platelet derived growth factor C
FNIP1	0.471273	0.007879	2.657215	Up	folliculin interacting protein 1
PFKFB2	0.470585	0.001594	3.156967	Up	6-phosphofructo-2-kinase/fructose-2,6-biphosphatase 2
CMPK2	0.469149	0.026406	2.220183	Up	cytidine/uridine monophosphate kinase 2
XRN1	0.468973	0.003035	2.964171	Up	5'-3' exoribonuclease 1
TLR2	0.468574	0.003335	2.935053	Up	toll like receptor 2
MPZL2	0.468537	0.01708	2.384983	Up	myelin protein zero like 2
EXOC8	0.468	0.000415	3.530221	Up	exocyst complex component 8
KIDINS220	0.464783	0.002146	3.069292	Up	kinase D interacting substrate 220
ATP11A	0.463847	0.004431	2.84575	Up	ATPase phospholipid transporting 11A
PIKFYVE	0.463471	0.004264	2.857932	Up	phosphoinositide kinase, FYVE-type zinc finger containing
STXBP3	0.463374	0.009506	2.593306	Up	syntaxin binding protein 3
JMJD1C	0.462846	0.005681	2.765644	Up	jumonji domain containing 1C
LTN1	0.462158	0.014597	2.442236	Up	listerin E3 ubiquitin protein ligase 1
RIC1	0.461569	0.001426	3.189272	Up	RIC1 homolog, RAB6A GEF complex partner 1
STK3	0.461466	0.023335	2.2679	Up	serine/threonine kinase 3
PLCXD2	0.460377	0.005265	2.790344	Up	phosphatidylinositol specific phospholipase C X domain containing 2
RELCH	0.459038	0.002683	3.001917	Up	RAB11 binding and LisH domain, coiled-coil and HEAT repeat containing
ARAP2	0.458995	0.001101	3.263317	Up	ArfGAP with RhoGAP domain, ankyrin repeat and PH domain 2

DUSP6	0.458953	0.000386	3.549441	Up	dual specificity phosphatase 6
CYP1B1	0.458398	0.035608	2.101377	Up	cytochrome P450 family 1 subfamily B member 1
CPEB2	0.458015	0.004118	2.869007	Up	cytoplasmic polyadenylation element binding protein 2
NR2C2	0.457728	0.003001	2.967678	Up	nuclear receptor subfamily 2 group C member 2
NEK7	0.457599	0.017419	2.377752	Up	NIMA related kinase 7
ZSCAN30	0.457517	0.006909	2.701197	Up	zinc finger and SCAN domain containing 30
DDX3X	0.456438	0.004613	2.832893	Up	DEAD-box helicase 3 X-linked
S1PR3	0.454986	0.00117	3.24607	Up	sphingosine-1-phosphate receptor 3
DTX3L	0.454597	0.00072	3.381886	Up	deltex E3 ubiquitin ligase 3L
PALLD	0.454374	0.004441	2.845022	Up	palladin, cytoskeletal associated protein
CYSLTR2	0.453903	0.020047	2.325458	Up	cysteinyl leukotriene receptor 2
LHFPL2	0.453535	0.006537	2.719566	Up	LHFPL tetraspan subfamily member 2
CPNE8	0.452797	0.014338	2.448675	Up	copine 8
DMTF1	0.451838	0.007929	2.655064	Up	cyclin D binding myb like transcription factor 1
TSPAN2	0.451757	0.008324	2.63862	Up	tetraspanin 2
PDCD6	0.451645	0.049278	1.966177	Up	programmed cell death 6
NBPF10	0.451359	0.003746	2.898773	Up	NBPF member 10
CCR1	0.450838	0.008855	2.6176	Up	C-C motif chemokine receptor 1
ATAD2B	0.450804	0.002266	3.052993	Up	ATPase family AAA domain containing 2B
STARD4	0.450748	0.020388	2.319127	Up	StAR related lipid transfer domain containing 4
ZNF107	0.450646	0.043654	2.017395	Up	zinc finger protein 107
KCTD9	0.449669	0.015138	2.42907	Up	potassium channel tetramerization domain containing 9
LPAL2	0.446958	0.043261	2.02118	Up	lipoprotein(a) like 2, pseudogene
GCNT2	0.444732	0.025931	2.227237	Up	glucosaminyl (N-acetyl) transferase 2 (I blood group)
TAF1	0.444342	0.000885	3.324719	Up	TATA-box binding protein associated factor 1
BACH1	0.444141	0.005237	2.792067	Up	BTB domain and CNC homolog 1
ZBP1	0.443862	0.022572	2.280597	Up	Z-DNA binding protein 1
SGMS1	0.443198	0.002962	2.971661	Up	sphingomyelin synthase 1
ZNF493	0.442938	0.016435	2.399105	Up	zinc finger protein 493
GBE1	0.44265	0.008172	2.644874	Up	1,4-alpha-glucan branching enzyme 1
ELOVL6	0.44258	0.026778	2.214741	Up	ELOVL fatty acid elongase 6
ATP13A3	0.442111	0.007679	2.665875	Up	ATPase 13A3
NCOA2	0.44199	0.019569	2.334514	Up	nuclear receptor coactivator 2
L3MBTL3	0.441871	0.001326	3.210238	Up	L3MBTL histone methyl-lysine binding protein 3
GPD2	0.440979	0.004645	2.830703	Up	glycerol-3-phosphate dehydrogenase 2
TRIM25	0.440618	0.021302	2.302594	Up	tripartite motif containing 25
OSBPL1A	0.440612	0.013652	2.466283	Up	oxysterol binding protein like 1A
PRKAB2	0.4396	0.007674	2.6661	Up	protein kinase AMP-activated non-catalytic subunit beta 2
TAF2	0.439468	0.005093	2.801082	Up	TATA-box binding protein associated factor 2
UTRN	0.43883	0.000345	3.578663	Up	utrophin
PTPN11	0.438193	0.001123	3.257843	Up	protein tyrosine phosphatase non-receptor type 11
OCRL	0.436079	0.004072	2.872541	Up	OCRL inositol polyphosphate-5-phosphatase
RIN2	0.435586	0.001649	3.147148	Up	Ras and Rabinteractor 2

AGFG1	0.435106	0.00011	3.867689	Up	ArfGAP with FG repeats 1
MYOF	0.435026	0.040756	2.046001	Up	myoferlin
STRN3	0.434837	0.025906	2.227622	Up	striatin 3
MORC3	0.434684	0.02161	2.297161	Up	MORC family CW-type zinc finger 3
HDAC9	0.434026	0.025695	2.230792	Up	histone deacetylase 9
TRIQK	0.432127	0.018346	2.358552	Up	triple QxxK/R motif containing
OTUD4	0.431727	0.004633	2.831527	Up	OTU deubiquitinase 4
ZBTB38	0.431317	0.005061	2.803145	Up	zinc finger and BTB domain containing 38
SMCHD1	0.430259	0.012051	2.510657	Up	structural maintenance of chromosomes flexible hinge domain containing 1
SERINC1	0.430229	0.001319	3.211763	Up	serine incorporator 1
NCOA4	0.429528	0.01661	2.395238	Up	nuclear receptor coactivator 4
LATS2	0.428786	0.008589	2.627975	Up	large tumor suppressor kinase 2
WDR44	0.428741	0.006739	2.709485	Up	WD repeat domain 44
DICER1	0.428022	0.005856	2.755748	Up	dicer 1, ribonuclease III
CDK17	0.427842	0.016842	2.390146	Up	cyclin dependent kinase 17
TOR1B	0.425407	0.002614	3.009857	Up	torsin family 1 member B
PIGA	0.423234	0.01659	2.395667	Up	phosphatidylinositol glycan anchor biosynthesis class A
CHM	0.422703	0.013686	2.465402	Up	CHM Rab escort protein
MED23	0.422273	0.011266	2.534336	Up	mediator complex subunit 23
FNDC3A	0.421932	0.017399	2.378169	Up	fibronectin type III domain containing 3A
IL1RN	0.421833	0.025276	2.237161	Up	interleukin 1 receptor antagonist
SINHCAF	0.420856	0.008281	2.64039	Up	SIN3-HDAC complex associated factor
SEC24D	0.420088	0.001415	3.191652	Up	SEC24 homolog D, COPII coat complex component
GCH1	0.419728	0.002971	2.970703	Up	GTP cyclohydrolase 1
TMEM161B	0.419209	0.02203	2.289849	Up	transmembrane protein 161B
ZNF236	0.419182	0.003806	2.893829	Up	zinc finger protein 236
GRAMD1B	0.419046	0.003831	2.891738	Up	GRAM domain containing 1B
LCLAT1	0.418707	0.024061	2.256156	Up	lysocardiolipinacyltransferase 1
EDEM3	0.41856	0.01889	2.347702	Up	ER degradation enhancing alpha-mannosidase like protein 3
LYST	0.416906	0.005139	2.798209	Up	lysosomal trafficking regulator
CEP170	0.416608	0.048765	1.97064	Up	centrosomal protein 170
DHRS9	0.416107	0.039574	2.058167	Up	dehydrogenase/reductase 9
PELI1	0.416033	0.024896	2.243009	Up	pellino E3 ubiquitin protein ligase 1
ASCC3	0.415261	0.01207	2.510091	Up	activating signal cointegrator 1 complex subunit 3
ELF1	0.415069	0.004448	2.844525	Up	E74 like ETS transcription factor 1
FAM8A1	0.415001	0.02173	2.295047	Up	family with sequence similarity 8 member A1
HEG1	0.413852	0.001768	3.126651	Up	heart development protein with EGF like domains 1
C2CD5	0.412617	0.01161	2.523775	Up	C2 calcium dependent domain containing 5
FCGR2C	0.410902	0.013546	2.469088	Up	Fc fragment of IgG receptor IIc (gene/pseudogene)
SYNJ1	0.410242	0.015988	2.409187	Up	synaptojanin 1
EGR1	0.409755	0.035369	2.104112	Up	early growth response 1
CSGALNACT2	0.408472	0.040405	2.049582	Up	chondroitin sulfate N-acetylgalactosaminyltransferase 2

SNX10	0.408391	0.015394	2.422964	Up	sorting nexin 10
SLC39A10	0.407287	0.023368	2.267358	Up	solute carrier family 39 member 10
CRYBG3	0.406991	0.011658	2.522319	Up	crystallin beta-gamma domain containing 3
XPR1	0.406939	0.000579	3.441304	Up	xenotropic and polytropic retrovirus receptor 1
FNDC3B	0.406209	0.027271	2.207611	Up	fibronectin type III domain containing 3B
ARFGEF2	0.40614	0.009731	2.585242	Up	ADP ribosylation factor guanine nucleotide exchange factor 2
LMBRD2	0.40591	0.005343	2.785611	Up	LMBR1 domain containing 2
VCAN	0.404576	0.005737	2.76246	Up	versican
CA2	0.404575	0.037933	2.075582	Up	carbonic anhydrase 2
KDM6A	0.404021	0.010202	2.56892	Up	lysine demethylase 6A
KCTD12	0.403551	0.002648	3.005943	Up	potassium channel tetramerization domain containing 12
NUP153	0.403336	0.006066	2.744188	Up	nucleoporin 153
HIPK3	0.403316	0.021801	2.293824	Up	homeodomain interacting protein kinase 3
ZEB2	0.403154	0.000352	3.573631	Up	zinc finger E-box binding homeobox 2
CYBB	0.402342	0.002199	3.061969	Up	cytochrome b-245 beta chain
ZBTB26	0.401612	0.028182	2.194738	Up	zinc finger and BTB domain containing 26
BIVM	0.400425	0.041705	2.036456	Up	basic, immunoglobulin-like variable motif containing
RASA2	0.400093	0.04108	2.042721	Up	RAS p21 protein activator 2
HIF1A	0.399901	0.032459	2.138717	Up	hypoxia inducible factor 1 subunit alpha
CLEC7A	0.399596	0.012296	2.503522	Up	C-type lectin domain containing 7A
RBL2	0.399297	0.013409	2.472706	Up	RB transcriptional corepressor like 2
ATG2B	0.398821	0.002885	2.979696	Up	autophagy related 2B
STX11	0.398085	0.030953	2.157671	Up	syntaxin 11
ABHD3	0.398036	0.019871	2.328768	Up	abhydrolase domain containing 3, phospholipase
PLA2G7	0.39779	0.040688	2.046691	Up	phospholipase A2 group VII
REV3L	0.397785	0.007245	2.685379	Up	REV3 like, DNA directed polymerase zeta catalytic subunit
ZNF518A	0.397482	0.014091	2.454926	Up	zinc finger protein 518A
C6orf120	0.39731	0.005535	2.774134	Up	chromosome 6 open reading frame 120
PTPRC	0.396086	0.011334	2.532236	Up	protein tyrosine phosphatase receptor type C
IL18R1	0.395525	0.019093	2.343709	Up	interleukin 18 receptor 1
TDRD7	0.394924	0.003651	2.906819	Up	tudor domain containing 7
DOCK8	0.394663	0.001922	3.101989	Up	dedicator of cytokinesis 8
ARHGAP12	0.394141	0.030593	2.162323	Up	Rho GTPase activating protein 12
RPRD1A	0.394082	0.003365	2.932246	Up	regulation of nuclear pre-mRNA domain containing 1A
TRAPPC11	0.393891	0.000477	3.493474	Up	trafficking protein particle complex subunit 11
CCR2	0.393582	0.00165	3.146958	Up	C-C motif chemokine receptor 2
CLIC5	0.393456	0.017938	2.366896	Up	chloride intracellular channel 5
PPAT	0.393438	0.041944	2.034075	Up	phosphoribosyl pyrophosphate amidotransferase
GAB1	0.393165	0.017134	2.38383	Up	GRB2 associated binding protein 1
CEP350	0.392768	0.002766	2.992577	Up	centrosomal protein 350
GORAB	0.392761	0.023692	2.262086	Up	golgin, RAB6 interacting
MEFV	0.392248	0.019729	2.33146	Up	MEFV innate immuity regulator, pyrin
FBXO34	0.391644	0.000131	3.825022	Up	F-box protein 34

TRAV20	0.39163	0.031921	2.145395	Up	T cell receptor alpha variable 20
USP15	0.391618	0.033248	2.129072	Up	ubiquitin specific peptidase 15
CASD1	0.391367	0.040342	2.050229	Up	CAS1 domain containing 1
SLC25A40	0.39116	0.015841	2.412555	Up	solute carrier family 25 member 40
IQGAP2	0.390755	0.009113	2.607801	Up	IQ motif containing GTPase activating protein 2
CLEC4E	0.390506	0.027279	2.207496	Up	C-type lectin domain family 4 member E
PPP1R15B	0.390227	0.007597	2.669473	Up	protein phosphatase 1 regulatory subunit 15B
ACBD5	0.389968	0.002107	3.074659	Up	acyl-CoA binding domain containing 5
HECTD1	0.389902	0.001668	3.143766	Up	HECT domain E3 ubiquitin protein ligase 1
IKZF2	0.389876	0.027241	2.208047	Up	IKAROS family zinc finger 2
UHRF1BP1L	0.389476	0.016424	2.39935	Up	UHRF1 binding protein 1 like
UFL1	0.3888	0.039196	2.062127	Up	UFM1 specific ligase 1
AKAP11	0.388765	0.014151	2.453402	Up	A-kinase anchoring protein 11
TRAPPC8	0.388485	0.017772	2.370331	Up	trafficking protein particle complex subunit 8
TNFSF10	0.388306	0.020728	2.31291	Up	TNF superfamily member 10
COG6	0.387762	0.006846	2.704255	Up	component of oligomericgolgi complex 6
WARS1	0.386642	0.023511	2.265025	Up	tryptophanyl-tRNAsynthetase 1
CLCN3	0.386468	0.005477	2.777524	Up	chloride voltage-gated channel 3
TRAPPC10	0.385542	0.003154	2.952294	Up	trafficking protein particle complex subunit 10
GCLC	0.38532	0.011444	2.528832	Up	glutamate-cysteine ligase catalytic subunit
LDLRAD3	0.385295	0.006772	2.707856	Up	low density lipoprotein receptor class A domain containing 3
SKIL	0.384195	0.01474	2.438713	Up	SKI like proto-oncogene
SPIN1	0.384042	0.003545	2.91601	Up	spindlin 1
PPIP5K2	0.383734	0.016677	2.393756	Up	diphosphoinositolpentakisphosphate kinase 2
IRAK3	0.383507	0.002362	3.040511	Up	interleukin 1 receptor associated kinase 3
EBLN3P	0.383325	0.014822	2.436693	Up	endogenous Bornavirus like nucleoprotein 3, pseudogene
IFI16	0.383204	0.025657	2.231371	Up	interferon gamma inducible protein 16
WDFY1	0.383168	0.009667	2.587536	Up	WD repeat and FYVE domain containing 1
TET3	0.382628	0.007009	2.6964	Up	tetmethylcytosinedioxygenase 3
SOS2	0.382154	0.019715	2.331731	Up	SOS Ras/Rho guanine nucleotide exchange factor 2
PI4K2B	0.382104	0.024069	2.256031	Up	phosphatidylinositol 4-kinase type 2 beta
KLF3	0.381856	0.008891	2.616233	Up	Kruppel like factor 3
FEM1C	0.381617	0.007599	2.669375	Up	fem-1 homolog C
CCNT2	0.381027	0.018972	2.346081	Up	cyclin T2
ETV3	0.380984	0.000373	3.558673	Up	ETS variant transcription factor 3
VEGFA	0.379914	0.015915	2.410855	Up	vascular endothelial growth factor A
HIPK1	0.379842	0.009573	2.590869	Up	homeodomain interacting protein kinase 1
TP53INP1	0.379314	0.044655	2.007888	Up	tumor protein p53 inducible nuclear protein 1
NBPF1	0.378995	0.011117	2.538987	Up	NBPF member 1
IMPACT	0.378782	0.003641	2.907724	Up	impact RWD domain protein
CSF2RB	0.378713	0.044547	2.008907	Up	colony stimulating factor 2 receptor subunit beta
KMT2C	0.377745	0.006614	2.715663	Up	lysine methyltransferase 2C
SF3B1	0.377663	0.017405	2.378045	Up	splicing factor 3b subunit 1

SORL1	0.377489	0.044566	2.008729	Up	sortilin related receptor 1
PCF11	0.377487	0.005299	2.788285	Up	PCF11 cleavage and polyadenylation factor subunit
GPR27	0.376251	0.040768	2.045882	Up	G protein-coupled receptor 27
ATP11C	0.376147	0.025269	2.237265	Up	ATPase phospholipid transporting 11C
NCOA3	0.375998	0.002432	3.031621	Up	nuclear receptor coactivator 3
GALNT7	0.375767	0.022564	2.280742	Up	polypeptide N-acetylgalactosaminyltransferase 7
AP4E1	0.375621	0.018448	2.356509	Up	adaptor related protein complex 4 subunit epsilon 1
OGT	0.37547	0.022376	2.283919	Up	O-linked N-acetylglucosamine (GlcNAc) transferase
TSC22D2	0.375371	0.000195	3.72517	Up	TSC22 domain family member 2
POC1B	0.375273	0.023967	2.257653	Up	POC1 centriolar protein B
FGL2	0.375164	0.003213	2.946611	Up	fibrinogen like 2
TXNDC16	0.374571	0.023248	2.269341	Up	thioredoxin domain containing 16
BCL2A1	0.374198	0.037786	2.077172	Up	BCL2 related protein A1
IDH1	0.374146	2.78E-05	4.190484	Up	isocitrate dehydrogenase (NADP(+)) 1
CPLANE1	0.373946	0.031629	2.149068	Up	ciliogenesis and planar polarity effector 1
SESTD1	0.373785	0.00479	2.8208	Up	SEC14 and spectrin domain containing 1
OXR1	0.372755	0.018463	2.356192	Up	oxidation resistance 1
USP33	0.372538	0.001897	3.105923	Up	ubiquitin specific peptidase 33
ZNF567	0.372356	0.025142	2.239214	Up	zinc finger protein 567
CLK4	0.371543	0.045697	1.998184	Up	CDC like kinase 4
SEC23A	0.370956	0.031083	2.156014	Up	SEC23 homolog A, COPII coat complex component
RDH10	0.370507	0.029967	2.170533	Up	retinol dehydrogenase 10
ITGB1	0.370416	0.008111	2.647427	Up	integrin subunit beta 1
NIPBL-DT	0.370194	0.023932	2.258217	Up	NIPBL divergent transcript
IRF9	0.370158	0.037124	2.084394	Up	interferon regulatory factor 9
VCPIP1	0.370059	0.013305	2.475511	Up	valosin containing protein interacting protein 1
LIPA	0.369766	0.001003	3.289638	Up	lipase A, lysosomal acid type
PPP1R3D	0.369745	0.02256	2.280797	Up	protein phosphatase 1 regulatory subunit 3D
UBR1	0.369542	0.005203	2.794189	Up	ubiquitin protein ligase E3 component n-recognin 1
PGM3	0.369193	0.009273	2.601818	Up	phosphoglucomutase 3
PRDM10	0.368926	0.028088	2.196054	Up	PR/SET domain 10
RASA1	0.368892	0.014294	2.449798	Up	RAS p21 protein activator 1
DDX5	0.368834	0.008775	2.620714	Up	DEAD-box helicase 5
CD46	0.368199	0.018396	2.357545	Up	CD46 molecule
ZNF606	0.368014	0.019954	2.327208	Up	zinc finger protein 606
PATL1	0.367965	0.000108	3.871479	Up	PAT1 homolog 1, processing body mRNA decay factor
CCDC146	0.367522	0.030549	2.162901	Up	coiled-coil domain containing 146
DISC1	0.366965	0.030637	2.161753	Up	DISC1 scaffold protein
EIF2AK3	0.366828	0.021624	2.29691	Up	eukaryotic translation initiation factor 2 alpha kinase 3
ARRDC4	0.3668	0.010538	2.557647	Up	arrestin domain containing 4
MARCHF7	0.366346	0.028077	2.196206	Up	membrane associated ring-CH-type finger 7
LATS1	0.366311	0.018033	2.364942	Up	large tumor suppressor kinase 1
ENPP4	0.364629	0.039683	2.057033	Up	ectonucleotidepyrophosphatase/phosphodiesterase 4

FAM234B	0.36462	0.005907	2.752893	Up	family with sequence similarity 234 member B
SLC40A1	0.364614	0.028837	2.185713	Up	solute carrier family 40 member 1
GASK1B	0.363997	0.023418	2.266547	Up	golgi associated kinase 1B
DZIP3	0.363816	0.008936	2.614494	Up	DAZ interacting zinc finger protein 3
CHURC1	0.36321	0.011139	2.538299	Up	churchill domain containing 1
TMEM123	0.363117	0.018154	2.362465	Up	transmembrane protein 123
RCOR1	0.362917	0.005673	2.766094	Up	REST corepressor 1
PHLPP1	0.362844	0.005577	2.771658	Up	PH domain and leucine rich repeat protein phosphatase 1
SLFN5	0.362459	0.010532	2.557864	Up	schlafen family member 5
PRRC1	0.362322	0.003038	2.963838	Up	proline rich coiled-coil 1
LONRF1	0.362268	0.00845	2.633551	Up	LON peptidase N-terminal domain and ring finger 1
MTM1	0.362194	0.009356	2.598747	Up	myotubularin 1
ZNF700	0.361419	0.04004	2.053334	Up	zinc finger protein 700
FAM111A	0.361241	0.007289	2.683331	Up	FAM111 trypsin like peptidase A
FMR1	0.360817	0.015711	2.415572	Up	FMRP translational regulator 1
DCLRE1A	0.360653	0.012181	2.506846	Up	DNA cross-link repair 1A
OSBPL11	0.360471	0.011496	2.527255	Up	oxysterol binding protein like 11
AP1G1	0.360464	0.000857	3.333775	Up	adaptor related protein complex 1 subunit gamma 1
PAPOLG	0.360369	0.007008	2.696472	Up	poly(A) polymerase gamma
ZNF585A	0.360084	0.026976	2.211869	Up	zinc finger protein 585A
PLEKHM3	0.359745	0.00803	2.650825	Up	pleckstrin homology domain containing M3
MEIS1	0.359715	0.031531	2.15031	Up	Meishomeobox 1
ITCH	0.358963	0.006144	2.739974	Up	itchy E3 ubiquitin protein ligase
ARRDC3	0.358603	0.030199	2.167474	Up	arrestin domain containing 3
PHF2	0.358488	0.007194	2.687718	Up	PHD finger protein 2
FCGR3A	0.356857	0.004074	2.872385	Up	Fc fragment of IgG receptor IIIa
ZUP1	0.356665	0.047846	1.978737	Up	zinc finger containing ubiquitin peptidase 1
PTPN12	0.356524	0.03693	2.08654	Up	protein tyrosine phosphatase non-receptor type 12
PRPF39	0.356505	0.040945	2.044088	Up	pre-mRNA processing factor 39
NFKBIZ	0.355294	0.036985	2.085925	Up	NFKB inhibitor zeta
CEPT1	0.355052	0.005403	2.781943	Up	choline/ethanolamine phosphotransferase 1
IGF2R	0.354946	0.036024	2.096655	Up	insulin like growth factor 2 receptor
CLASP2	0.353658	0.013603	2.467581	Up	cytoplasmic linker associated protein 2
CDK5R1	0.352976	0.044915	2.005447	Up	cyclin dependent kinase 5 regulatory subunit 1
SPOPL	0.35271	0.034396	2.115394	Up	speckle type BTB/POZ protein like
PEX1	0.352524	0.020694	2.313516	Up	peroxisomal biogenesis factor 1
USF3	0.352329	0.009583	2.590534	Up	upstream transcription factor family member 3
ELF2	0.352303	0.007186	2.688104	Up	E74 like ETS transcription factor 2
RCBTB1	0.351412	0.029218	2.180539	Up	RCC1 and BTB domain containing protein 1
PARP12	0.35131	0.03397	2.120424	Up	poly(ADP-ribose) polymerase family member 12
GALC	0.349336	0.001908	3.10423	Up	galactosylceramidase
SCAF8	0.349032	0.018158	2.362387	Up	SR-related CTD associated factor 8
ADAR	0.348872	0.004896	2.813821	Up	adenosine deaminase RNA specific

SNRK	0.348798	0.00845	2.633537	Up	SNF related kinase
EOGT	0.348618	0.047177	1.984703	Up	EGF domain specific O-linked N-acetylglucosaminetransferase
TRGC1	0.348097	0.043865	2.015376	Up	T cell receptor gamma constant 1
USP25	0.348022	0.004209	2.862059	Up	ubiquitin specific peptidase 25
TNKS2	0.347883	0.014319	2.449153	Up	tankyrase 2
ZBTB1	0.347831	0.013823	2.461831	Up	zinc finger and BTB domain containing 1
TMED8	0.347631	0.02685	2.21369	Up	transmembrane p24 trafficking protein family member 8
DENND5A	0.347212	0.003228	2.945181	Up	DENN domain containing 5A
PARP8	0.34716	0.027766	2.200571	Up	poly(ADP-ribose) polymerase family member 8
UBR2	0.346801	0.007849	2.658503	Up	ubiquitin protein ligase E3 component n-recognin 2
NR2C1	0.345866	0.026565	2.217844	Up	nuclear receptor subfamily 2 group C member 1
PRKAR1A	0.345794	0.0147	2.439688	Up	protein kinase cAMP-dependent type I regulatory subunit alpha
TRIO	0.345648	0.001756	3.128662	Up	trio Rho guanine nucleotide exchange factor
ARFGEF1	0.345035	0.005192	2.794861	Up	ADP ribosylation factor guanine nucleotide exchange factor 1
CPOX	0.344978	0.022371	2.284002	Up	coproporphyrinogen oxidase
SENP6	0.344654	0.005449	2.779238	Up	SUMO specific peptidase 6
ZFR	0.344401	0.014019	2.456787	Up	zinc finger RNA binding protein
WDR11	0.344319	0.003862	2.889216	Up	WD repeat domain 11
RB1CC1	0.34424	0.047821	1.978955	Up	RB1 inducible coiled-coil 1
TBC1D8	0.343055	0.017591	2.37412	Up	TBC1 domain family member 8
MTR	0.343021	0.01288	2.487067	Up	5-methyltetrahydrofolate-homocysteine methyltransferase
PTAR1	0.342936	0.042993	2.023777	Up	protein prenyltransferase alpha subunit repeat containing 1
SLC6A6	0.34254	0.032415	2.139252	Up	solute carrier family 6 member 6
WASHC4	0.342275	0.034383	2.115546	Up	WASH complex subunit 4
NUP58	0.342266	0.035245	2.105532	Up	nucleoporin 58
BRWD3	0.341667	0.025147	2.239134	Up	bromodomain and WD repeat domain containing 3
RANBP6	0.341496	0.041281	2.040692	Up	RAN binding protein 6
LYPLA1	0.341423	0.028062	2.196414	Up	lysophospholipase 1
LDLR	0.340577	0.023359	2.267519	Up	low density lipoprotein receptor
LPGAT1	0.340091	0.020106	2.324359	Up	lysophosphatidylglycerolacyltransferase 1
NUS1	0.340026	0.038396	2.070606	Up	NUS1 dehydrodolichyldiphosphate synthase subunit
TIA1	0.339287	0.0381	2.073773	Up	TIA1 cytotoxic granule associated RNA binding protein
PWWP2A	0.339134	0.006521	2.720359	Up	PWWP domain containing 2A
ZBTB37	0.339104	0.0227	2.278441	Up	zinc finger and BTB domain containing 37
LPIN2	0.33881	0.012596	2.494979	Up	lipin 2
PANK3	0.338709	0.008849	2.617821	Up	pantothenate kinase 3
TLR6	0.338522	0.008635	2.626179	Up	toll like receptor 6
FGD6	0.338495	0.015096	2.430056	Up	FYVE, RhoGEF and PH domain containing 6
NNT	0.338077	0.0082	2.643723	Up	nicotinamide nucleotide transhydrogenase
SRGAP2	0.337383	0.015744	2.414797	Up	SLIT-ROBO Rho GTPase activating protein 2
SDE2	0.336883	0.019595	2.334011	Up	SDE2 telomere maintenance homolog
ERO1B	0.3363	0.034728	2.111518	Up	endoplasmic reticulum oxidoreductase 1 beta
SIRT1	0.335886	0.045022	2.00445	Up	sirtuin 1

TOX	0.335858	0.014988	2.432677	Up	thymocyte selection associated high mobility group box
BIRC6	0.335585	0.000723	3.380816	Up	baculoviral IAP repeat containing 6
ALDH1A1	0.335523	0.024396	2.250834	Up	aldehyde dehydrogenase 1 family member A1
SVIL	0.334479	0.023136	2.271176	Up	supervillin
SMG1	0.334437	0.020164	2.323275	Up	SMG1 nonsense mediated mRNA decay associated PI3K related kinase
VPS13C	0.33431	0.018011	2.365385	Up	vacuolar protein sorting 13 homolog C
UBR5	0.334257	0.003782	2.89577	Up	ubiquitin protein ligase E3 component n-recognin 5
SLC36A1	0.334115	0.035685	2.100493	Up	solute carrier family 36 member 1
NEMP1	0.334107	0.024745	2.245355	Up	nuclear envelope integral membrane protein 1
NOD2	0.334077	0.031011	2.15693	Up	nucleotide binding oligomerization domain containing 2
RNF111	0.333585	0.017755	2.370682	Up	ring finger protein 111
ARMT1	0.33344	0.00173	3.133004	Up	acidic residue methyltransferase 1
AHCYL2	0.333396	0.004365	2.850504	Up	adenosylhomocysteinase like 2
SLC36A4	0.333152	0.024413	2.250564	Up	solute carrier family 36 member 4
SEMA6B	-1.56564	0.000374	-3.55773	Down	semaphorin 6B
HBG2	-1.4958	0.014941	-2.43381	Down	hemoglobin subunit gamma 2
HBG1	-1.29798	0.013291	-2.47587	Down	hemoglobin subunit gamma 1
RAP1GAP	-1.24886	0.019481	-2.33619	Down	RAP1 GTPase activating protein
IGLV10-54	-1.1921	0.003009	-2.96685	Down	immunoglobulin lambda variable 10-54
ASAP1-IT2	-0.94099	0.000439	-3.51538	Down	ASAP1 intronic transcript 2
IGLV7-43	-0.87467	0.012142	-2.50798	Down	immunoglobulin lambda variable 7-43
GK-IT1	-0.87444	0.01086	-2.54716	Down	GK intronic transcript 1
MYL9	-0.81478	0.012731	-2.49121	Down	myosin light chain 9
IGHG3	-0.80547	0.038376	-2.07082	Down	immunoglobulin heavy constant gamma 3 (G3m marker)
ZBTB32	-0.80502	0.000678	-3.39839	Down	zinc finger and BTB domain containing 32
IGHV3-15	-0.79361	0.003284	-2.93978	Down	immunoglobulin heavy variable 3-15
IGKJ1	-0.78767	0.006012	-2.74714	Down	immunoglobulin kappa joining 1
IGKV2-24	-0.78694	0.020572	-2.31575	Down	immunoglobulin kappa variable 2-24
KEL	-0.77524	0.003452	-2.9243	Down	Kellmetallo-endopeptidase (Kell blood group)
IGLV3-25	-0.76869	0.013573	-2.46836	Down	immunoglobulin lambda variable 3-25
IGLC7	-0.767	0.028814	-2.18602	Down	immunoglobulin lambda constant 7
PCSK1N	-0.75391	0.015159	-2.42856	Down	proproteinconvertasesubtilisin/kexin type 1 inhibitor
FRMD4A	-0.75023	0.001698	-3.13852	Down	FERM domain containing 4A
KLF1	-0.72964	0.013451	-2.4716	Down	Kruppel like factor 1
EFNA3	-0.72659	0.017921	-2.36725	Down	ephrin A3
IGLC3	-0.71894	0.01058	-2.55626	Down	immunoglobulin lambda constant 3 (Kern-Oz+ marker)
CRIP2	-0.71503	0.003641	-2.90769	Down	cysteine rich protein 2
MEMO1	-0.71182	0.001076	-3.26985	Down	Methylation modifier for class I HLA
AZU1	-0.70691	0.040408	-2.04956	Down	azurocidin 1
RNU4-62P	-0.70231	0.004796	-2.82044	Down	RNA, U4 small nuclear 62, pseudogene
TSHZ2	-0.6979	0.002939	-2.97406	Down	teashirt zinc finger homeobox 2
PPP1R14A	-0.69612	0.005847	-2.75626	Down	protein phosphatase 1 regulatory inhibitor subunit 14A
GCAT	-0.68862	0.024863	-2.24352	Down	glycine C-acetyltransferase

TRBV15	-0.6846	0.001675	-3.14247	Down	T cell receptor beta variable 15
SAMD14	-0.68433	0.032843	-2.134	Down	sterile alpha motif domain containing 14
ZBTB20	-0.67808	0.000368	-3.56233	Down	zinc finger and BTB domain containing 20
TGFB1I1	-0.67268	0.002989	-2.96891	Down	transforming growth factor beta 1 induced transcript 1
PHGDH	-0.65507	0.001951	-3.09755	Down	phosphoglycerate dehydrogenase
TRBV19	-0.64892	0.002473	-3.02659	Down	T cell receptor beta variable 19
RPL10P3	-0.643	0.002098	-3.07603	Down	ribosomal protein L10 pseudogene 3
HS3ST1	-0.63815	0.02664	-2.21675	Down	heparansulfate-glucosamine 3-sulfotransferase 1
GRAP	-0.61852	0.000387	-3.549	Down	GRB2 related adaptor protein
CAVIN1	-0.61438	0.001873	-3.10974	Down	caveolae associated protein 1
PWP2	-0.60552	0.036134	-2.09541	Down	PWP2 small subunit processome component
LIMS2	-0.60498	0.00566	-2.76687	Down	LIM zinc finger domain containing 2
CCDC34	-0.60441	0.006032	-2.74602	Down	coiled-coil domain containing 34
RPL13P2	-0.59862	0.027886	-2.19888	Down	ribosomal protein L13 pseudogene 2
IGLV3-19	-0.59368	0.04444	-2.00992	Down	immunoglobulin lambda variable 3-19
C9orf78	-0.58629	0.028286	-2.19329	Down	chromosome 9 open reading frame 78
SHPK	-0.58468	0.001672	-3.14302	Down	sedoheptulokinase
RPS15AP17	-0.58348	0.018968	-2.34615	Down	ribosomal protein S15a pseudogene 17
ARL4D	-0.5786	0.022294	-2.28533	Down	ADP ribosylation factor like GTPase 4D
SLC14A1	-0.5722	0.002501	-3.02326	Down	solute carrier family 14 member 1 (Kidd blood group)
POU2F2	-0.57193	0.002374	-3.03893	Down	POU class 2 homeobox 2
MRC2	-0.56976	0.027611	-2.20277	Down	mannose receptor C type 2
PAX5	-0.56773	0.015783	-2.41389	Down	paired box 5
NT5M	-0.56654	0.009235	-2.60325	Down	5',3'-nucleotidase, mitochondrial
TMEM238	-0.56576	0.008126	-2.64677	Down	transmembrane protein 238
PKIG	-0.56136	0.003885	-2.88735	Down	cAMP-dependent protein kinase inhibitor gamma
RPS28P7	-0.56072	0.004418	-2.84664	Down	ribosomal protein S28 pseudogene 7
IGHG2	-0.55981	0.049539	-1.96393	Down	immunoglobulin heavy constant gamma 2 (G2m marker)
TRBV7-9	-0.5532	0.010029	-2.57483	Down	T cell receptor beta variable 7-9
PI16	-0.55208	0.004785	-2.82115	Down	peptidase inhibitor 16
FN3K	-0.54797	0.001548	-3.16558	Down	fructosamine 3 kinase
IGKV3-20	-0.54499	0.024995	-2.24148	Down	immunoglobulin kappa variable 3-20
FHIT	-0.54334	0.006912	-2.70106	Down	fragile histidine triad diadenosinetriphosphatase
SELENOM	-0.53751	0.009878	-2.58006	Down	selenoprotein M
PRKAR1B	-0.53702	9.73E-05	-3.8972	Down	protein kinase cAMP-dependent type I regulatory subunit beta
ST6GALNAC4	-0.53447	0.013214	-2.47795	Down	ST6 N-acetylgalactosaminide alpha-2,6-sialyltransferase 4
NAPSB	-0.53429	0.006951	-2.69918	Down	napsin B aspartic peptidase, pseudogene
GP9	-0.53352	0.026445	-2.21961	Down	glycoprotein IX platelet
RPL26P6	-0.53133	0.024277	-2.25272	Down	ribosomal protein L26 pseudogene 6
TRAV8-1	-0.52699	0.048666	-1.97151	Down	T cell receptor alpha variable 8-1
PYCR3	-0.52231	0.005595	-2.7706	Down	pyrroline-5-carboxylate reductase 3
TNFRSF13B	-0.5198	0.022606	-2.28003	Down	TNF receptor superfamily member 13B
CD79B	-0.51591	0.004015	-2.877	Down	CD79b molecule

ZGLP1	-0.51539	0.008683	-2.62429	Down	zinc finger GATA like protein 1
ZNF714	-0.51471	0.004407	-2.84749	Down	zinc finger protein 714
ATG9B	-0.51124	0.001925	-3.10156	Down	autophagy related 9B
RN7SL600P	-0.50987	0.039361	-2.06039	Down	RNA, 7SL, cytoplasmic 600, pseudogene
NDUFA13	-0.50939	0.011579	-2.52472	Down	NADH:ubiquinoneoxidoreductase subunit A13
CCDC106	-0.50893	0.002213	-3.06002	Down	coiled-coil domain containing 106
CHCHD6	-0.50661	0.001829	-3.11662	Down	coiled-coil-helix-coiled-coil-helix domain containing 6
BEND5	-0.50539	0.00118	-3.24359	Down	BEN domain containing 5
LMTK3	-0.50504	0.005584	-2.77128	Down	lemur tyrosine kinase 3
FXYD7	-0.50359	0.025758	-2.22985	Down	FXYD domain containing ion transport regulator 7
EFNA4	-0.50095	0.008563	-2.62902	Down	ephrin A4
C12orf57	-0.50001	0.002137	-3.07051	Down	chromosome 12 open reading frame 57
PNPLA7	-0.49486	0.007359	-2.68014	Down	patatin like phospholipase domain containing 7
INKA1	-0.49424	0.020021	-2.32595	Down	inka box actin regulator 1
GAMT	-0.49406	0.001604	-3.1551	Down	guanidinoacetate N-methyltransferase
TENT5C	-0.49205	0.019444	-2.3369	Down	terminal nucleotidyltransferase 5C
CYP20A1	-0.48764	0.00196	-3.09619	Down	cytochrome P450 family 20 subfamily A member 1
NT5DC2	-0.48748	0.034568	-2.11339	Down	5'-nucleotidase domain containing 2
CHMP4A	-0.48595	0.018489	-2.35568	Down	charged multivesicular body protein 4A
ZNF358	-0.48145	0.008482	-2.63225	Down	zinc finger protein 358
PODXL2	-0.48049	0.017053	-2.38556	Down	podocalyxin like 2
C16orf74	-0.47969	0.001882	-3.1082	Down	chromosome 16 open reading frame 74
ITGA2B	-0.47651	0.048538	-1.97263	Down	integrin subunit alpha 2b
PURA	-0.47608	0.001303	-3.21525	Down	purine rich element binding protein A
ABCB9	-0.47492	0.016638	-2.39462	Down	ATP binding cassette subfamily B member 9
NUCKS1P1	-0.47416	0.024136	-2.25496	Down	nuclear casein kinase and cyclin dependent kinase substrate 1 pseudogene 1
ZC3H6	-0.47239	0.025336	-2.23624	Down	zinc finger CCCH-type containing 6
TOP2A	-0.47031	0.012076	-2.5099	Down	DNA topoisomerase II alpha
RABEP2	-0.46999	0.005742	-2.76214	Down	rabaptin, RAB GTPase binding effector protein 2
RPS21	-0.46961	0.00092	-3.314	Down	ribosomal protein S21
TMSB4XP4	-0.46862	0.004621	-2.83234	Down	TMSB4X pseudogene 4
DPM2	-0.46764	0.017715	-2.37152	Down	dolichyl-phosphate mannosyltransferase subunit 2, regulatory
ZNF593	-0.46212	0.010171	-2.56996	Down	zinc finger protein 593
HSPBP1	-0.46082	0.006124	-2.74104	Down	HSPA (Hsp70) binding protein 1
SEC62	-0.45972	0.015262	-2.42611	Down	SEC62 homolog, preprotein translocation factor
TNFRSF4	-0.45871	0.033726	-2.12334	Down	TNF receptor superfamily member 4
GNAO1	-0.45841	0.046748	-1.98858	Down	G protein subunit alpha o1
NOP53	-0.45616	0.001891	-3.10684	Down	NOP53 ribosome biogenesis factor
PPBP	-0.45597	0.030646	-2.16164	Down	pro-platelet basic protein
NOXA1	-0.45542	0.039955	-2.05422	Down	NADPH oxidase activator 1
RPS29	-0.45369	0.006099	-2.74241	Down	ribosomal protein S29
GNB1L	-0.45331	0.003924	-2.88421	Down	G protein subunit beta 1 like

FNDC10	-0.45304	0.033141	-2.13037	Down	fibronectin type III domain containing 10
RPL13P12	-0.45284	0.004106	-2.86993	Down	ribosomal protein L13 pseudogene 12
MYBL2	-0.45211	0.049877	-1.96102	Down	MYB proto-oncogene like 2
MAL	-0.451	0.004681	-2.82821	Down	mal, T cell differentiation protein
MZT2B	-0.45047	0.002862	-2.98219	Down	mitotic spindle organizing protein 2B
TAX1BP3	-0.44482	0.007218	-2.68661	Down	Tax1 binding protein 3
RABAC1	-0.4443	0.011457	-2.52845	Down	Rab acceptor 1
ARL2	-0.44399	0.001986	-3.09232	Down	ADP ribosylation factor like GTPase 2
ARPC1B	-0.44224	0.001651	-3.14667	Down	actin related protein 2/3 complex subunit 1B
SIT1	-0.44217	0.002191	-3.06307	Down	signaling threshold regulating transmembrane adaptor 1
CCDC85B	-0.4411	0.019597	-2.33397	Down	coiled-coil domain containing 85B
PTCD1	-0.44047	3.53E-05	-4.13618	Down	pentatricopeptide repeat domain 1
PRRT3	-0.4389	0.000769	-3.36389	Down	proline rich transmembrane protein 3
NENF	-0.43871	0.004512	-2.83995	Down	neudesinneurotrophic factor
FBXO10	-0.4382	0.016208	-2.4042	Down	F-box protein 10
IGFBP4	-0.43819	0.007425	-2.67717	Down	insulin like growth factor binding protein 4
TRBV5-1	-0.43811	0.014686	-2.44003	Down	T cell receptor beta variable 5-1
PFDN4	-0.43698	0.026052	-2.22543	Down	prefoldin subunit 4
GGT1	-0.43665	0.00142	-3.19058	Down	gamma-glutamyltransferase 1
FBLN7	-0.43646	0.035888	-2.09819	Down	fibulin 7
NBL1	-0.43619	0.045624	-1.99885	Down	NBL1, DAN family BMP antagonist
C14orf132	-0.43551	0.02019	-2.3228	Down	chromosome 14 open reading frame 132
TRAV23DV6	-0.43539	0.048866	-1.96976	Down	T cell receptor alpha variable 23/delta variable 6
TRPM4	-0.43528	0.026401	-2.22026	Down	transient receptor potential cation channel subfamily M member 4
FAM174C	-0.43415	0.010202	-2.5689	Down	family with sequence similarity 174 member C
LRRC29	-0.43221	0.016501	-2.39763	Down	leucine rich repeat containing 29
SNRNP25	-0.43162	0.00139	-3.1967	Down	small nuclear ribonucleoprotein U11/U12 subunit 25
GPR55	-0.43054	0.001841	-3.11483	Down	G protein-coupled receptor 55
PPDPF	-0.43	0.009193	-2.6048	Down	pancreatic progenitor cell differentiation and proliferation factor
TRBD1	-0.42995	0.022616	-2.27986	Down	T cell receptor beta diversity 1
ESF1	-0.42994	0.013225	-2.47765	Down	ESF1 nucleolar pre-rRNA processing protein homolog
LRRCC1	-0.42928	0.020791	-2.31176	Down	leucine rich repeat and coiled-coil centrosomal protein 1
GCHFR	-0.42895	0.041726	-2.03624	Down	GTP cyclohydrolase I feedback regulator
RPL37P2	-0.42837	0.0425	-2.02859	Down	ribosomal protein L37 pseudogene 2
RPL13	-0.42827	0.001989	-3.09193	Down	ribosomal protein L13
ALKBH7	-0.42786	0.006162	-2.73905	Down	alkB homolog 7
PF4	-0.42623	0.019051	-2.34454	Down	platelet factor 4
F2RL3	-0.42604	0.037816	-2.07684	Down	F2R like thrombin or trypsin receptor 3
SNTA1	-0.42596	0.013394	-2.47311	Down	syntrophin alpha 1
HDHD3	-0.42454	0.001149	-3.25119	Down	haloaciddehalogenase like hydrolase domain containing 3
GAREM2	-0.42436	0.014387	-2.44745	Down	GRB2 associated regulator of MAPK1 subtype 2
UBXN6	-0.42375	0.041822	-2.03529	Down	UBX domain protein 6
NOSIP	-0.42193	0.001539	-3.16721	Down	nitric oxide synthase interacting protein

RPLP2	-0.42078	0.002313	-3.04673	Down	ribosomal protein lateral stalk subunit P2
DNAJC2	-0.42011	0.038845	-2.06583	Down	DnaJ heat shock protein family (Hsp40) member C2
RPS14	-0.41928	0.00296	-2.97185	Down	ribosomal protein S14
ZNF91	-0.418	0.012503	-2.49762	Down	zinc finger protein 91
NFIA	-0.4174	0.019303	-2.33962	Down	nuclear factor I A
RPL13AP20	-0.41631	0.002491	-3.02442	Down	ribosomal protein L13a pseudogene 20
DENND5B	-0.41617	0.034319	-2.1163	Down	DENN domain containing 5B
SWSAP1	-0.41504	0.00982	-2.5821	Down	SWIM-type zinc finger 7 associated protein 1
LHPP	-0.41497	0.003628	-2.9088	Down	phospholysinephosphohistidine inorganic pyrophosphate phosphatase
CD27	-0.41394	0.007929	-2.65507	Down	CD27 molecule
MCRIP1	-0.41249	0.024348	-2.2516	Down	MAPK regulated corepressor interacting protein 1
PHLDB3	-0.4124	0.012134	-2.50821	Down	pleckstrin homology like domain family B member 3
P2RX5	-0.41142	0.024486	-2.24942	Down	purinergic receptor P2X 5
ARRDC5	-0.41018	0.029395	-2.17815	Down	arrestin domain containing 5
MZT2A	-0.41015	0.000303	-3.6124	Down	mitotic spindle organizing protein 2A
KRT18	-0.40943	0.015526	-2.41986	Down	keratin 18
EIF5B	-0.4094	0.015145	-2.4289	Down	eukaryotic translation initiation factor 5B
BMERB1	-0.40902	0.045373	-2.00118	Down	bMERB domain containing 1
RITA1	-0.40814	0.00405	-2.87428	Down	RBPJ interacting and tubulin associated 1
MRPL2	-0.4071	0.03296	-2.13257	Down	mitochondrial ribosomal protein L2
ZNF524	-0.40704	0.034292	-2.11663	Down	zinc finger protein 524
RRN3P3	-0.40597	0.011742	-2.51981	Down	RRN3 pseudogene 3
BAG1	-0.40554	0.021842	-2.2931	Down	BAG cochaperone 1
EEF1DP2	-0.40519	0.002375	-3.0388	Down	eukaryotic translation elongation factor 1 delta pseudogene 2
VEGFB	-0.40451	0.001478	-3.17901	Down	vascular endothelial growth factor B
ANKRD12	-0.40276	0.037916	-2.07576	Down	ankyrin repeat domain 12
FBXL15	-0.40272	0.021508	-2.29895	Down	F-box and leucine rich repeat protein 15
CCDC142	-0.40253	0.003405	-2.92855	Down	coiled-coil domain containing 142
SH2D3A	-0.40072	0.001491	-3.1764	Down	SH2 domain containing 3A
METTL26	-0.40041	0.006464	-2.72329	Down	methyltransferase like 26
C12orf43	-0.39984	0.000136	-3.81449	Down	chromosome 12 open reading frame 43
LTB	-0.39766	0.00151	-3.17277	Down	lymphotoxin beta
FAM133B	-0.3966	0.023209	-2.26997	Down	family with sequence similarity 133 member B
SNHG19	-0.3964	0.028847	-2.18558	Down	small nucleolar RNA host gene 19
NAT14	-0.39577	0.032137	-2.1427	Down	N-acetyltransferase 14 (putative)
KDF1	-0.39473	0.049433	-1.96484	Down	keratinocyte differentiation factor 1
PRXL2A	-0.39306	0.03194	-2.14516	Down	peroxiredoxin like 2A
ELOF1	-0.39281	0.003068	-2.96085	Down	elongation factor 1
MBD3	-0.39213	0.015498	-2.42054	Down	methyl-CpG binding domain protein 3
ITM2C	-0.3907	0.042749	-2.02615	Down	integral membrane protein 2C
DUSP18	-0.39021	0.019325	-2.33921	Down	dual specificity phosphatase 18
POU2F1	-0.38979	0.003601	-2.91113	Down	POU class 2 homeobox 1
MGLL	-0.38963	0.01704	-2.38585	Down	monoglyceride lipase

HSPG2	-0.3872	0.024374	-2.25118	Down	heparansulfate proteoglycan 2
ASCC2	-0.38651	0.021134	-2.30559	Down	activating signal cointegrator 1 complex subunit 2
SREK1IP1	-0.38454	0.020228	-2.3221	Down	SREK1 interacting protein 1
SNRPN	-0.38432	0.040017	-2.05357	Down	small nuclear ribonucleoprotein polypeptide N
TJP3	-0.38395	0.044265	-2.01157	Down	tight junction protein 3
CAPN5	-0.38347	0.029036	-2.18299	Down	calpain 5
SHISAL2A	-0.38325	0.005469	-2.77803	Down	shisa like 2A
RPS15	-0.38314	0.022832	-2.27623	Down	ribosomal protein S15
CPTP	-0.38187	0.020593	-2.31537	Down	ceramide-1-phosphate transfer protein
ZBTB7A	-0.3817	0.008407	-2.63526	Down	zinc finger and BTB domain containing 7A
PC	-0.38113	0.029322	-2.17913	Down	pyruvate carboxylase
SNHG8	-0.38042	0.025923	-2.22736	Down	small nucleolar RNA host gene 8
GPT2	-0.37875	0.035881	-2.09827	Down	glutamic--pyruvic transaminase 2
HEXIM2	-0.37863	0.025432	-2.23477	Down	HEXIM P-TEFb complex subunit 2
BCL7C	-0.37843	0.030245	-2.16686	Down	BAF chromatin remodeling complex subunit BCL7C
RPL18A	-0.37755	0.048417	-1.97369	Down	ribosomal protein L18a
NACA4P	-0.37717	0.037952	-2.07537	Down	NACA family member 4, pseudogene
FLYWCH1	-0.37709	0.011381	-2.53076	Down	FLYWCH-type zinc finger 1
NME4	-0.37705	0.014638	-2.44122	Down	NME/NM23 nucleoside diphosphate kinase 4
ACP5	-0.37682	0.011026	-2.54186	Down	acid phosphatase 5, tartrate resistant
TRAPPC6A	-0.37667	0.008704	-2.62348	Down	trafficking protein particle complex subunit 6A
RPL36	-0.37633	0.021961	-2.29105	Down	ribosomal protein L36
TMUB1	-0.37552	0.007327	-2.68163	Down	transmembrane and ubiquitin like domain containing 1
PNOC	-0.37533	0.045755	-1.99765	Down	prepronociceptin
ROGDI	-0.37524	0.025409	-2.23513	Down	rogdi atypical leucine zipper
ANTKMT	-0.37504	0.041095	-2.04257	Down	adenine nucleotide translocase lysine methyltransferase
ATP5F1D	-0.37499	0.021166	-2.30501	Down	ATP synthase F1 subunit delta
VPREB3	-0.37499	0.046499	-1.99083	Down	V-set pre-B cell surrogate light chain 3
C1orf122	-0.37412	0.00883	-2.61855	Down	chromosome 1 open reading frame 122
PUSL1	-0.37375	0.020115	-2.3242	Down	pseudouridine synthase like 1
RPS19	-0.37343	0.008447	-2.63366	Down	ribosomal protein S19
HHLA3	-0.37262	0.029994	-2.17017	Down	HERV-H LTR-associating 3
TNK1	-0.37185	0.036403	-2.09239	Down	tyrosine kinase non receptor 1
MARCHF9	-0.37168	0.000998	-3.29121	Down	membrane associated ring-CH-type finger 9
CCR7	-0.37164	0.016192	-2.40456	Down	C-C motif chemokine receptor 7
NDUFS8	-0.37089	0.010363	-2.56348	Down	NADH:ubiquinoneoxidoreductase core subunit S8
DMAC2L	-0.37087	0.002852	-2.98325	Down	distal membrane arm assembly component 2 like
ZCRB1	-0.37084	0.005918	-2.75228	Down	zinc finger CCHC-type and RNA binding motif containing 1
NINJ2	-0.3707	0.021705	-2.29549	Down	ninjurin 2
CCDC85C	-0.37057	0.015366	-2.42364	Down	coiled-coil domain containing 85C
TM7SF2	-0.37044	0.023776	-2.26073	Down	transmembrane 7 superfamily member 2
GIPC1	-0.37041	0.009037	-2.61065	Down	GIPC PDZ domain containing family member 1
CD6	-0.37018	0.008059	-2.64959	Down	CD6 molecule

PRR7	-0.37017	0.032725	-2.13544	Down	proline rich 7, synaptic
TRBV10-3	-0.36952	0.047346	-1.98319	Down	T cell receptor beta variable 10-3
C19orf48	-0.36939	0.015882	-2.41161	Down	multidrug resistance-related protein
CTDSPL	-0.36938	0.044763	-2.00687	Down	CTD small phosphatase like
PDE6B	-0.36744	0.000453	-3.50719	Down	phosphodiesterase 6B
RPS9	-0.36715	0.001075	-3.27011	Down	ribosomal protein S9
ALDOC	-0.3671	0.001294	-3.21727	Down	aldolase, fructose-bisphosphate C
RPS15AP1	-0.36658	0.037758	-2.07748	Down	ribosomal protein S15a pseudogene 1
DCP1A	-0.36586	0.000779	-3.36025	Down	decapping mRNA 1A
PRDX2	-0.36572	0.009164	-2.60587	Down	peroxiredoxin 2
ELAC1	-0.36521	0.010375	-2.56307	Down	elaCribonuclease Z 1
DNPH1	-0.36486	0.015081	-2.43043	Down	2'-deoxynucleoside 5'-phosphate N-hydrolase 1
ENDOG	-0.36484	0.047213	-1.98438	Down	endonuclease G
FAHD1	-0.36392	0.002766	-2.9926	Down	fumarylacetoacetate hydrolase domain containing 1
ZNF611	-0.36388	0.011903	-2.51502	Down	zinc finger protein 611
MRPL23	-0.36321	0.015304	-2.42511	Down	mitochondrial ribosomal protein L23
CD7	-0.36267	0.03555	-2.10203	Down	CD7 molecule
THAP3	-0.36155	0.003008	-2.96688	Down	THAP domain containing 3
RPL29P11	-0.36037	0.01757	-2.37455	Down	ribosomal protein L29 pseudogene 11
RPL29	-0.36017	0.003124	-2.95524	Down	ribosomal protein L29
INF2	-0.35941	0.004187	-2.86374	Down	inverted formin 2
APBB1	-0.35922	0.00588	-2.75437	Down	amyloid beta precursor protein binding family B member 1
FAU	-0.35807	0.017444	-2.37722	Down	FAU ubiquitin like and ribosomal protein S30 fusion
GADD45GIP1	-0.35772	0.010383	-2.56281	Down	GADD45G interacting protein 1
ILF3-DT	-0.35746	0.004946	-2.81055	Down	ILF3 divergent transcript
RPL18	-0.35695	0.013837	-2.46148	Down	ribosomal protein L18
TRBC2	-0.35667	0.014194	-2.45233	Down	T cell receptor beta constant 2
MCRIP2	-0.3553	0.021913	-2.29188	Down	MAPK regulated corepressor interacting protein 2
TMEM40	-0.35413	0.035856	-2.09856	Down	transmembrane protein 40
TONSL	-0.35384	0.020513	-2.31682	Down	tonsoku like, DNA repair protein
ANKRD39	-0.35369	0.010007	-2.5756	Down	ankyrin repeat domain 39
VPS51	-0.35336	0.007174	-2.68865	Down	VPS51 subunit of GARP complex
NMRAL1	-0.35226	0.018759	-2.35028	Down	NmrA like redox sensor 1
MRPS17	-0.35175	0.038273	-2.07192	Down	mitochondrial ribosomal protein S17
RPLP1	-0.35146	0.002613	-3.00998	Down	ribosomal protein lateral stalk subunit P1
RPL23AP42	-0.35116	0.025561	-2.23281	Down	ribosomal protein L23a pseudogene 42
RUNX3	-0.35092	0.026754	-2.2151	Down	RUNX family transcription factor 3
REEP6	-0.35045	0.043635	-2.01758	Down	receptor accessory protein 6
DCLRE1C	-0.35024	0.013129	-2.48025	Down	DNA cross-link repair 1C
CCDC120	-0.34902	0.004839	-2.81757	Down	coiled-coil domain containing 120
ZNF428	-0.34891	0.008866	-2.61717	Down	zinc finger protein 428
POLR2J3	-0.34862	0.037521	-2.08005	Down	RNA polymerase II subunit J3
SPIB	-0.34853	0.027128	-2.20967	Down	Spi-B transcription factor

AQP3	-0.34832	0.010319	-2.56496	Down	aquaporin 3 (Gill blood group)
SVIP	-0.34781	0.001862	-3.11137	Down	small VCP interacting protein
CCDC124	-0.34668	0.021461	-2.29978	Down	coiled-coil domain containing 124
TRBV7-6	-0.34644	0.042672	-2.0269	Down	T cell receptor beta variable 7-6
RPS5	-0.34569	0.009463	-2.59486	Down	ribosomal protein S5
BIN1	-0.34562	0.003818	-2.89278	Down	bridging integrator 1
MAF1	-0.34496	0.009817	-2.5822	Down	MAF1 homolog, negative regulator of RNA polymerase III
ZNF517	-0.34464	0.004366	-2.85046	Down	zinc finger protein 517
CWF19L2	-0.34442	0.026623	-2.217	Down	CWF19 like cell cycle control factor 2
MTCO2P12	-0.34438	0.027375	-2.20612	Down	MT-CO2 pseudogene 12
TMIGD2	-0.34389	0.031623	-2.14915	Down	transmembrane and immunoglobulin domain containing 2
LAGE3	-0.34354	0.027773	-2.20048	Down	L antigen family member 3
RPL19	-0.34341	0.001996	-3.09087	Down	ribosomal protein L19
MRPS34	-0.34339	0.022359	-2.28421	Down	mitochondrial ribosomal protein S34
SOX12	-0.3424	0.005056	-2.80343	Down	SRY-box transcription factor 12
ADK	-0.34157	0.01727	-2.3809	Down	adenosine kinase
NUDT18	-0.3412	0.019994	-2.32647	Down	nudix hydrolase 18
ECSIT	-0.34119	0.005678	-2.76581	Down	ECSIT signaling integrator
TMEM156	-0.34078	0.01493	-2.43407	Down	transmembrane protein 156
WDR18	-0.34068	0.034446	-2.11481	Down	WD repeat domain 18
ZNF444	-0.34024	0.003207	-2.94713	Down	zinc finger protein 444
SLC35E3	-0.33903	0.028847	-2.18557	Down	solute carrier family 35 member E3
PCYT2	-0.33887	0.004332	-2.85292	Down	phosphate cytidylyltransferase 2, ethanolamine
NAGS	-0.33883	0.049862	-1.96114	Down	N-acetylglutamate synthase
DCXR	-0.3387	0.02248	-2.28216	Down	dicarbonyl and L-xylulosereductase
ABHD14A	-0.33857	0.017177	-2.38289	Down	abhydrolase domain containing 14A
FBXL8	-0.33841	0.03326	-2.12894	Down	F-box and leucine rich repeat protein 8
RPL27	-0.33827	0.006777	-2.70762	Down	ribosomal protein L27
PPIG	-0.33814	0.03116	-2.15502	Down	peptidylprolylisomerase G
RPL8	-0.338	0.016616	-2.3951	Down	ribosomal protein L8
RPL21P11	-0.33729	0.028214	-2.1943	Down	ribosomal protein L21 pseudogene 11
NME3	-0.33652	0.028029	-2.19688	Down	NME/NM23 nucleoside diphosphate kinase 3
LENG1	-0.3363	0.001051	-3.27657	Down	leukocyte receptor cluster member 1
AMDHD2	-0.33592	0.026607	-2.21723	Down	amidohydrolase domain containing 2
RPL10	-0.3354	0.012325	-2.5027	Down	ribosomal protein L10
EEF1D	-0.33501	0.001315	-3.21268	Down	eukaryotic translation elongation factor 1 delta
C1orf56	-0.33448	0.023954	-2.25786	Down	chromosome 1 open reading frame 56
NFIC	-0.33371	0.013657	-2.46615	Down	nuclear factor I C
LGALS3	-0.33359	0.04945	-1.96469	Down	galectin 3
MED16	-0.33191	0.015722	-2.41531	Down	mediator complex subunit 16
RPL12	-0.33186	0.016435	-2.3991	Down	ribosomal protein L12
YJU2	-0.33146	0.014902	-2.43475	Down	YJU2 splicing factor homolog
HSPB1	-0.33126	0.038703	-2.06733	Down	heat shock protein family B (small) member 1

EXOSC4	-0.32927	0.019889	-2.32844	Down	exosome component 4
RPS2	-0.32916	0.022849	-2.27595	Down	ribosomal protein S2
LTBP3	-0.3283	0.014216	-2.45177	Down	latent transforming growth factor beta binding protein 3
SMDT1	-0.32825	0.049949	-1.9604	Down	single-pass membrane protein with aspartate rich tail 1
ZNF688	-0.32772	0.010097	-2.57249	Down	zinc finger protein 688
DPP7	-0.32724	0.021129	-2.30567	Down	dipeptidyl peptidase 7
SLC29A2	-0.32709	0.025931	-2.22725	Down	solute carrier family 29 member 2
RAB3IP	-0.32681	0.013257	-2.4768	Down	RAB3A interacting protein
ZNF71	-0.3264	0.009916	-2.57876	Down	zinc finger protein 71
B3GAT3	-0.32611	0.014071	-2.45544	Down	beta-1,3-glucuronyltransferase 3
POLR2L	-0.32608	0.034861	-2.10997	Down	RNA polymerase II, I and III subunit L
CSKMT	-0.32603	0.025082	-2.24014	Down	citrate synthase lysine methyltransferase
POLR1E	-0.32593	0.001653	-3.14645	Down	RNA polymerase I subunit E
TCF4	-0.32549	0.033702	-2.12362	Down	transcription factor 4
TMEM134	-0.32529	0.011701	-2.52104	Down	transmembrane protein 134
OLFM2	-0.32524	0.04297	-2.024	Down	olfactomedin 2
PDLIM1	-0.32523	0.007639	-2.66761	Down	PDZ and LIM domain 1
PRRC2C	-0.32473	0.031845	-2.14635	Down	proline rich coiled-coil 2C
CLUAP1	-0.32374	0.022091	-2.28879	Down	clusterin associated protein 1
KCNK6	-0.32359	0.019019	-2.34517	Down	potassium two pore domain channel subfamily K member 6
NSMCE1	-0.32342	0.007067	-2.69368	Down	NSE1 homolog, SMC5-SMC6 complex component
IFI27L2	-0.32321	0.048793	-1.9704	Down	interferon alpha inducible protein 27 like 2
CCDC61	-0.32297	0.009673	-2.58732	Down	coiled-coil domain containing 61
TFPT	-0.32288	0.004252	-2.85886	Down	TCF3 fusion partner
EPS8L2	-0.32273	0.042125	-2.03228	Down	EPS8 like 2
SEPTIN1	-0.32196	0.00964	-2.58848	Down	septin 1
RPL3	-0.32195	0.004634	-2.83146	Down	ribosomal protein L3
TNFAIP8L1	-0.32177	0.000995	-3.29204	Down	TNF alpha induced protein 8 like 1
SORBS3	-0.32153	0.028128	-2.1955	Down	sorbin and SH3 domain containing 3
SLC2A4RG	-0.3209	0.015081	-2.43042	Down	SLC2A4 regulator
SGF29	-0.3209	0.011209	-2.53612	Down	SAGA complex associated factor 29
RPL13A	-0.31981	0.013721	-2.46449	Down	ribosomal protein L13a
FOXP1	-0.31949	0.021326	-2.30217	Down	forkhead box P1
RPL37A	-0.31898	0.00455	-2.83728	Down	ribosomal protein L37a
RPL28	-0.3178	0.043754	-2.01644	Down	ribosomal protein L28
PPP1R13L	-0.3176	0.044051	-2.0136	Down	protein phosphatase 1 regulatory subunit 13 like
LTA	-0.317	0.024771	-2.24495	Down	lymphotoxin alpha
NUDT16L1	-0.31698	0.001553	-3.16462	Down	nudix hydrolase 16 like 1
FBL	-0.31696	0.006111	-2.74175	Down	fibrillarin
RABL6	-0.31651	0.016894	-2.38901	Down	RAB, member RAS oncogene family like 6
UBL7	-0.31461	0.017143	-2.38364	Down	ubiquitin like 7
POLR2I	-0.31412	0.041014	-2.04339	Down	RNA polymerase II subunit I
RPL38	-0.31384	0.017208	-2.38224	Down	ribosomal protein L38

PLPP1	-0.31371	0.037754	-2.07751	Down	phospholipid phosphatase 1
BAD	-0.31367	0.034791	-2.11078	Down	BCL2 associated agonist of cell death
TRBC1	-0.3134	0.016747	-2.39222	Down	T cell receptor beta constant 1
BUD23	-0.31338	0.000686	-3.39512	Down	BUD23 rRNAmethyltransferase and ribosome maturation factor
TCF7	-0.31274	0.030493	-2.16362	Down	transcription factor 7
TLE5	-0.31196	0.003064	-2.96128	Down	TLE family member 5, transcriptional modulator
DTX1	-0.3115	0.029945	-2.17081	Down	deltex E3 ubiquitin ligase 1
PEBP1	-0.3109	0.005279	-2.78947	Down	phosphatidylethanolamine binding protein 1
FAM89B	-0.31075	0.036899	-2.08688	Down	family with sequence similarity 89 member B
YDJC	-0.31071	0.012222	-2.50566	Down	YdjCchitooligosaccharidedeacetylase homolog
MPV17L2	-0.31036	0.014187	-2.4525	Down	MPV17 mitochondrial inner membrane protein like 2
RPL35	-0.30927	0.026148	-2.224	Down	ribosomal protein L35
UBOX5	-0.30895	0.006095	-2.74264	Down	U-box domain containing 5
NHP2	-0.30883	0.028606	-2.18888	Down	NHP2 ribonucleoprotein
HDAC11	-0.30868	0.031172	-2.15487	Down	histone deacetylase 11
AKT1S1	-0.30855	0.028869	-2.18527	Down	AKT1 substrate 1
PHACTR4	-0.30682	0.004163	-2.86552	Down	phosphatase and actin regulator 4
NEK8	-0.30679	0.029384	-2.17829	Down	NIMA related kinase 8
TTF1	-0.30638	0.012971	-2.48456	Down	transcription termination factor 1
BOLA1	-0.30637	0.01314	-2.47996	Down	bolA family member 1
NDUFB11	-0.30616	0.027049	-2.21081	Down	NADH:ubiquinoneoxidoreductase subunit B11
UPF3B	-0.30609	0.020211	-2.32242	Down	UPF3B regulator of nonsense mediated mRNA decay
ATAD3A	-0.30603	0.013348	-2.47434	Down	ATPase family AAA domain containing 3A
AGMAT	-0.306	0.039529	-2.05864	Down	agmatinase
NAXE	-0.3057	0.028047	-2.19663	Down	NAD(P)HX epimerase
EVA1C	-0.30553	0.014308	-2.44944	Down	eva-1 homolog C
BEX3	-0.30529	0.0319	-2.14566	Down	brain expressed X-linked 3
RPS27	-0.30485	0.019199	-2.34165	Down	ribosomal protein S27
TMEM204	-0.30464	0.046355	-1.99215	Down	transmembrane protein 204
TMEM256	-0.30412	0.014802	-2.43719	Down	transmembrane protein 256
MGMT	-0.30399	0.046748	-1.98858	Down	O-6-methylguanine-DNA methyltransferase
AP5S1	-0.30372	0.0102	-2.56897	Down	adaptor related protein complex 5 subunit sigma 1
RNASEH2C	-0.30311	0.002503	-3.02295	Down	ribonuclease H2 subunit C
DDIT4	-0.303	0.042694	-2.02669	Down	DNA damage inducible transcript 4
DNAJC30	-0.3025	0.021065	-2.30681	Down	DnaJ heat shock protein family (Hsp40) member C30
POLD2	-0.30245	0.011501	-2.52711	Down	DNA polymerase delta 2, accessory subunit
TAF3	-0.30208	0.029439	-2.17756	Down	TATA-box binding protein associated factor 3
HCFC1R1	-0.3019	0.026186	-2.22344	Down	host cell factor C1 regulator 1
MPHOSPH8	-0.30173	0.022732	-2.27791	Down	M-phase phosphoprotein 8
TNRC6C	-0.3016	0.019677	-2.33246	Down	trinucleotide repeat containing adaptor 6C
NUBP2	-0.30143	0.034522	-2.11392	Down	nucleotide binding protein 2
CHMP6	-0.30113	0.032504	-2.13816	Down	charged multivesicular body protein 6
ZNF395	-0.3009	0.002883	-2.97997	Down	zinc finger protein 395

RSBN1L	-0.29972	0.02994	-2.17089	Down	round spermatid basic protein 1 like
C19orf53	-0.29882	0.02842	-2.19144	Down	chromosome 19 open reading frame 53
C8orf82	-0.29846	0.030098	-2.1688	Down	chromosome 8 open reading frame 82
ALKBH4	-0.29826	0.008345	-2.63776	Down	alkB homolog 4, lysine demethylase
RDH11	-0.29789	0.019843	-2.32931	Down	retinol dehydrogenase 11
ZNF791	-0.29784	0.026426	-2.21989	Down	zinc finger protein 791
UCP2	-0.29771	0.025882	-2.22798	Down	uncoupling protein 2
TCOF1	-0.29709	0.005977	-2.74902	Down	treacle ribosome biogenesis factor 1
ARFRP1	-0.29703	0.00392	-2.88449	Down	ADP ribosylation factor related protein 1
RARG	-0.29683	0.027975	-2.19763	Down	retinoic acid receptor gamma
YIF1B	-0.29677	0.025338	-2.23621	Down	Yip1 interacting factor homolog B, membrane trafficking protein
RPS3	-0.29657	0.012769	-2.49014	Down	ribosomal protein S3
SH3GLB2	-0.29597	0.006605	-2.71611	Down	SH3 domain containing GRB2 like, endophilin B2
THAP7	-0.29589	0.013689	-2.46532	Down	THAP domain containing 7
PRORP	-0.29573	0.049657	-1.96291	Down	protein only RNase P catalytic subunit
PGM2L1	-0.29563	0.031884	-2.14586	Down	phosphoglucomutase 2 like 1
SIRPG	-0.29333	0.030691	-2.16105	Down	signal regulatory protein gamma
BCAS4	-0.29277	0.039157	-2.06253	Down	breast carcinoma amplified sequence 4
RBMX2	-0.29275	0.005782	-2.75989	Down	RNA binding motif protein X-linked 2
NBDY	-0.29252	0.005205	-2.79406	Down	negative regulator of P-body association
SLC25A6	-0.29236	0.019528	-2.33529	Down	solute carrier family 25 member 6
HAUS8	-0.2923	0.005316	-2.78723	Down	HAUS augmin like complex subunit 8
PLEKHB1	-0.29208	0.04181	-2.03541	Down	pleckstrin homology domain containing B1
PAFAH1B3	-0.29201	0.024926	-2.24254	Down	platelet activating factor acetylhydrolase 1b catalytic subunit 3
YIPF4	-0.29112	0.033686	-2.12381	Down	Yip1 domain family member 4
CCDC12	-0.29111	0.024702	-2.24604	Down	coiled-coil domain containing 12
FCMR	-0.29107	0.014754	-2.43837	Down	Fc fragment of IgM receptor
GRWD1	-0.29104	0.026912	-2.2128	Down	glutamate rich WD repeat containing 1
NAA10	-0.29072	0.028357	-2.19231	Down	N-alpha-acetyltransferase 10, NatA catalytic subunit
FLYWCH2	-0.29058	0.037917	-2.07575	Down	FLYWCH family member 2
PSPN	-0.29043	0.014853	-2.43593	Down	persephin
ZNRD2	-0.29043	0.030942	-2.15781	Down	zinc ribbon domain containing 2
SNPH	-0.2904	0.037563	-2.07959	Down	syntaphilin
RPL26	-0.28931	0.039167	-2.06243	Down	ribosomal protein L26
DBP	-0.28899	0.029037	-2.18298	Down	D-box binding PAR bZIP transcription factor
RRP1	-0.28855	0.017434	-2.37742	Down	ribosomal RNA processing 1
MRPL34	-0.28831	0.001748	-3.13002	Down	mitochondrial ribosomal protein L34
RPL14	-0.28775	0.007623	-2.66832	Down	ribosomal protein L14
KDM8	-0.28774	0.005678	-2.76582	Down	lysine demethylase 8
LGMN	-0.28755	0.03066	-2.16145	Down	legumain
DCTPP1	-0.28739	0.026959	-2.21211	Down	dCTPpyrophosphatase 1
APOBEC3C	-0.28721	0.022923	-2.27472	Down	apolipoprotein B mRNA editing enzyme catalytic subunit 3C
MRPL4	-0.28714	0.039467	-2.05928	Down	mitochondrial ribosomal protein L4

CSNK2B	-0.28574	0.005952	-2.75039	Down	casein kinase 2 beta
RPL36AL	-0.28562	0.008816	-2.61909	Down	ribosomal protein L36a like
LYRM4	-0.2854	0.005905	-2.75303	Down	LYR motif containing 4
RPS4X	-0.28534	0.029502	-2.17671	Down	ribosomal protein S4 X-linked
RPL10A	-0.2852	0.004172	-2.86482	Down	ribosomal protein L10a
CD5	-0.28518	0.035312	-2.10476	Down	CD5 molecule
GNL1	-0.28466	0.002093	-3.07673	Down	G protein nucleolar 1 (putative)
ZNF581	-0.28437	0.020531	-2.3165	Down	zinc finger protein 581
ABHD14B	-0.28434	0.013805	-2.46229	Down	abhydrolase domain containing 14B
CD3E	-0.28433	0.038656	-2.06783	Down	CD3e molecule
ZNF763	-0.28417	0.028747	-2.18694	Down	zinc finger protein 763
SPINDOC	-0.28308	0.014998	-2.43243	Down	spindlininteractor and repressor of chromatin binding
RGS10	-0.2829	0.031074	-2.15612	Down	regulator of G protein signaling 10
EIF3G	-0.28195	0.014967	-2.43317	Down	eukaryotic translation initiation factor 3 subunit G
PHF14	-0.28132	0.047285	-1.98374	Down	PHD finger protein 14
MRPL24	-0.28121	0.015086	-2.43032	Down	mitochondrial ribosomal protein L24
PARL	-0.28091	0.023533	-2.26466	Down	presenilin associated rhomboid like
PQBP1	-0.28089	0.002224	-3.05852	Down	polyglutamine binding protein 1
MRPS18A	-0.2804	0.012725	-2.49137	Down	mitochondrial ribosomal protein S18A
SNRPA	-0.28038	0.019837	-2.32942	Down	small nuclear ribonucleoprotein polypeptide A
NDUFAF3	-0.28035	0.01943	-2.33717	Down	NADH:ubiquinoneoxidoreductase complex assembly factor 3

Table 2 The enriched GO terms of the up and down regulated differentially expressed genes

GO ID	CATEGORY	GO Name	Adjusted p value	negative log10 of adjusted p value	Gene Count	Gene
			Up regulated genes			
GO:0051716	BP	cellular response to stimulus	4.69E-14	13.32861286	242	BATF2,IFIT2,IFITM3,IFIT3,IFIT1,OAS3,GBP1,CLEC4D,DOCK4,KCNJ2,CD274,CEACAM1,P2RY14,ATOH8,PARP14,ACSL1,CLIC2,DDX60,GPR141,PARP9,ABTB2,DDX58,PLSCR1,TRIM22,STAT1,ARG1,SIPA1L2,TLR4,LRRK2,ADAM9,VNN1,ABCA1,EIF2AK2,IFIT5,IFIH1,STAT2,TAFA2,RAPGEF2,TNFAIP6,TLR5,PTGS2,TGFA,F2RL1,CYP2D6,TRIM5,RSAD2,CR1,OAS2,CMTM1,HCAR2,FAS,SHTN1,KIF16B,PMAIP1,IL18RAP,FBN2,RUFY4,IFI35,PDK4,KLRC1,RNF213,LIG4,ZDHHC17,NRIP1,HIP1,C9ORF72,JAK2,APC,TMOD2,PIK3AP1,SHPRH,TCP11L2,MCTP2,TLR8,PKN2,NOTCH2,CENPJ,CHMP5,PDGFC,FNIP1,CMPK2,XRN1,TLR2,KIDINS220,PIKFYVE,STXBP3,STK3,PLCXD2,ARAP2,DUSP6,CYP1B1,CPEB2,NR2C2,NEK7,DDX3X,S1PR3,DTX3L,CYSLTR2,CPNE8,PDCD6,CCR1,KCTD9,GCNT2,TAF1,BACH1,ZBP1,SGMS1,NCOA2,TRIM25,PRKAB2,TAF2,PTPN11,OCRL,RIN2,STRN3,MORC3,HDAC9,OTUD4,ZBTB38,SMCHD1,NCOA4,LATS2,DICER1,PIGA,CHM,IL1RN,SINHCAF,GCH1,ZNF236,GRAMD1B,EDEM3,LYST,PELI1,ASCC3,ELF1,FAM8A1,HEG1,C2CD5,EGR1,SNX10,SLC39A10,XPR1,ARFGEF2,LMBRD2,CA2,HIPK3,ZEB2,CYBB,RASA2,HIF1A,CLEC7A,PLA2G7,REV3L,PTPRC,IL18R1,DOCK8,ARHGAP12,CCR2,GAB1,GORAB,MEFV,USP15,IQGAP2,CLEC4E,PPP1R15B,UFL1,AKAP11,TNFSF10,GCLC,SKIL,IRAK3,IFI16,WDFY1,SOS2,KLF3,ETV3,VEGFA,HIPK1,TP53INP1,IMPACT,CSF2RB,SORL1,GPR27,NCOA3,OGT,BCL2A

						1,OXR1,USP33,ITGB1,IRF9,VCPIP1,UBR1,RASA1,DDX5,CD46,DISC1,EIF2AK3,MARCHF7,LATS1,SLC40A1,CHURC1,PHLPP1,MTM1,FAM111A,FMR1,DCLRE1A,AP1G1,ARRDC3,FCGR3A,PTPN12,NFKBIZ,IGF2R,CLASP2,CDK5R1,ADAR,SNRK,USP25,TNKS2,ZBTB1,UBR2,NR2C1,PRKAR1A,TRIO,ARFGEF1,WDR11,RB1CC1,MTR,LDLR,NUS1,LPIN2,TLR6,SRGAP2,SDE2,SIRT1,BIRC6,ALDH1A1,SMG1,VPS13C,UBR5,NOD2,RNF111,ARMT1
GO:0065007	BP	biological regulation	4.30E-13	12.366875	352	SERPING1,BATF2,IFIT2,IFITM3,IFIT3,IFIT1,ETV7,OAS3,APOBEC3B,GBP1,CLEC4D,DOCK4,HES4,KCNJ2,CD274,CEACAM1,P2RY14,ATOH8,PARP14,ACSL1,HERC5,CLIC2,DDX60,GPR141,PARP9,DDX58,PLSCR1,TRIM22,STAT1,ARG1,SIPA1L2,TLR4,LRRK2,OTX1,ADAM9,VNN1,ABCA1,EIF2AK2,IFIT5,IFIH1,STAT2,TAFA2,RAPGEF2,TNFAIP6,TLR5,HELZ2,PLAGL1,PTGS2,TGFA,F2RL1,CYP2D6,ZNF117,DMXL2,TRIM5,RSAD2,CR1,ATP10D,OAS2,CMTM1,HCAR2,FAS,SHTN1,KIF16B,PMAIP1,IL18RAP,NFXL1,FBN2,RUFY4,SRGAP2B,KDM1B,IFI35,BTAF1,PDK4,KIAA1109,KLRC1,RNF213,LIG4,ZNF217,PAPSS2,ACSL4,ZDHHC17,TET2,NRIP1,ZCCHC4,MYSM1,HIP1,AFF1,C9ORF72,JAK2,APC,TMOD2,PIK3AP1,RNF19A,NTNG2,ATP8A1,TCP11L2,TMLHE,MCTP2,SAMD4A,FRY,TLR8,RP2,MX2,MED13L,PKN2,NOTCH2,CENPJ,ZBTB11,CHMP5,PDGFC,FNIP1,PFKFB2,XRN1,TLR2,EXOC8,KIDINS220,ATP11A,PIKFYVE,STXBP3,JMJD1C,RIC1,STK3,PLCXD2,ARAP2,DUSP6,CYP1B1,CPEB2,NR2C2,NEK7,ZSCAN30,DDX3X,S1PR3,DTX3L,CYSLTR2,LHFPL2,DMTF1,PDCD6,CCR1,ATAD2B,STARD4,ZNF107,KCTD9,GCNT2,TAF1,BACH1,ZBP1,SGMS1,ZNF493,GBE1,ELOVL6,ATP13A3,NCOA2,L3MBTL3,TRIM25,PRKAB2,TAF2,UTRN,PTPN11,OCRL,RIN2,AGFG1,STRN3,MORC3,HDAC9,OTUD4,ZBTB38,SMCHD1,SERINC1,NCOA4,LATS2,DICER1,CDK17,CHM,MED23,IL1RN,SINHCAF,GCH1,TMEM161B,ZNF236,GRAMD1B,DHRS9,PELI1,ELF1,HEG1,C2CD5,SYNJ1,EGR1,SNX10,SLC39A10

						,XPR1,ARFGEF2,LMBRD2,CA2,KDM6A,NUP153,HIPK3,ZEB2,CYBB,ZBTB26,RASA2,HIF1A,CLEC7A,RBL2,STX11,PLA2G7,ZNF518A,PTPRC,IL18R1,TDRD7,DOCK8,ARHGAP12,RPRD1A,TRAPPC11,CCR2,CLIC5,GAB1,GORAB,MEFV,USP15,SLC25A40,IQGAP2,CLEC4E,PPP1R15B,HECTD1,IKZF2,UFL1,AKAP11,TNFSF10,WARS1,CLCN3,GCLC,LDLRAD3,SKIL,IRAK3,IFI16,WDFY1,TET3,SOS2,KLF3,CCNT2,ETV3,VEGFA,HIPK1,TP53INP1,IMPACT,CSF2RB,KMT2C,SF3B1,SORL1,GPR27,ATP11C,NCOA3,OGT,TSC22D2,POC1B,FGL2,BCL2A1,IDH1,SESTD1,OXR1,USP33,ZNF567,CLK4,SEC23A,RDH10,ITGB1,IRF9,VCPIP1,LIPA,PPP1R3D,UBR1,PRDM10,RASA1,DDX5,CD46,ZNF606,PATL1,DISC1,EIF2AK3,ARRDC4,MARCHF7,LATS1,ENPP4,SLC40A1,CHURC1,TMEM123,RCOR1,PHLPP1,PRRC1,MTM1,ZNF700,FAM111A,FMR1,OSBPL11,AP1G1,ZNF585A,MEIS1,ARRDC3,PHF2,FCGR3A,ZUP1,PTPN12,NFKBIZ,IGF2R,CLASP2,CDK5R1,SPOPL,USF3,ELF2,SCAF8,ADAR,SNRK,USP25,TNKS2,ZBTB1,DENND5A,UBR2,NR2C1,PRKAR1A,TRIO,ARFGEF1,SENP6,WDR11,RB1CC1,TBC1D8,SLC6A6,WASHC4,NUP58,BRWD3,LYPLA1,LDLR,LPGAT1,NUS1,TIA1,PWWP2A,ZBTB37,LPIN2,TLR6,FGD6,SRGAP2,SDE2,SIRT1,TOX,BIRC6,ALDH1A1,SVIL,SMG1,VPS13C,UBR5,NOD2,RNF111,ARMT1
GO:0012505	CC	endomembrane system	7.20E-13	12.14272694	173	SERPING1,IFIT2,IFITM3,TMTC1,GBP1,CLEC4D,DOCK4,KCNJ2,CD274,CEACAM1,SAMD9L,ACSL1,CLEC12A,PLSCR1,TRIM22,ARG1,TLR4,LRRK2,VNN1,ABCA1,RAPGEF2,TNFAIP6,PLAGL1,GCA,PTGS2,TGFA,F2RL1,CYP2D6,ANKRD50,DMXL2,TRIM5,RSAD2,CR1,ATP10D,KIF16B,FCHO2,LPCAT2,C1GALT1,ACSL4,ZDHHC17,HIP1,C9ORF72,JAK2,APC,ATP8A1,MCTP2,TLR8,RP2,MX2,WDFY3,NOTCH2,CHMP5,PDGFC,TLR2,EXOC8,KIDINS220,ATP11A,PIKFYVE,STXBP3,RIC1,RELCH,CYP1B1,DDX3X,DTX3L,LHFPL2,PDCD6,STARD4,GCNT2,SGMS1,ELOVL6,ATP13A3,OSBPL1A,OCRL,AGFG1,MYOF,STRN3,TRIQK,SERINC1,WDR44,TOR1B

						,PIGA,FNDC3A,SEC24D,GCH1,GRAMD1B,LCLAT1,EDEM3,DHRS9,FAM8A1,SYNJ1,CSGALNACT2,SNX10,XPR1,ARFGEF2,VCAN,NUP153,CYBB,ATG2B,STX11,C6ORF120,PTPRC,TRAPPC11,CLIC5,GORAB,CASD1,IQGAP2,PPP1R15B,UHRF1BP1L,UFL1,TRAPPC8,COG6,CLCN3,TRAPPC10,SKIL,WDFY1,PI4K2B,VEGFA,SORL1,ATP11C,GALNT7,AP4E1,FGL2,TXNDC16,IDH1,USP33,SEC23A,RDH10,ITGB1,VCPIP1,CD46,DISC1,EIF2AK3,ARRDC4,ENPP4,FAM234B,SLC40A1,GASK1B,PRRC1,MTM1,OSBPL11,AP1G1,PLEKHM3,ARRDC3,CEPT1,IGF2R,CLASP2,EOGT,USP25,TNKS2,ZBTB1,DENND5A,PRKAR1A,ARFGEF1,WDR11,RB1CC1,WASHC4,NUP58,LYPLA1,LDLR,LPGAT1,NUS1,LPIN2,TLR6,FGD6,SDE2,ERO1B,SIRT1,BIRC6,VPS13C,SLC36A1,NEMP1,NOD2,AHCYL2
GO:0005622	CC	intracellular anatomical structure	6.00E-08	7.221916574	420	SERPING1,BATF2,IFIT2,IFITM3,IFIT3,IFIT1,ETV7,OAS3,TMTC1,APOBEC3B,GBP1,CLEC4D,DOCK4,HES4,KCNJ2,CD274,CEACAM1,SAMD9L,XAF1,ATOH8,PARP14,KLHL2,ACSL1,HERC5,CLIC2,CLEC12A,DDX60,PARP9,DDX58,MFAP3,PLSCR1,TRIM22,ZCCHC2,STAT1,ARG1,SIPA1L2,TLR4,LRRK2,OTX1,DDX60L,VNN1,ABCA1,EIF2AK2,IFIT5,IFIH1,IFI44,STAT2,TAFA2,RAPGEF2,TNFAIP6,HELZ2,FBXO30,PLAGL1,GCA,PTGS2,TGFA,TASOR2,F2RL1,CYP2D6,ANKRD50,ZNF117,DMXL2,TRIM5,RSAD2,N4BP2,CR1,ATP10D,OAS2,ITPRID2,FAS,SAMD9,SHTN1,KIF16B,PMAIP1,FCHO2,NFXL1,RTP4,RUFY4,SRGAP2B,KDM1B,IFI35,BTAF1,PDK4,FAR2,KIAA1109,LPCAT2,C1GALT1,RNF213,LIG4,ZNF217,PAPSS2,ACSL4,ZDHHC17,TET2,NRIP1,ZCCHC4,MYSM1,HIP1,AFF1,C9ORF72,JAK2,APC,TMOD2,PIK3AP1,NBPF3,RNF19A,ATP8A1,SHPRH,TMLHE,MCTP2,SAMD4A,FRY,TLR8,RP2,MX2,WDFY3,MED13L,PKN2,NOTCH2,CENPJ,ZBTB11,MIS18BP1,CHMP5,PDGFC,FNIP1,PFKFB2,CMPK2,XRN1,TLR2,MPZL2,EXOC8,KIDINS220,ATP11A,PIKFYVE,STXBP3,JMJD1C,LTN1,RIC1,STK3,PLCXD2,RELCH,ARAP2,DUSP6,CYP1B1,CPEB2,NR2C2,NEK7,ZSCAN30,DD

X3X,S1PR3,DTX3L,PALLD,LHF
PL2,DMTF1,TSPAN2,PDCD6,CC
R1,ATAD2B,STARD4,ZNF107,G
CNT2,TAF1,BACH1,ZBP1,SGMS
1,ZNF493,GBE1,ELOVL6,ATP13
A3,NCOA2,L3MBTL3,GPD2,TRI
M25,OSBPL1A,PRKAB2,TAF2,U
TRN,PTPN11,OCRL,RIN2,AGFG
1,MYOF,STRN3,MORC3,HDAC9,
TRIQK,OTUD4,ZBTB38,SMCHD
1,SERINC1,NCOA4,LATS2,WDR
44,DICER1,CDK17,TOR1B,PIGA,
CHM,MED23,FNDC3A,IL1RN,SI
NHCAF,SEC24D,GCH1,ZNF236,
GRAMD1B,LCLAT1,EDEM3,LY
ST,CEP170,DHRS9,PELI1,ASCC3
,ELF1,FAM8A1,C2CD5,SYNJ1,E
GR1,CSGALNACT2,SNX10,XPR
1,ARFGEF2,VCAN,CA2,KDM6A,
NUP153,HIPK3,ZEB2,CYBB,ZBT
B26,BIVM,RASA2,HIF1A,CLEC7
A,RBL2,ATG2B,STX11,PLA2G7,
REV3L,ZNF518A,C6ORF120,PTP
RC,TDRD7,DOCK8,ARHGAP12,
RPRD1A,TRAPPC11,CCR2,CLIC
5,PPAT,GAB1,CEP350,GORAB,
MEFV,USP15,CASD1,SLC25A40,
IQGAP2,CLEC4E,PPP1R15B,AC
BD5,HECTD1,IKZF2,UHRF1BP1
L,UFL1,AKAP11,TRAPPC8,COG
6,WARS1,CLCN3,TRAPPC10,GC
LC,SKIL,PPIP5K2,IRAK3,IFI16,
WDFY1,TET3,SOS2,PI4K2B,KLF
3,FEM1C,CCNT2,ETV3,VEGFA,
HIPK1,TP53INP1,NBPF1,IMPAC
T,KMT2C,SF3B1,SORL1,PCF11,
ATP11C,NCOA3,GALNT7,AP4E1
,OGT,POC1B,FGL2,TXNDC16,B
CL2A1,IDH1,SESTD1,OXR1,USP
33,ZNF567,CLK4,SEC23A,RDH1
0,ITGB1,IRF9,VCPIP1,LIPA,PPP1
R3D,UBR1,PGM3,PRDM10,RAS
A1,DDX5,CD46,ZNF606,PATL1,
CCDC146,DISC1,EIF2AK3,ARRD
C4,MARCHF7,LATS1,ENPP4,FA
M234B,SLC40A1,GASK1B,DZIP3
,TMEM123,RCOR1,PHLPP1,SLF
N5,PRRC1,LONRF1,MTM1,ZNF7
00,FAM111A,FMR1,DCLRE1A,O
SBPL11,AP1G1,PAPOLG,ZNF585
A,PLEKHM3,MEIS1,ARRDC3,PH
F2,ZUP1,PTPN12,PRPF39,NFKBI
Z,CEPT1,IGF2R,CLASP2,CDK5R
1,SPOPL,PEX1,USF3,ELF2,RCBT
B1,PARP12,GALC,SCAF8,ADAR,
SNRK,EOGT,USP25,TNKS2,ZBT
B1,DENND5A,UBR2,NR2C1,PRK
AR1A,TRIO,ARFGEF1,CPOX,SE
NP6,ZFR,WDR11,RB1CC1,MTR,
PTAR1,WASHC4,NUP58,BRWD3
,RANBP6,LYPLA1,LDLR,LPGAT

						1,NUS1,TIA1,PWWP2A,ZBTB37,LPIN2,PANK3,TLR6,FGD6,NNT,SRGAP2,SDE2,ERO1B,SIRT1,TOX,BIRC6,ALDH1A1,SVIL,SMG1,VPS13C,UBR5,SLC36A1,NEMP1,NOD2,RNF111,AHCYL2
GO:0043167	MF	ion binding	1.21E-08	7.916559407	203	OAS3,APOBEC3B,GBP1,CLEC4D,KCNJ2,XAF1,ACSL1,DDX60,PARP9,DDX58,PLSCR1,TRIM22,ZCCHC2,ARG1,LRRK2,ADAM9,DDX60L,ABCA1,EIF2AK2,IFIH1,RAPGEF2,TNFAIP6,HELZ2,FBXO30,PLAGL1,GCA,PTGS2,CYP2D6,ZNF117,TRIM5,RSAD2,N4BP2,ATP10D,OAS2,KIF16B,FCHO2,NFXL1,FBN2,RUFY4,KDM1B,BTAF1,PDK4,LPCAT2,C1GALT1,RNF213,LIG4,ZNF217,PAPSS2,ACSL4,TET2,ZCCHC4,MYSM1,HIP1,ZSWIM6,JAK2,RNF19A,ATP8A1,SHPRH,TMLHE,MCTP2,RP2,MX2,WDFY3,PKN2,NOTCH2,ZBTB11,PFKFB2,CMPK2,ATP11A,PIKFYVE,JMJD1C,LTN1,STK3,ARAP2,CYP1B1,NR2C2,NEK7,ZSCAN30,DDX3X,DTX3L,CPNE8,PDCD6,ATAD2B,ZNF107,TAF1,ZNF493,GBE1,ATP13A3,L3MBTL3,GPD2,TRIM25,UTRN,AGFG1,MYOF,MORC3,HDAC9,ZBTB38,SMCHD1,LATS2,DICER1,CDK17,TOR1B,SEC24D,GCH1,ZNF236,GRAMD1B,EDEM3,ASCC3,HEG1,C2CD5,EGR1,CSGALNACT2,XPR1,VCAN,CA2,KDM6A,NUP153,HIPK3,ZEB2,CYBB,ZBTB26,RASA2,CLEC7A,REV3L,ZNF518A,PPAT,MEFV,IQGAP2,CLEC4E,HECTD1,IKZF2,TNFSF10,WARS1,CLCN3,GCLC,PPIP5K2,IRAK3,WDFY1,TET3,PI4K2B,KLF3,HIPK1,KMT2C,ATP11C,GALNT7,OGT,IDH1,SESTD1,USP33,ZNF567,CLK4,SEC23A,ITGB1,UBR1,PGM3,PRDM10,DDX5,ZNF606,EIF2AK3,MARCHF7,LATS1,ENPP4,SLC40A1,DZIP3,CHURC1,PHLPP1,SLFN5,LONRF1,ZNF700,DCLRE1A,PAPOLG,ZNF585A,PLEKHM3,PHF2,ZUP1,CEPT1,IGF2R,CDK5R1,PEX1,PARP12,ADAR,SNRK,TNKS2,ZBTB1,UBR2,NR2C1,PRKAR1A,TRIO,ZFR,MTR,LDLR,NUS1,ZBTB37,PANK3,FGD6,ERO1B,SIRT1,SVIL,SMG1,UBR5,NOD2,RNF111,ARMT1
GO:0019899	MF	enzyme binding	1.82687E-05	4.7382926	83	GBP1,DOCK4,CEACAM1,PARP14,PARP9,DDX58,PLSCR1,TRIM22,STAT1,LRRK2,ADAM9,ABCA1

						,STAT2,PTGS2,DMXL2,TRIM5,FAS,NRIP1,C9ORF72,JAK2,APC,RNF19A,SHPRH,PKN2,NOTCH2,CENPJ,FNIP1,PFKFB2,EXOC8,RIC1,DTX3L,PRKAB2,UTRN,PTPN11,OCRL,RIN2,STRN3,HDAC9,CHM,GCH1,LYST,EGR1,SNX10,HIF1A,PTPRC,RPRD1A,IQGAP2,UFL1,AKAP11,WARS1,IRAK3,CCNT2,ETV3,SORL1,PCF11,NCOA3,USP33,ITGB1,PPP1R3D,RASA1,EIF2AK3,MARCHF7,LATS1,DZIP3,RCOR1,AP1G1,IGF2R,CLASP2,CDK5R1,SPOPL,SCAF8,USP25,TNKS2,DENND5A,NR2C1,PRKAR1A,RB1CC1,LDLR,FGD6,SRGAP2,SIRT1,NOD2,ARMT1
			Down regulated genes			
GO:0009058	BP	biosynthetic process	1.94E-07	6.712880634	171	ZBTB32,KLF1,AZU1,TSHZ2,GCAT,ZBTB20,TGFB1I1,PHGDH,HS3ST1,CAVIN1,POU2F2,PAX5,PKIG,ST6GALNAC4,PYCR3,ZGLP1,ZNF714,NDUFA13,BEND5,GAMT,ZNF358,PURA,ZC3H6,TOP2A,RPS21,DPM2,ZNF593,TNFRSF4,NOP53,RPS29,MYBL2,CCDC85B,PTCD1,GGT1,GCHFR,RPL13,PF4,RPLP2,DNAJC2,RPS14,ZNF91,NFIA,EIF5B,RITA1,MRPL2,ZNF524,VEGFB,NAT14,ELOF1,MBD3,ITM2C,POU2F1,MGLL,ASCC2,RPS15,ZBTB7A,PC,GPT2,HEXIM2,BCL7C,RPL18A,NME4,ACP5,RPL36,ANTKMT,ATP5F1D,RPS19,CCR7,NDUFS8,DMAC2L,TM7SF2,GIPC1,RPS9,ALDOC,DCP1A,PRDX2,ZNF611,MRPL23,THAP3,RPL29,APBB1,FAU,GADD45GIP1,RPL18,MRPS17,RPLP1,RUNX3,SPIB,SVIP,CCDC124,RPS5,BIN1,MAF1,ZNF517,RPL19,MRPS34,SOX12,ADK,ZNF444,PCYT2,NAGS,RPL27,RPL8,NME3,AMDHD2,RPL10,EEF1D,NFIC,MED16,RPL12,HSPB1,RPS2,ZNF688,ZNF71,B3GAT3,POLR2L,POLR1E,TCF4,PDLIM1,TFPT,RPL3,SORBS3,SLC2A4RG,SGF29,RPL13A,RPL37A,RPL28,PPP1R13L,POLR2I,RPL38,PLPP1,TCF7,TLE5,DTX1,MPV17L2,RPL35,NHP2,TTF1,NDUFB11,UPF3B,AGMAT,RPS27,DNAJC30,POLD2,TAF3,MPHOSPH8,TNRC6C,ZNF395,ZNF791,TCOF1,RARG,RPS3,THAP7,RPL26,DBP,MRPL34,RPL14,KDM8,MRPL4,RPL36AL,RPS4X,RPL10A,ZNF581,ABHD14B,ZNF763,SPINDOC,EIF3G,PHF

						14,MRPL24,PQBP1,MRPS18A
GO:1901564	BP	organonitrogen compound metabolic process	0.000379938	3.420287697	169	KEL,PCSK1N,EFNA3,AZU1,GCAT,ZBTB20,TGFB1I1,PHGDH,HS3ST1,SHPK,PAX5,NT5M,PKIG,PI16,FN3K,FHIT,PRKAR1B,ST6GALNAC4,GP9,PYCR3,NDUFA13,LMTK3,PNPLA7,GAMT,CHMP4A,PURA,ABCB9,RPS21,DPM2,HSPBP1,NOP53,RPS29,ARL2,PTCD1,FBXO10,PFDN4,GGT1,TRPM4,RPL13,SNTA1,UBXN6,NOSIP,RPLP2,RPS14,CD27,EIF5B,MRPL2,VEGFB,FBXL15,SH2D3A,ELOF1,MBD3,ITM2C,DUSP18,ASCC2,CAPN5,RPS15,CPTP,ZBTB7A,PC,GPT2,HEXIM2,RPL18A,NME4,RPL36,TMUB1,ANTKMT,ATP5F1D,RPS19,TNK1,MARCHF9,CCR7,NDUFS8,DMAC2L,GIPC1,CD6,PRR7,CTDSPL,RPS9,ALDOC,DCP1A,DNPH1,MRPL23,RPL29,APBB1,FAU,GADD45GIP1,RPL18,ANKRD39,MRPS17,RPLP1,RUNX3,SVIP,RPS5,BIN1,RPL19,MRPS34,ADK,NUDT18,NAGS,DCXR,FBXL8,RPL27,PPIG,RPL8,NME3,AMDHD2,RPL10,EEF1D,LGALS3,RPL12,HSPB1,RPS2,DPP7,B3GAT3,CSKMT,NSMCE1,RPL3,SGF29,RPL13A,RPL37A,RPL28,FBL,UBL7,RPL38,PLPP1,BAD,DTX1,PEBP1,MPV17L2,RPL35,UBOX5,HDAC11,AKT1S1,NEK8,NDUFB11,UPF3B,AGMAT,NAXE,BEX3,RPS27,MGMT,DDIT4,DNAJC30,TAF3,TNRC6C,CHMP6,ALKBH4,TCOF1,RPS3,THAP7,NAA10,RPL26,MRPL34,RPL14,KDM8,LGMN,DCTPP1,APOBEC3C,MRPL4,RPL36AL,RPS4X,RPL10A,ABHD14B,CD3E,EIF3G,MRPL24,PARL,MRPS18A
GO:0070013	CC	intracellular organelle lumen	1.95488E-05	4.708880544	177	ZBTB32,KEL,KLF1,AZU1,GCAT,ZBTB20,TGFB1I1,HS3ST1,CAVIN1,PWP2,C9ORF78,ARL4D,POU2F2,PAX5,NT5M,FHIT,SELENOM,ZGLP1,NDUFA13,CCDC106,C12ORF57,TENT5C,PODXL2,TOP2A,RPS21,ZNF593,NOP53,PPBP,RPS29,MYBL2,MZT2B,TAX1BP3,ARL2,PTCD1,IGFBP4,TRPM4,SNRNP25,ESF1,GCHFR,RPL13,ALKBH7,PF4,HDHD3,NOSIP,DNAJC2,RPS14,NFIA,LHPP,MZT2A,KRT18,RITA1,MRPL2,BAG1,VEGFB,ANKRD12,ELOF1,MBD3,DUSP18,POU2F1,MGLL,HSPG2,ASCC2,SNRPN,TJP3,RPS15,ZBTB7A,PC,SNHG8,GPT2,HEXIM2,FLYW

						CH1,NME4,RPL36,TMUB1,ATP5F1D,RPS19,NDUFS8,ZCRB1,PRR7,C19ORF48,RPS9,ALDOC,ELAC1,FAHD1,MRPL23,APBB1,FAU,GADD45GIP1,RPL18,TONSL,VPS51,NMRAL1,MRPS17,RUNX3,DCLRE1C,AQP3,RPS5,MAF1,LAGE3,RPL19,MRPS34,SOX12,ADK,ECSIT,WDR18,NAGS,RPL27,PPIG,EEF1D,NFIC,LGALS3,MED16,RPL12,EXOSC4,RPS2,SMDT1,DPP7,SLC29A2,POLR2L,POLR1E,OLFM2,CLUAP1,NSMCE1,TFPT,RPL3,SLC2A4RG,SGF29,RPL13A,PPP1R13L,FBL,POLR2I,BUD23,TCF7,DTX1,MPV17L2,RPL35,UBOX5,NHP2,HDAC11,AKT1S1,TTF1,UPF3B,ATAD3A,NAXE,RPS27,MGMT,AP5S1,POLD2,TAF3,HCFC1R1,MPHOSPH8,TNRC6C,ZNF395,ALKBH4,TCOF1,RARG,RPS3,SH3GLB2,THAP7,PRORP,GRWD1,NAA10,RPL26,RRP1,MRPL34,KDM8,LGMN,DCTPP1,MRPL4,LYRM4,RPS4X,ABHD14B,PHF14,MRPL24,PQBP1,MRPS18A,SNRPA
GO:0005737	CC	cytoplasm	6.79874E-05	4.167571412	286	RAP1GAP,MYL9,KEL,PCSK1N,FRMD4A,CRIP2,MEMO1,AZU1,PPP1R14A,GCAT,SAMD14,ZBTB20,TGFB1I1,PHGDH,HS3ST1,GRAP,CAVIN1,LIMS2,C9ORF78,SHPK,ARL4D,POU2F2,PAX5,NT5M,PKIG,FN3K,FHIT,SELENOM,PRKAR1B,ST6GALNAC4,PYCR3,ATG9B,NDUFA13,CCDC106,CHCHD6,BEND5,LMTK3,C12ORF57,PNPLA7,GAMT,TENT5C,CHMP4A,PODXL2,ITGA2B,PURA,ABCB9,TOP2A,RABEP2,RPS21,DPM2,SEC62,NOP53,PPBP,NOXA1,RPS29,MAL,MZT2B,TAX1BP3,RABAC1,ARL2,ARPC1B,CCDC85B,PTCD1,NENF,FBXO10,IGFBP4,PFDN4,TRPM4,FAM174C,SNRNP25,LRRCC1,GCHFR,RPL13,ALKBH7,PF4,SNTA1,UBXN6,NOSIP,RPLP2,DNAJC2,RPS14,DENND5B,LHPP,MCRIP1,P2RX5,ARRDC5,MZT2A,KRT18,EIF5B,RITA1,MRPL2,BAG1,VEGFB,ANKRD12,FBXL15,KDF1,PRXL2A,MBD3,ITM2C,DUSP18,POU2F1,MGLL,HSPG2,SNRPN,CAPN5,RPS15,CPTP,ZBTB7A,PC,GPT2,HEXIM2,RPL18A,FLYWCH1,NME4,ACP5,TRAPPC6A,RPL36,TMUB1,ROGDI,ANTKMT,ATP5F1D,VPREB3,PUSL1,RPS19,TNK1,MARCHF9,CCR7,NDUFS8,DMAC2L,ZCRB1,TM7SF2,GIP

						C1,PRR7,RPS9,ALDOC,DCP1A,PRDX2,ELAC1,DNPH1,ENDOG,FAHD1,MRPL23,RPL29,INF2,APBB1,FAU,GADD45GIP1,RPL18,MCRIP2,TONSL,VPS51,NMRAL1,MRPS17,RPLP1,RUNX3,REEP6,DCLRE1C,CCDC120,SPIB,AQP3,SVIP,CCDC124,RPS5,BIN1,MAF1,LAGE3,RPL19,MRPS34,ADK,NUDT18,ECSIT,WDR18,SLC35E3,PCYT2,NAGS,DCXR,ABHD14A,FBXL8,RPL27,PPIG,RPL8,NME3,AMDHD2,RPL10,EEF1D,LGALS3,RPL12,HSPB1,EXOSC4,RPS2,SMDT1,DPP7,RAB3IP,B3GAT3,POLR2L,CSKMT,TMEM134,OLFM2,PDLIM1,PRRC2C,IFI27L2,CCDC61,TFPT,EPS8L2,SEPTIN1,RPL3,TNFAIP8L1,SORBS3,SLC2A4RG,RPL13A,RPL37A,RPL28,PPP1R13L,RABL6,UBL7,RPL38,BAD,BUD23,DTX1,PEBP1,FAM89B,MPV17L2,RPL35,AKT1S1,PHACTR4,NEK8,TTF1,BOLA1,NDUFB11,UPF3B,ATAD3A,AGMAT,NAXE,BEX3,RPS27,AP5S1,DDIT4,DNAJC30,HCFC1R1,MPHOSPH8,TNRC6C,NUBP2,CHMP6,ZNF395,ALKBH4,RDH11,UCP2,TCOF1,ARFRP1,RARG,YIF1B,RPS3,SH3GLB2,PRORP,PGM2L1,BCAS4,NBDY,SLC25A6,HAUS8,PLEKHB1,PAFAH1B3,YIPF4,GRWD1,NAA10,SNPH,RPL26,MRPL34,RPL14,KDM8,LGMN,DCTPP1,APOBEC3C,MRPL4,RPL36AL,LYRM4,RPS4X,RPL10A,ABHD14B,CD3E,RGS10,EIF3G,MRPL24,PARL,PQBP1,MRPS18A,NDUFAF3
GO:0005198	MF	structural molecule activity	7.65844E-06	5.115859553	51	MYL9,RPS21,RPS29,MAL,ARPC1B,RPL13,SNTA1,RPLP2,RPS14,KRT18,MRPL2,HSPG2,RPS15,RPL18A,RPL36,RPS19,RPS9,MRPL23,RPL29,FAU,RPL18,MRPS17,RPLP1,RPS5,RPL19,MRPS34,RPL27,RPL8,RPL10,RPL12,RPS2,RPL3,SORBS3,RPL13A,RPL37A,RPL28,RPL38,RPL35,UPF3B,RPS27,RPS3,RPL26,MRPL34,RPL14,MRPL4,RPL36AL,RPS4X,RPL10A,GNL1,MRPL24,MRPS18A
GO:0003676	MF	nucleic acid binding	0.283943271	0.546768419	132	ZBTB32,KLF1,TSHZ2,ZBTB20,CAVIN1,PWP2,POU2F2,PAX5,ZGLP1,BEND5,TENT5C,ZNF358,PURA,ZC3H6,TOP2A,RPS21,ZNF593,NOP53,RPS29,MYBL2,PTCD1,ESF1,RPL13,NOSIP,DNAJC2,RPS14,ZNF91,NFIA,SWSAP1,KRT18,EIF5B,MRPL2,ZNF524,FAM133B

,NAT14,ELOF1,MBD3,POU2F1,S
REK1IP1,SNRPN,RPS15,ZBTB7A
,HEXIM2,RPL18A,FLYWCH1,RP
L36,PUSL1,RPS19,ZCRB1,RPS9,
DCP1A,ENDOG,ZNF611,MRPL2
3,THAP3,RPL29,FAU,RPL18,MR
PS17,RUNX3,DCLRE1C,SPIB,CC
DC124,RPS5,MAF1,ZNF517,RPL
19,SOX12,ADK,ZNF444,RPL27,P
PIG,RPL8,RPL10,EEF1D,NFIC,L
GALS3,RPL12,HSPB1,EXOSC4,R
PS2,ZNF688,ZNF71,POLR2L,POL
R1E,TCF4,PRRC2C,TFPT,RPL3,S
LC2A4RG,RPL13A,RPL37A,RPL
28,NUDT16L1,FBL,POLR2I,RPL3
8,BUD23,TCF7,PEBP1,RPL35,NH
P2,TTF1,UPF3B,RPS27,MGMT,P
OLD2,TNRC6C,ZNF395,ZNF791,
TCOF1,RARG,RPS3,THAP7,RBM
X2,GRWD1,FLYWCH2,RPL26,D
BP,RRP1,RPL14,APOBEC3C,MR
PL4,RPS4X,RPL10A,ZNF581,ZNF
763,EIF3G,MRPL24,PQBP1,MRP
S18A,SNRPA

Table 3 The enriched pathway terms of the up and down regulated differentially expressed genes

Pathway ID	Pathway Name	Adjusted p value	Negative log10 of adjusted p value	Gene Count	Gene
		Up regulated genes			
REAC:R-HSA-168256	Immune System	0.000140591	3.852041534	95	SERPING1,IFIT2,IFITM3,IFIT3,IFIT1,OAS3,GBP1,CLEC4D,CD274,CEACAM1,XAF1,KLHL2,HERC5,CLEC12A,DDX58,TRIM22,STAT1,ARG1,TLR4,VNN1,EIF2AK2,IFIT5,IFIH1,STAT2,TNFAIP6,TLR5,FBXO30,GCA,PTGS2,TRIM5,RSAD2,CR1,OAS2,IL18RAP,IFI35,KLRC1,RNF213,JAK2,PIK3AP1,RNF19A,ATP8A1,TLR8,MX2,TLR2,ATP11A,LTN1,DUSP6,DDX3X,DTX3L,CCR1,ZBP1,TRIM25,OSBPL1A,PTPN11,IL1RN,SEC24D,PELI1,EGR1,NUP153,CYBB,HIF1A,CLEC7A,C6ORF120,PTPRC,IL18R1,CCR2,MEFV,IQGAP2,CLEC4E,HECTD1,UFL1,IRAK3,IFI16,SOS2,VEGFA,CSF2RB,FGL2,IDH1,SEC23A,ITGB1,IRF9,UBR1,CD46,ENPP4,DZIP3,LONRF1,AP1G1,FCGR3A,PTPN12,IGF2R,ADAR,UBR2,TLR6,NOD2,RNF111
REAC:R-HSA-1280215	Cytokine Signaling in Immune system	0.001405014	2.852319352	42	IFIT2,IFITM3,IFIT3,IFIT1,OAS3,GBP1,XAF1,HERC5,DDX58,TRIM22,STAT1,EIF2AK2,IFIT5,STAT2,PTGS2,TRIM5,RSAD2,OAS2,IL18RAP,IFI35,JAK2,MX2,DUSP6,CCR1,TRIM25,PTPN11,IL1RN,PELI1,EGR1,NUP153,HIF1A,IL18R1,CCR2,IRAK3,SOS2,VEGFA,CSF2RB,ITGB1,IRF9,PTPN12,ADAR,NOD2
REAC:R-HSA-983169	Class I MHC mediated antigen processing & presentation	0.315029726	0.501648465	20	KLHL2,HERC5,TLR4,FBXO30,RNF213,RNF19A,TLR2,LTN1,DTX3L,SEC24D,CYBB,HECTD1,UFL1,SEC23A,UBR1,DZIP3,LONRF1,UBR2,TLR6,RNF111
REAC:R-HSA-556833	Metabolism of lipids	0.318371036	0.497066449	33	ACSL1,ABCA1,HELZ2,PTGS2,CYP2D6,FAR2,LPCAT2,ACSL4,MED13L,PIKFYVE,CYP1B1,STARD4,SGMS1,ELOVL6,NCOA2,GPD2,OSBPL1A,PRKAB2,OCRL,MED23,SEC24D,LCLAT1,SYNJ1,ABHD3,ACBD5,PI4K2B,NCOA3,SEC23A,MTM1,CEPT1,GALC,LPGAT1,LPIN2
REAC:R-HSA-1483257	Phospholipid metabolism	0.433484677	0.363026249	12	LPCAT2,PIKFYVE,GPD2,OCRL,LCLAT1,SYNJ1,ABHD3,PI4K2B,MTM1,CEPT1,LPGAT1,LPIN2
REAC:R-HSA-199991	Membrane Trafficking	0.443515755	0.353090948	27	TGFA,KIF16B,FCHO2,HIP1,CHM

					P5,EXOC8,STXBP3,RIC1,PRKAB2,OCRL,RIN2,AGFG1,TOR1B,CHM,SEC24D,C2CD5,SYNJ1,TRAPPC11,TRAPPC8,COG6,TRAPPC10,AP4E1,SEC23A,AP1G1,IGF2R,DENND5A,LDLR
		Down regulated genes			
REAC:R-HSA-156842	Eukaryotic Translation Elongation	2.21E-30	29.65512539	35	RPS21,RPS29,RPL13,RPLP2,RPS14,RPS15,RPL18A,RPL36,RPS19,RPS9,RPL29,FAU,RPL18,RPLP1,RPS5,RPL19,RPL27,RPL8,RPL10,EEF1D,RPL12,RPS2,RPL3,RPL13A,RPL37A,RPL28,RPL38,RPL35,RPS27,RPS3,RPL26,RPL14,RPL36AL,RPS4X,RPL10A
REAC:R-HSA-1643685	Disease	0.000368188	3.433929964	66	IGLV7-43,IGLV3-25,IGLC3,IGLV3-19,IGHG2,IGKV3-20,PRKAR1B,ST6GALNAC4,GP9,FXYD7,CHMP4A,ITGA2B,RPS21,DPM2,NOXA1,RPS29,ARPC1B,GGT1,RPL13,RPLP2,RPS14,MBD3,HSPG2,RPS15,PC,RPL18A,RPL36,RPS19,ZCRB1,RPS9,PRDX2,RPL29,FAU,RPL18,RPLP1,RPS5,RPL19,DCXR,RPL27,RPL8,RPL10,RPL12,RPS2,B3GAT3,POLR2L,RPL3,RPL13A,RPL37A,RPL28,POLR2I,RPL38,BAD,PEBP1,RPL35,HDAC11,AKT1S1,RPS27,TAF3,CHMP6,RPS3,SLC25A6,RPL26,RPL14,RPL36AL,RPS4X,RPL10A
REAC:R-HSA-1266738	Developmental Biology	0.000592869	3.227041427	48	RAP1GAP,MYL9,EFNA3,EFNA4,ITGA2B,RPS21,RPS29,ARPC1B,RPL13,RPLP2,RPS14,KRT18,RPS15,RPL18A,RPL36,RPS19,RPS9,RPL29,FAU,RPL18,RPLP1,RPS5,RPL19,RPL27,RPL8,RPL10,MED16,RPL12,RPS2,POLR2L,TCF4,RPL3,RPL13A,RPL37A,RPL28,POLR2I,RPL38,RPL35,UPF3B,RPS27,RARG,RPS3,PSPN,RPL26,RPL14,RPL36AL,RPS4X,RPL10A
REAC:R-HSA-5368286	Mitochondrial translation initiation	0.003768495	2.423832	9	MRPL2,MRPL23,GADD45GIP1,MRPS17,MRPS34,MRPL34,MRPL4,MRPL24,MRPS18A
REAC:R-HSA-392499	Metabolism of proteins	0.100368079	0.998404389	62	FN3K,ST6GALNAC4,TOP2A,RPS21,DPM2,RPS29,ARL2,FBXO10,IGFBP4,PFDN4,RPL13,RPLP2,RPS14,EIF5B,MRPL2,FBXL15,HSPG2,RPS15,RPL18A,TRAPPC6A,RPL36,RPS19,RPS9,MRPL23,RPL29,FAU,GADD45GIP1,RPL18,MRPS17,RPLP1,RPS5,RPL19,MRPS34,FBXL8,RPL27,RPL8,AMDHD2,RPL10,EEF1D,RPL12,RPS2,NSMCE1,TFPT,RPL3,RPL13A,RPL37A,RPL28,RPL38,RPL35,TTF1,RPS27,RPS3,RPL26,MRPL34,RPL14,MRPL4,RPL36AL,RPS4X,RPL10A,EIF3G,MRPL24,MRPS18A
REAC:R-HSA-2029507	The citric acid (TCA) cycle and respiratory electron transport	0.231970991	0.634566322	9	NDUFA13,ATP5F1D,NDUFS8,DMAC2L,FAHD1,ECSIT,NDUFB11,UCP2,NDUFAF3

Table 4 Topology table for up and down regulated genes

Regulation	Node	Degree	Betweenness	Stress	Closeness
Up	EGR1	518	0.155691	51097908	0.373483
Up	SIRT1	314	0.080189	32134000	0.36686
Up	STAT1	223	0.049509	22461952	0.360228
Up	LRRK2	164	0.030545	13490182	0.347112
Up	HIF1A	156	0.031431	15278362	0.358132
Up	DDX5	156	0.021312	13124370	0.353754
Up	APC	134	0.03062	8157278	0.352549
Up	DDX3X	129	0.01346	7508184	0.353317
Up	SF3B1	125	0.017765	7636820	0.356112
Up	ITCH	125	0.022984	9612406	0.341769
Up	LIG4	123	0.028987	6646986	0.322992
Up	PTPN11	122	0.025132	7810708	0.344261
Up	DISC1	117	0.024269	5646774	0.319364
Up	NCOA3	108	0.014326	8210920	0.34684
Up	USP15	106	0.021378	8044676	0.339028
Up	HDAC9	96	0.01859	4353434	0.345214
Up	JAK2	92	0.01367	4674124	0.345337
Up	SKIL	90	0.019069	4779812	0.343216
Up	ITGB1	88	0.020231	6343496	0.339146
Up	PRKAR1A	85	0.015974	5349082	0.343168
Up	PLSCR1	84	0.021078	4243846	0.350339
Up	EIF2AK2	81	0.011589	4309902	0.345779
Up	FAS	79	0.012899	4058128	0.354192
Up	SEC23A	76	0.013578	5658738	0.33792
Up	UBR5	69	0.009193	3786410	0.341529
Up	RBL2	69	0.011976	4158150	0.340548
Up	SVIL	67	0.011621	3322418	0.340167
Up	TAF1	63	0.011788	3175596	0.341002
Up	IFIT3	60	0.004025	1299464	0.320205
Up	RASA1	59	0.009402	3115094	0.336774
Up	TLR4	58	0.010616	3186120	0.335056
Up	NCOA2	58	0.006941	2732602	0.341433
Up	PTPN12	57	0.010002	2421710	0.338061
Up	DDX58	56	0.006503	1834648	0.337498
Up	RB1CC1	56	0.008398	2355384	0.340667
Up	STK3	55	0.009833	1712866	0.340238
Up	NRIP1	54	0.00827	3272078	0.342105
Up	PTPRC	53	0.008794	2245892	0.332854
Up	TLR2	52	0.005513	2069040	0.319406
Up	MED23	52	0.00655	2458958	0.334918
Up	NOD2	50	0.007945	2448312	0.33501
Up	OGT	50	0.005936	2454148	0.335033
Up	IFIT2	49	0.00407	1266226	0.315325
Up	IFIT1	49	0.004249	1046646	0.323529
Up	DZIP3	49	0.005721	1898762	0.331832
Up	NUP153	48	0.007755	2222394	0.352089
Up	RCOR1	47	0.005941	1928750	0.336331
Up	IRF9	47	0.004901	1168868	0.323982
Up	LATS1	45	0.006286	1648222	0.338933
Up	STAT2	45	0.004441	1404884	0.344188
Up	UBR1	43	0.006883	1966348	0.330254
Up	TRIM5	43	0.00492	1419914	0.336354
Up	RNF111	42	0.003349	1439100	0.334756
Up	PDCD6	40	0.004532	1868828	0.334641
Up	PRKAB2	39	0.009131	1791642	0.331492
Up	VEGFA	39	0.004753	1575996	0.337803

Up	PTGS2	39	0.003263	1647510	0.334964
Up	WARS1	38	0.007643	1386458	0.343531
Up	ABCA1	37	0.009943	1770442	0.350794
Up	STRN3	36	0.00712	1163202	0.340024
Up	TRIM25	36	0.005366	1043530	0.340262
Up	ZFR	36	0.004606	1607878	0.335287
Up	UTRN	35	0.009868	1586706	0.340548
Up	ELF1	35	0.005117	1379662	0.332717
Up	IDH1	34	0.005267	1446080	0.330771
Up	OTUD4	34	0.005666	1056004	0.334434
Up	TIA1	33	0.003322	1355074	0.333883
Up	USP25	33	0.005798	1286746	0.337522
Up	GAB1	32	0.003575	736882	0.306809
Up	HIPK3	32	0.004394	1067342	0.337007
Up	TNKS2	32	0.007932	1127420	0.333448
Up	XRN1	32	0.00463	1166800	0.332308
Up	NR2C1	32	0.002237	881234	0.333906
Up	NR2C2	31	0.002628	842738	0.315223
Up	BACH1	30	0.003883	1156962	0.330479
Up	DICER1	29	0.003258	1048798	0.328914
Up	SMG1	29	0.003881	944060	0.333562
Up	LATS2	29	0.002866	932064	0.334964
Up	AFF1	28	0.004083	854336	0.344921
Up	AP1G1	28	0.007669	984640	0.330748
Up	LDLR	27	0.004527	823592	0.345288
Up	CYBB	27	0.003654	730344	0.338933
Up	KDM6A	27	0.003959	815862	0.331267
Up	BCL2A1	26	0.003065	536256	0.304046
Up	CSF2RB	26	0.002156	669768	0.337498
Up	USP33	26	0.002994	730842	0.333402
Up	CDK5R1	26	0.004459	939900	0.345386
Up	FMR1	26	0.003111	963508	0.332263
Up	EXOC8	26	0.006786	1054730	0.338226
Up	AGFG1	25	0.002709	802666	0.332626
Up	PHLPP1	25	0.00394	865598	0.331425
Up	IGF2R	25	0.00464	1190522	0.331628
Up	PKN2	25	0.002459	733000	0.333768
Up	TNFSF10	24	0.00253	533778	0.299292
Up	VCPIP1	24	0.003847	626002	0.331041
Up	KMT2C	24	0.002698	821542	0.331832
Up	BIRC6	24	0.003247	830228	0.330187
Up	IRAK3	24	0.004322	1008336	0.329784
Up	LYST	24	0.00515	1052670	0.329493
Up	NOTCH2	23	0.003516	733162	0.32858
Up	CHMP5	23	0.00412	696206	0.325217
Up	IFIH1	22	0.001947	527982	0.33386
Up	CLASP2	22	0.00263	721240	0.332922
Up	ZEB2	22	0.001047	587914	0.331289
Up	HERC5	22	0.001864	592046	0.344237
Up	DTX3L	22	0.001464	651102	0.325544
Up	MARCHF7	22	0.00212	515132	0.323465
Up	MEIS1	21	0.003315	2580846	0.284877
Up	PELI1	21	0.001105	479568	0.32927
Up	SOS2	21	9.67E-04	345366	0.30029
Up	KCTD12	21	0.001914	677242	0.328669
Up	PPAT	21	0.002572	660286	0.328758
Up	SEC24D	21	0.00203	616138	0.324826
Up	ADAR	21	0.001844	835666	0.348481
Up	SRGAP2	20	0.002579	564926	0.333562
Up	RPRD1A	20	0.002845	718856	0.331357
Up	SHTN1	20	0.002265	377498	0.340667
Up	IFIT5	20	0.001655	410358	0.334227
Up	ARFGEF2	20	0.003033	463622	0.334388
Up	NNT	19	0.00332	653754	0.330479
Up	ARFGEF1	3	2.70E-05	11908	0.263209
Up	IFITM3	3	0	0	0.267246
Up	GBP1	3	0	0	0.267246
Up	PMAIP1	2	1.31E-05	2106	0.240063
Up	TAF2	2	3.21E-05	21792	0.272381
Up	RSAD2	2	0	0	0.266076

Up	STXBP3	2	6.84E-05	61250	0.282691
Up	CEP170	2	0	0	0.255317
Up	PALLD	2	2.08E-04	29096	0.260209
Up	F2RL1	1	0	0	0.250981
Up	N4BP2	1	0	0	0.248848
Up	CLEC7A	1	0	0	0.242095
Up	AKAP11	1	0	0	0.255505
Up	ELF2	1	0	0	0.271939
Up	SLC6A6	1	0	0	0.271939
Up	C1GALT1	1	0	0	0.271939
Up	PDGFC	1	0	0	0.271939
Up	DMTF1	1	0	0	0.271939
Up	NUP58	1	0	0	0.260669
Up	TLR8	1	0	0	0.264844
Up	XAF1	1	0	0	0.264844
Up	CD274	1	0	0	0.25611
Up	CEACAM1	1	0	0	0.25611
Up	ZBP1	1	0	0	0.24941
Up	TGFA	1	0	0	0.230985
Up	KCNJ2	1	0	0	0.230985
Up	TASOR2	1	0	0	0.241951
Up	PARP9	1	0	0	0.245605
Up	RANBP6	1	0	0	0.24738
Up	ARRDC4	1	0	0	0.254728
Up	GCA	1	0	0	0.254728
Up	ARRDC3	1	0	0	0.254728
Up	CENPJ	1	0	0	0.247846
Up	ZNF107	1	0	0	0.252074
Up	LONRF1	1	0	0	0.24442
Up	TRIO	1	0	0	0.242071
Up	TLR5	1	0	0	0.250981
Up	ZNF217	1	0	0	0.251695
Up	CD46	1	0	0	0.253269
Up	OAS2	1	0	0	0.250955
Up	GCLC	1	0	0	0.271939
Up	TRAPPC10	1	0	0	0.188559
Up	IL18R1	1	0	0	0.271939
Up	DENND5A	1	0	0	0.265814
Up	DCLRE1A	1	0	0	0.268411
Up	HIPK1	1	0	0	0.255532
Up	ASCC3	1	0	0	0.255532
Up	OXR1	1	0	0	0.24415
Up	FBXO30	1	0	0	0.260669
Up	ATG2B	1	0	0	0.260042
Up	L3MBTL3	1	0	0	0.257685
Up	C9orf72	1	0	0	0.254116
Up	PRRC1	1	0	0	0.248556
Up	OSBPL11	1	0	0	0.248556
Up	CLK4	1	0	0	0.271939
Up	SERINC1	1	0	0	0.249052
Up	TMLHE	1	0	0	0.25405
Up	FBXO34	1	0	0	0.256638
Up	RELCH	1	0	0	0.252362
Up	HECTD1	1	0	0	0.260669
Down	CSNK2B	222	0.056174	17631706	0.362025
Down	RPS3	176	0.012295	9257168	0.355799
Down	RPS2	156	0.009378	5766964	0.357054
Down	RPS4X	145	0.005665	5003802	0.351962
Down	HDAC11	130	0.030131	5932312	0.351402
Down	CCDC85B	129	0.032481	5281170	0.319155
Down	RPS19	126	0.008243	5318220	0.350768
Down	RPS14	123	0.005871	5083400	0.348056
Down	RPL18	122	0.003792	3647522	0.353189
Down	RPL19	115	0.0038	2987980	0.351199
Down	RPL3	112	0.006259	4717518	0.348655
Down	RPL14	111	0.003611	2989780	0.351047
Down	RPS5	110	0.004451	3267918	0.34863
Down	FBL	109	0.011851	5023504	0.34868
Down	RPL13	106	0.006492	4256224	0.360015
Down	RPS9	104	0.00379	3744910	0.350794

Down	RPL18A	103	0.004506	2954966	0.348156
Down	RPL12	101	0.003356	2961874	0.349031
Down	RPS21	100	0.006374	2945134	0.350515
Down	HSPB1	100	0.01647	7946014	0.342033
Down	RPL8	99	0.00578	3226670	0.346124
Down	EEF1D	99	0.014903	6249736	0.341697
Down	RPL10A	98	0.003901	2869994	0.354373
Down	RPLP1	97	0.009168	4520058	0.348956
Down	RPL37A	96	0.003973	2574564	0.34519
Down	ZNRD2	91	0.016749	5308632	0.341361
Down	KRT18	89	0.019649	7044288	0.348505
Down	POU2F1	82	0.013443	5840974	0.339834
Down	RPL10	78	0.003095	2523704	0.34573
Down	RPL36	72	0.002491	2063476	0.343507
Down	RPLP2	72	0.00291	2184006	0.343507
Down	RPL38	71	0.004592	2141760	0.34295
Down	RPS27	71	0.006415	2530570	0.344066
Down	SNTA1	69	0.018872	2462930	0.300346
Down	APBB1	69	0.009676	2780082	0.343289
Down	SNRPA	68	0.008238	3614266	0.342853
Down	RPL35	67	0.003092	2148100	0.341937
Down	TOP2A	64	0.005513	4072480	0.341409
Down	RPS15	62	0.004076	1866096	0.336494
Down	RPL27	61	0.002978	1678152	0.338485
Down	PRDX2	58	0.008991	3958342	0.336657
Down	RPL29	57	0.002603	1419924	0.339478
Down	BAG1	57	0.007676	3434558	0.336238
Down	LGALS3	56	0.00845	1865196	0.324544
Down	RPS29	55	0.002489	832996	0.340024
Down	PHGDH	54	0.005938	2441924	0.343434
Down	RPL26	53	0.002942	1758546	0.339952
Down	MBD3	53	0.006462	1870582	0.339549
Down	FAU	53	0.001131	1036104	0.34225
Down	NFIC	52	0.010634	3092564	0.347783
Down	TCF4	51	0.008284	1807164	0.349633
Down	MRPL23	50	0.007556	1265756	0.336447
Down	NUBP2	46	0.006086	1674116	0.330636
Down	MED16	46	0.006184	1909986	0.333906
Down	ECSIT	44	0.006864	1020928	0.308934
Down	RABAC1	43	0.01234	2137826	0.335982
Down	BIN1	43	0.0067	2582058	0.308698
Down	PAFAH1B3	43	0.006128	2093888	0.338391
Down	ARPC1B	42	0.005643	1431032	0.337288
Down	UBXN6	42	0.007469	1807124	0.333425
Down	GIPC1	41	0.009058	1572624	0.330951
Down	RARG	41	0.008772	1169788	0.334664
Down	EIF3G	40	0.004085	1322146	0.333516
Down	RPL28	40	0.001195	931888	0.338344
Down	BAD	39	0.004502	1531146	0.32188
Down	EXOSC4	39	0.009295	1821656	0.326134
Down	ASCC2	38	0.007002	1168692	0.337662
Down	HSPBP1	38	0.003444	1325910	0.3329
Down	PQBP1	38	0.006776	1400710	0.33785
Down	MYBL2	36	0.004044	3335808	0.306075
Down	NFIA	35	0.002543	824542	0.294756
Down	LAGE3	35	0.006065	1324068	0.325566
Down	NUDT18	35	0.007306	684202	0.279892
Down	RUNX3	35	0.00354	1330910	0.334319
Down	UPF3B	33	0.003086	1140422	0.329694
Down	PEBP1	33	0.00281	1236570	0.330726
Down	TLE5	32	0.00485	1046816	0.334388
Down	SNRPN	32	0.002554	849514	0.336984
Down	TCOF1	32	0.00472	1623208	0.332399
Down	NENF	31	0.003779	689502	0.33538
Down	RPL13A	31	0.003028	1650092	0.325304
Down	POLR1E	30	0.004456	818072	0.333837
Down	ATAD3A	30	0.001638	1033330	0.324978
Down	CHMP4A	30	0.004822	904830	0.333997
Down	WDR18	30	0.002192	817698	0.332195
Down	CD3E	28	0.006746	1235934	0.333676

Down	UBL7	28	0.003366	798026	0.332149
Down	NDUFS8	27	0.005599	1024420	0.32188
Down	TGFB1I1	27	0.003891	793770	0.335079
Down	SORBS3	26	0.003948	3906396	0.273361
Down	TONSL	26	0.003067	864156	0.33138
Down	MRPL24	26	0.004476	853098	0.326835
Down	PURA	25	0.003175	1040344	0.348481
Down	CAVIN1	25	0.002887	661460	0.335264
Down	GRWD1	25	0.001986	1011652	0.324891
Down	UBOX5	25	0.00154	616704	0.331109
Down	ZBTB7A	24	0.001803	493312	0.323637
Down	POU2F2	24	0.001553	739578	0.332786
Down	PPBP	24	0.0049	805220	0.293386
Down	MRPL4	24	0.003024	868942	0.325609
Down	SH3GLB2	24	0.004486	768154	0.324588
Down	MRPL2	24	0.002496	599756	0.325719
Down	GADD45GIP1	23	0.002025	652996	0.338179
Down	TFPT	23	0.004884	2734812	0.296445
Down	PDLIM1	22	0.00278	722376	0.324566
Down	DCTPP1	22	0.002215	760632	0.326791
Down	EIF5B	22	0.001181	612952	0.331719
Down	DTX1	21	0.001238	435252	0.334802
Down	POLR2L	21	0.00407	851400	0.327121
Down	NAA10	21	0.002348	526556	0.339312
Down	TAF3	20	0.001056	228098	0.286708
Down	KLF1	20	0.001571	516082	0.334802
Down	THAP7	20	0.002718	952806	0.294025
Down	RAB3IP	20	0.004665	3742314	0.232365
Down	FBXL15	19	0.002406	562466	0.330187
Down	TNRC6C	19	0.002762	4923668	0.276407
Down	RABEP2	19	0.001975	540152	0.32838
Down	RABL6	19	0.003071	2190512	0.281398
Down	HBG1	19	0.001005	288998	0.307838
Down	PFDN4	18	0.003287	554480	0.328114
Down	TCF7	3	2.27E-04	42330	0.276958
Down	NDUFA13	3	1.25E-04	23576	0.258686
Down	PF4	2	1.02E-05	16122	0.257617
Down	TRAPPC6A	2	3.62E-04	307310	0.255036
Down	ARL4D	2	6.90E-06	2180	0.25389
Down	MEMO1	2	8.81E-05	20782	0.264642
Down	MAL	1	0	0	0.250981
Down	NDUFAF3	1	0	0	0.243514
Down	SLC25A6	1	0	0	0.259459
Down	EPS8L2	1	0	0	0.250206
Down	CD79B	1	0	0	0.249743
Down	PRKAR1B	1	0	0	0.255505
Down	YJU2	1	0	0	0.271939
Down	ELOF1	1	0	0	0.271939
Down	LRRC29	1	0	0	0.271939
Down	PDE6B	1	0	0	0.271939
Down	ANKRD12	1	0	0	0.254688
Down	ACP5	1	0	0	0.230361
Down	GAMT	1	0	0	0.265814
Down	ZNF71	1	0	0	0.265814
Down	HBG2	1	0	0	0.250838
Down	DNPH1	1	0	0	0.248277
Down	CHMP6	1	0	0	0.250386
Down	FAHD1	1	0	0	0.245941
Down	ROGDI	1	0	0	0.242071
Down	C9orf78	1	0	0	0.248492
Down	ZNF593	1	0	0	0.248277
Down	BUD23	1	0	0	0.248938
Down	PTCD1	1	0	0	0.248403
Down	CD5	1	0	0	0.251943
Down	PC	1	0	0	0.244457
Down	MYL9	1	0	0	0.257685
Down	ATP5F1D	1	0	0	0.245036
Down	ADK	1	0	0	0.271939
Down	UCP2	1	0	0	0.268411
Down	BEX3	1	0	0	0.241951

Down	ZNF91	1	0	0	0.245419
Down	TTF1	1	0	0	0.251097
Down	PHLDB3	1	0	0	0.268411
Down	LIMS2	1	0	0	0.252074
Down	SVIP	1	0	0	0.248721
Down	THAP3	1	0	0	0.250968
Down	NAT14	1	0	0	0.2515
Down	ZNF428	1	0	0	0.24415
Down	CCDC124	1	0	0	0.25695
Down	CCDC120	1	0	0	0.241951
Down	AGMAT	1	0	0	0.25533
Down	ITM2C	1	0	0	0.271939
Down	TSHZ2	1	0	0	0.255572
Down	NDUFB11	1	0	0	0.226846
Down	NOP53	1	0	0	0.25695
Down	ZNF581	1	0	0	0.259459
Down	DPP7	1	0	0	0.249436
Down	NOSIP	1	0	0	0.271939
Down	SIT1	1	0	0	0.25611

Table 5 MiRNA - hub gene and TF – hub gene topology table

Regulation	Target Genes	Degree	MicroRNA	Regulation	Target Genes	Degree	TF
Up	DDX3X	187	hsa-mir-149-3p	Up	EGR1	53	LMO2
Up	DDX5	145	hsa-mir-500b-5p	Up	DDX5	51	MYCN
Up	NCOA3	143	hsa-mir-548y	Up	NCOA3	48	SIN3B
Up	EGR1	129	hsa-mir-518b	Up	STAT1	42	IRF8
Up	HIF1A	101	hsa-mir-16-5p	Up	HIF1A	40	GATA1
Up	SF3B1	89	hsa-mir-181c-3p	Up	DISC1	37	RUNX1
Up	APC	80	hsa-mir-148a-3p	Up	USP15	34	AP1S2
Up	SIRT1	70	hsa-mir-520c-3p	Up	APC	34	HOXB4
Up	LIG4	57	hsa-mir-501-3p	Up	SIRT1	33	TBX3
Up	USP15	50	hsa-mir-20a-5p	Up	DDX3X	32	PDX1
Up	STAT1	48	hsa-mir-449a	Up	LIG4	31	KDM6A
Up	PTPN11	43	hsa-mir-30d-3p	Up	PTPN11	29	TCF3
Up	ITCH	34	hsa-mir-27a-3p	Up	SF3B1	29	NANOG
Up	LRRK2	11	hsa-mir-4476	Up	ITCH	17	BCL3
Up	DISC1	8	hsa-mir-30d-5p	Up	LRRK2	16	CNOT3
Down	RPS3	50	hsa-mir-5699-3p	Down	RPS14	45	RCOR3
Down	RPS4X	40	hsa-mir-532-3p	Down	RPL3	44	DMRT1
Down	RPS14	40	hsa-mir-503-5p	Down	RPS19	42	SREBF1
Down	FBL	39	hsa-mir-31-5p	Down	RPL18	36	FOXP3
Down	RPL3	32	hsa-mir-365b-3p	Down	RPS5	35	POU5F1
Down	RPL18	29	hsa-mir-550a-3-5p	Down	CSNK2B	35	SOX11
Down	RPL13	27	hsa-mir-495-3p	Down	FBL	33	GATA2
Down	RPL19	26	hsa-mir-23b-3p	Down	RPL14	29	FOXO3
Down	RPS19	26	hsa-mir-320e	Down	RPS3	27	AR
Down	RPS2	20	hsa-mir-378d	Down	RPL13	24	ESR2
Down	RPL14	16	hsa-mir-424-5p	Down	RPL19	24	RARG
Down	RPS5	16	hsa-mir-103a-3p	Down	HDAC11	24	MITF
Down	CCDC85B	11	hsa-mir-603	Down	RPS2	22	RELA
Down	CSNK2B	9	hsa-mir-124-3p	Down	CCDC85B	19	PPARD
Down	HDAC11	4	hsa-mir-1306-5p	Down	RPS4X	15	XRN2

Figures

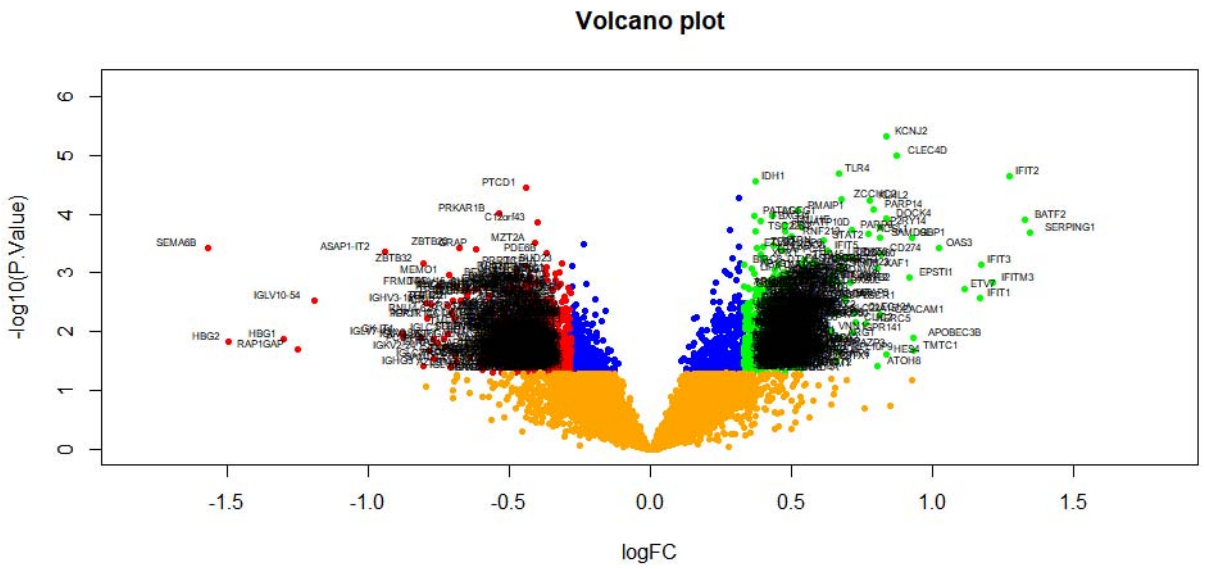

Fig. 1. Volcano plot of differentially expressed genes. Genes with a significant change of more than two-fold were selected. Green dot represented up regulated significant genes and red dot represented down regulated significant genes.

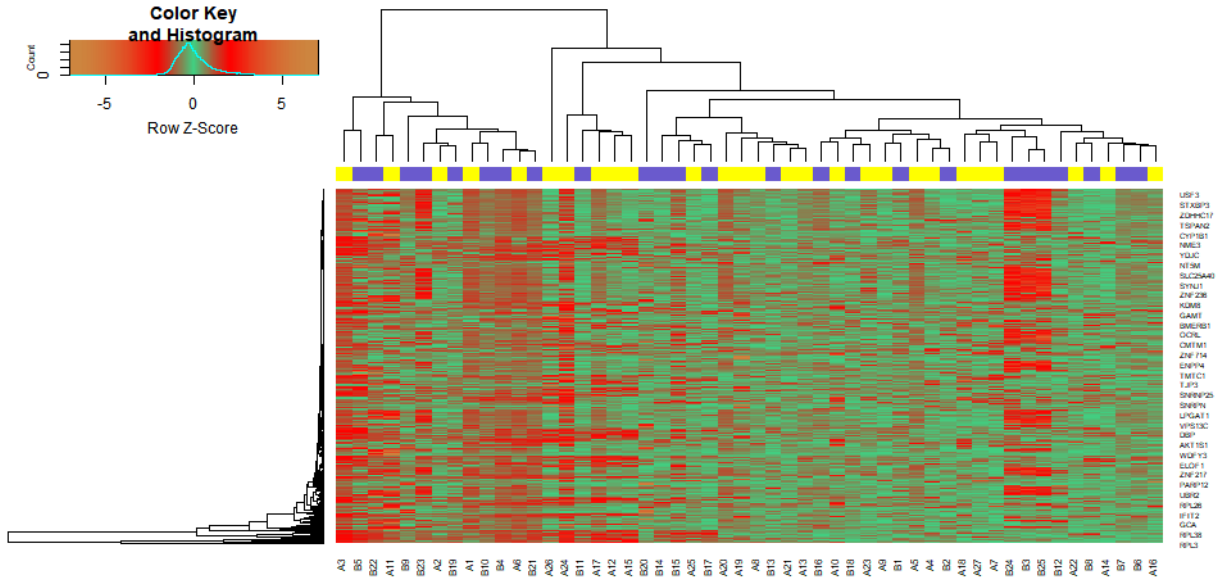

Fig. 2. Heat map of differentially expressed genes. Legend on the top left indicate log fold change of genes. (A1 – A76 = CAD samples; B1 – B62 = normal control samples)

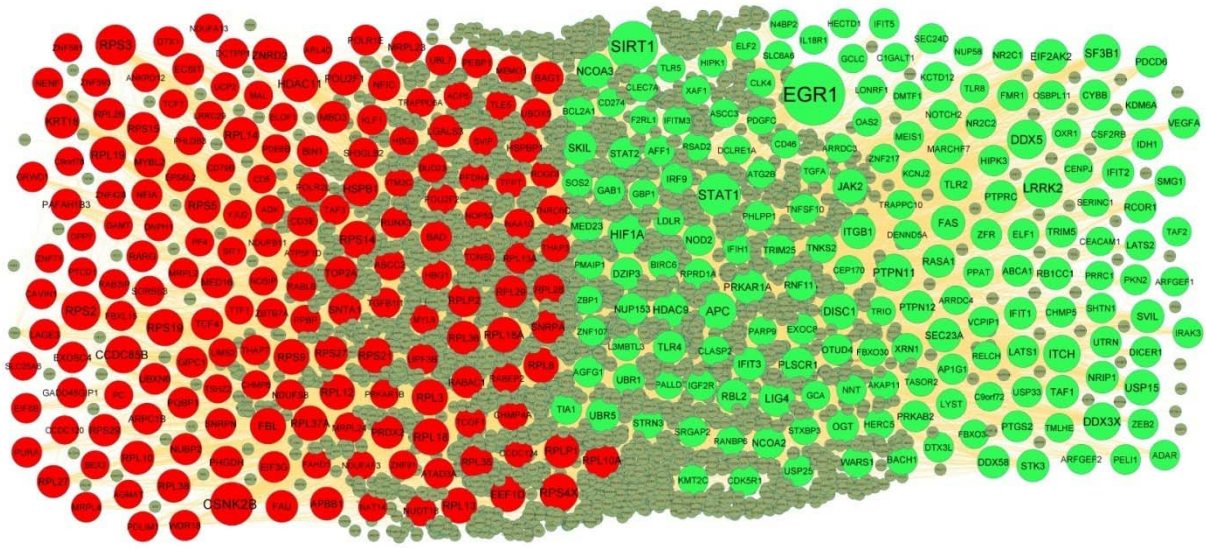

Fig. 3. PPI network of DEGs. Up regulated genes are marked in green; down regulated genes are marked in red

Fig. 4. Modules selected from the DEG PPI between patients with FSGS and normal controls. (A) The most significant module was obtained from PPI network with 26 nodes and 78 edges for up regulated genes (B) The most significant module was obtained from PPI network with 29 nodes and 230 edges for down regulated genes. Up regulated genes are marked in green; down regulated genes are marked in red

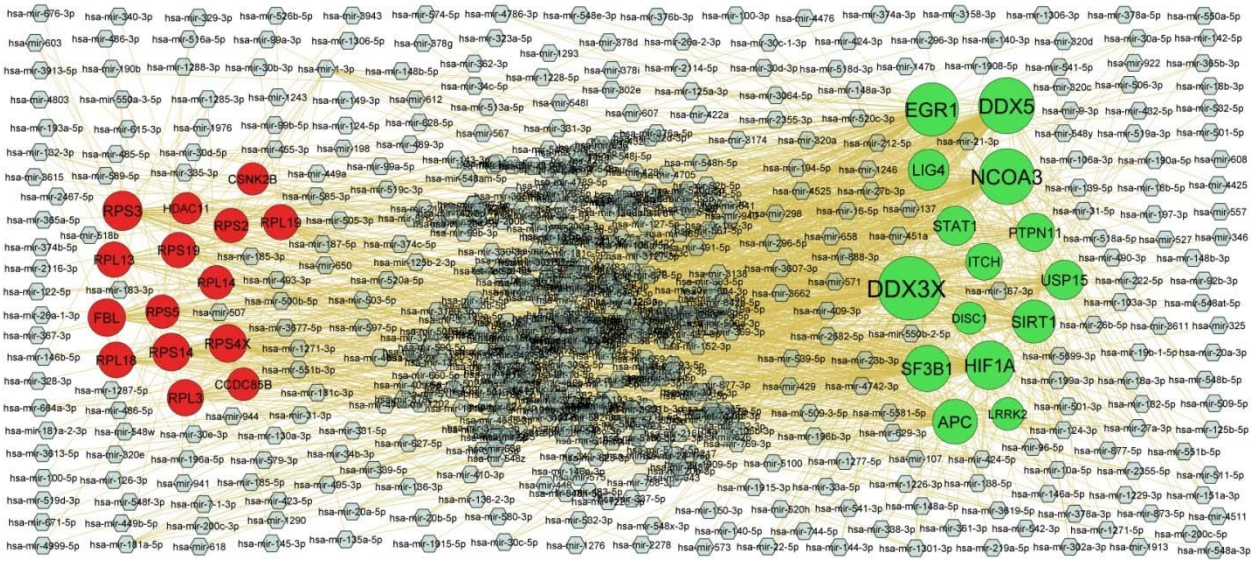

Fig. 5. Target gene - miRNA regulatory network between target genes. The blue color diamond nodes represent the key miRNAs; up regulated genes are marked in green; down regulated genes are marked in red.

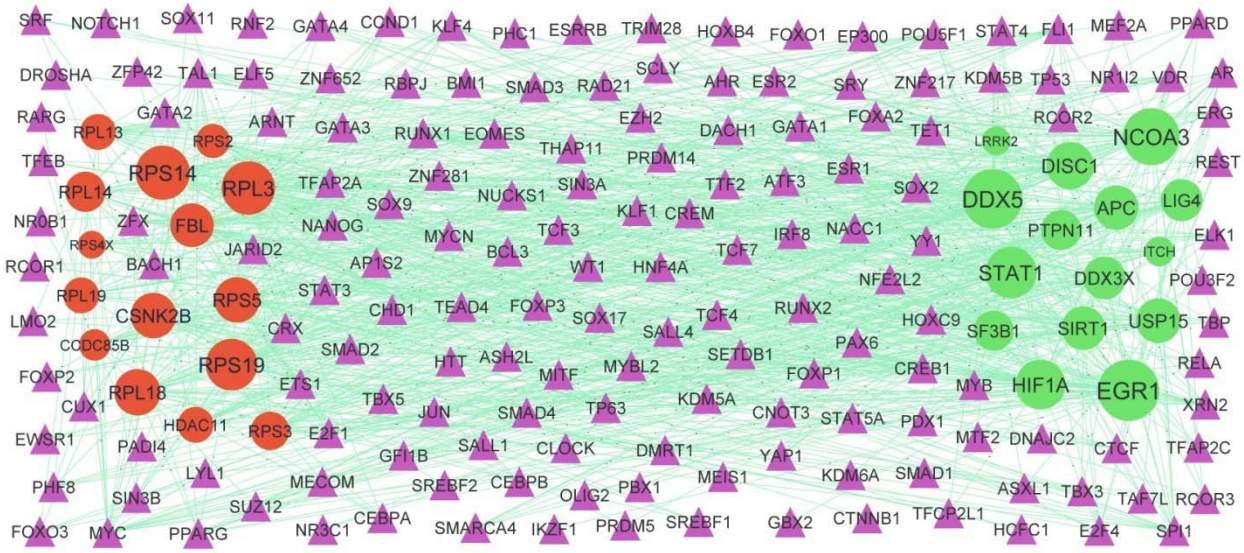

Fig. 6. Target gene - TF regulatory network between target genes. The violet color triangle nodes represent the key TFs; up regulated genes are marked in green; down regulated genes are marked in red.

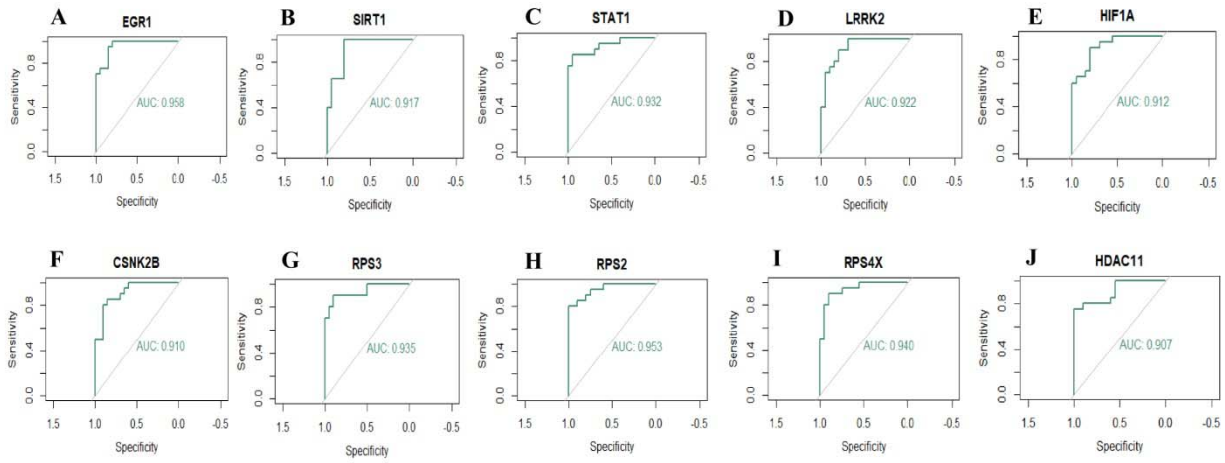

Fig. 7. ROC curve analyses of hub genes. A) EGR1 B) SIRT1 C) STAT1 D) LRRK2 E) HIF1A F) CSNK2B G) RPS3 H) RPS2 I) RPS4X J) HDAC11